

Chimera State in Multiplex Networks

Ph.D. Thesis

By
SAPTARSHI GHOSH



DISCIPLINE OF PHYSICS
INDIAN INSTITUTE OF TECHNOLOGY INDORE
JANUARY 2020

Chimera State in Multiplex Networks

A THESIS

*Submitted in partial fulfillment of the
requirements for the award of the degree
of
DOCTOR OF PHILOSOPHY*

by
SAPTARSHI GHOSH



**DISCIPLINE OF PHYSICS
INDIAN INSTITUTE OF TECHNOLOGY INDORE
JANUARY 2020**



INDIAN INSTITUTE OF TECHNOLOGY INDORE

CANDIDATE'S DECLARATION

I hereby certify that the work which is being presented in the thesis entitled "Chimera State in Multiplex Networks" in the partial fulfillment of the requirements for the award of the degree of DOCTOR OF PHILOSOPHY and submitted in the DISCIPLINE OF PHYSICS, Indian Institute of Technology Indore, is an authentic record of my own work carried out during the time period from December 2014 to August 2019 under the supervision of Prof. Sarika Jalan, Professor, Indian Institute of Technology Indore, India.

The matter presented in this thesis has not been submitted by me for the award of any other degree of this or any other institute.

Signature of the student with date
SAPTARSHI GHOSH

This is to certify that the above statement made by the candidate is correct to the best of my/our knowledge.

Signature of Thesis Supervisor with date

Prof. SARIKA JALAN

SAPTARSHI GHOSH has successfully given his/her Ph.D. Oral Examination held on 8/1/2020.

Signature of Chairperson (OEB)
Date:

Signature of External Examiner
Date: 8/1/2020

Signature(s) of Thesis Supervisor(s)
Date: 08.01.2020

Signature of PSPC Member #1
Date: 8/1/2020

Signature of PSPC Member #2
Date: 8/1/2020

Signature of Convener, DPGC
Date: 8-01-2020

Signature of Head of Discipline
Date: 08.01.2020

This Thesis is

Dedicated

to

My Beloved Grandparents

Dadubhai, Didibhai & Sundordida

Acknowledgements

The pursuit of the Ph.D. is a life-changing journey for me, both insanely beautiful and absolutely terrifying and, it wouldn't have been possible without constant guidance and support from my supervisor, **Prof. Sarika Jalan**. I wish to place on record my deep sense of gratitude and reverence to her for providing me an opportunity to be part of the Complex Systems Lab. She has always been a steady source of inspiration to me, and her constant encouragement, support as well as reprimand has enabled me to draw out the best in me. I can never forget one awe-inspiring snippet of advice from her;

Fearing the unavoidable will only slow you down...

Accept it as inevitable..... and push through your fear...

because the other side is as beautiful as you dreamed it to be.....

which helped me to evolve not only as a better researcher but also as a better person and responsible citizen for both the society and the nation.

I humbly thank **the Director**, IIT Indore, for providing the necessary amenities required for involved research. I am grateful to my PSPC committee members, **Dr. Rajesh Kumar**, and **Dr. Kapil Ahuja** for scrutinizing my work and lending insightful suggestions at different phases of my Ph.D. I am also thankful to the **DPGC convener**, **Head (Physics)**, all the **faculty members** and **staff** of Discipline of Physics, IIT Indore for their timely help and support throughout. I humbly acknowledge the sincere efforts of all the staff members of the Academic Office (especially **Tapesh Sir and Bindu Ma'am**), Accounts Section (especially **Sunny Sir**), R&D Section, IT Section and Central Library, IIT Indore whose constant support ascertained smooth functioning of my research work. I am also thankful to Health Center, IIT Indore for their relentless help for my physical well-being.

I would also take this opportunity to thank my fellowship sponsoring agency, **Department of Science and Technology, India**, for selecting me as an **INSPIRE** fellow and my collaborator, **Dr. Anna Zakharova** (TU Berlin) for her help and support during my research work.

My heartfelt gratitude to all my present and past colleagues at Complex Systems Lab, **Aradhana**, **Sanjiv**, **Camellia** and **Aparna** for their love, care, support and guidance throughout, **Alok** for his insightful suggestions on anything and everything, **Pramod** for being a stress-buster friend and **Priodyuti** for always being the voice of reason and an extremely helpful research partner, **Dr. Ajaydeep** for being a mentor, **Rahul** for always being there for any help, **Anil** for being a very easy-going research partner, **Vasundhara & Tanu** for their help and for keeping the lab atmosphere jovial and alive, **Ankit** for his unique insights and our newest member **Sanket and Ritho** for all their support. I would also like to sincerely thank my other past colleagues, **Bibhabasu**, **Jakub**, **Leo** (my co-authors and friends), **Sudeep**, **Krishna**, **Amit**, **Ankush**, **Palak**, **Parth**, **Madhoolika**, **Loïc**, **Richa**, **Naveen**, **Pramodini**, **Neeraj** for providing a challenging yet conducive atmosphere for my research and helping me to enjoy this journey.

On personal front, I am lucky to have **Camellia** and **Aparna**, my sisters, helping me through the darkest storms during this journey and lending their shoulder for support regardless. I am ever grateful to my dear friends and comrades-in-arms **Pramod**, **Priodyuti**, **Madhurima**, **Abhishek**, **Anirban**, **Deepika** for being there for me any and every time. Of course, the story remains incomplete without mentioning our cutest friend and my first model for DSLR Photoshoot, **Coco**. I am fortunate to have some amazing friends, **Anirudh**, **Manojit**, **Samsul**, **Kushal**, **Siddhartha**, **Mithun**, **Sayan**, **Dipayan**, **Sudhir**, **Anupama**, **Pragati**, **Suchismita**, **Thaksen**, **Mahesh**, **Najim**, **Sudeep**, **Tamalika**, **Ankita**, **Sampa**, **the present and past members of whole Saraswati Puja gang** and many others, making my stay at Indore, an unforgettable one. The list are by no means complete, and I apologize for not being able to list everyone. But know that, you will always be a part of my fond memories of time here, at IIT Indore.

I am indebted to my all my teachers, **Rana Sir**, **Prashanta Sir**, **Bappa Da**, my teachers from **Mekhliganj High School**, **Kajol Sir**, **Ranjan Sir**, **Ratul Sir**, **English Sir**, **MG Sir**, **AK sir**, **BP sir**, **MC & MK ma'am**, my teachers at **IIT Kanpur** (especially my project mentor **Prof. H.C. Verma** and **Dr. Krishnacharya** and

Dr. Deshdeep Sahdev), who laid the foundation of education for me, enabling me to reach this far. I also forever indebted to **Ujjwal Sir** (Dr. Ujjwal Sen) without whom I wouldn't have started on this path.

I am incredibly grateful to my evergreen friends, **Rohan, Ashu, Biplab, Manoj, Bappa, Debu, my entire brotherhood of y14IITK including Avishek, Niladri, Amartya, Debasmit, Utpal, Bivas, Shayoree, Piyali, Kaushali, Anirban, Shamreen and all others** for keeping the craziness alive in me.

Words fall short for expressing my gratitude towards my parents, my loving **mother** and **father** who has been my pillar of strength through all ups and downs. I can't thank them enough for believing in me, encouraging and supporting me to chase my dreams. This would be incomplete without mentioning my **damsel**, *who-must-not-be-named* for showering me with unconditional love and keeping up with my quirkiness.

Finally, I thank my **ancestors** and almighty **God** for enabling me to live this beautiful life, meeting these amazing people, and helping me to chase my dream.

Saptarshi Ghosh

Synopsis

Introduction

The dynamical systems theory, which deals with the temporal evolution of the state of interacting constituent entities of a system, forms the foundation of this thesis. The study of dynamics originated in the 1600s when Newton and Leibniz developed calculus to study the trajectories of celestial bodies [4]. However, before the twentieth century, investigation of a dynamical system could only be achieved for smaller cases due to the requirement of sophisticated mathematical techniques to solve higher-order systems. Only recent advancements in the fast computing and easily available vast amount of information enabled us to investigate and solve large complex systems found in the real-world. Network science, which describes the interaction architecture among the constituent entities of a system, helped us in mathematically modeling complex systems in terms of networks. A network which is a collection of nodes (or the constituent entities) and edges (interactions or links among the entities), sketches the collective dynamics of the entire system in terms of coupled differential or difference equations. Starting from cognitive functions arising from dynamics of the neural networks to the formation of public opinions arising from dynamics of the social networks, the wide range and variety of applications demonstrate the baffling scale in which network science operates. Moreover, it shows the reason for the success of network science in providing a combined mathematical framework to investigate complex systems across fields spanning the entire spectrum of science and technology [9].

In the late twentieth century, the phenomenon of synchronization, which at heart narrates a correlated dynamics between the interacting entities, has emerged as one of the biggest success stories in the study of dynamics on networks, building on the works on dynamical systems theory, mean-field theory, manifold theory, and bifurcation theory [11]. However, at the dawn of the twenty-first century, an exotic partial synchronization state, termed as chimera, describing dynamical symmetry

breaking in an identically coupled network has been reported, attracting considerable interest in the past two decades and forming the main focus of this thesis.

A chimera state refers to a hybrid dynamics, which displays coexistence of coherence - incoherence in a network of identical entities coupled in a symmetric fashion. In 2002, Kuramoto and Battogtokh reported a peculiar coexistence of coherent and incoherent dynamics on an array of identical phase oscillators arranged in a regular network, under certain special conditions [2]. Later on, Abrams and Strogatz christened this dynamical state as a chimera and provided a firm understanding over its strange appearance [3]. In the last two decades, the chimera state has been investigated both theoretically and experimentally, providing new understanding and insights as well as applications [32] to various fields including neuroscience.

However, the majority of the studies is primarily focused on exploring chimera states in various systems having diverse underlying dynamics. Minimal emphasis has been paid to incorporate the new-found multiplex structure of the networks in the investigation of the emergent chimera state. The recent multiplex approach to network science, incorporating the existence of various types of interactions (edges) between the same pair of entities (nodes) by segregating them in different layers, provided a more realistic portrayal of the complex systems [87]. Furthermore, the inclusion of multiplex framework presents a wide variety of dynamical behaviors, which may be impossible to capture through single-layer framework [53].

This thesis aims to provide a complete report on the emergence of the chimera state in multiplex networks adding a new dimension to the study of chimera state. We first report the appearance of chimera state in multiplex networks demonstrating required special conditions. We further demonstrate the impact of delay, inhibitions, and non-identicality of the layers on the collective dynamical behavior of the chimera state in multiplex networks. We also provide a recipe to engineer the chimera state. The findings obtained through our systematic investigation, demonstrate the role of several crucial factors, which controls the emergence of chimera state in the multiplex network, commonly found in real-world complex systems.

Objectives

- To demonstrate the emergence of chimera state in networks incorporating the multiplex architecture.
- To investigate the impact of several factors including delay, non-identical layers, and inhibition on the enhancement or suppression of chimera state in multiplex networks.
- To provide a technique to gain control in designing of the chimera states for both single- and multiplex networks.

Theoretical Framework

This thesis presents a comprehensive investigation of emerging chimera state in multiplex networks. However, sketching on the full canvas, we aggregated several studies in the thesis pertaining to the investigation of the collective dynamical behavior of complex systems, represented in terms of both single layer (monoplex) and multiplex networks.

First, we describe the construction of the network and the governing equations that we have used to showcase our findings. We have considered an undirected multiplex network (consisting of $2N$ nodes distributed in two layers) represented by the adjacency matrix $\mathcal{A}_{(2N \times 2N)}$ such that [87],

$$\mathcal{A} = \begin{pmatrix} A^1 & I \\ I & A^2 \end{pmatrix} \quad (1)$$

Here, each layer of the multiplex network (consisting of N nodes) is encoded by adjacency matrices A^1, A^2 , respectively. The connectivity of the s^{th} layer is described

by $(A^s; s = 1, 2)$. Each element of the layers is defined as

$$A_{i,j}^s = \begin{cases} 1 & \text{if } i \text{ is connected } j \\ 0 & \text{otherwise} \end{cases} \quad (2)$$

The matrix $A_{(N \times N)}^s$ is a symmetric matrix ($A_{ij}^s = A_{ji}^s$), representing bi-directional connections and with zero diagonal entries ($A_{ii}^s = 0$) depicting no self-connection. $I_{(N \times N)}$ is a unit matrix representing one to one connection between the mirror nodes across layers of the multiplex network. We consider bi-directional inter-layer connections which maintain symmetric coupling environment required for defining a chimera state.

Furthermore, we represent the dynamical state of the nodes of the network at time t by a real variable $z_i^t \in \mathbb{R}, \forall_{i=1, \dots, 2N}$. The local dynamics of the nodes is realized as the famous logistic map $z_i^{t+1} = \mu z_i^t (1 - z_i^t)$ in chaotic regime ($\mu = 4.0$) [26]. Adding the network architecture, the dynamical evolution equation for the whole network can be written as [52]

$$z_i^{t+1} = f(z_i^t) + \frac{\varepsilon}{(k_i)} \sum_{j=1}^{2N} \mathcal{A}_{ij} [f(z_j^t) - f(z_i^t)] \quad (3)$$

where ε represents the overall coupling strength ($0 \leq \varepsilon \leq 1$) and $k_i = (\sum_{j=1}^{2N} \mathcal{A}_{ij})$ is the normalizing factor. The function $f(z^t)$ is the logistic map described above.

Primarily, the layers of the multiplex network are represented by the regular 1D ring networks with periodic boundary conditions, where each node is connected to its P neighbors on each side. Thus all the nodes in the regular 1D ring network possess same node degree $\langle k \rangle = 2P$. Although, 1D ring network generally describes a special class of regular networks, in the following, we will use regular or 1D ring network interchangeably to describe 1D regular ring network throughout the thesis, unless specified otherwise. We further describe the node degree by the coupling radius r , defined as $r = \frac{\langle k \rangle}{2N} = \frac{P}{N}$, with N being number of nodes in the regular network in each layer of the multiplex network.

We further describe the equation governing the temporal evolution, incorporating

the time delay τ as [53]

$$z_i^{t+1} = f(z_i^t) + \frac{\varepsilon}{(k_i)} \sum_{j=1}^{2N} \mathcal{A}_{ij} [f(z_j^{t-\tau}) - f(z_i^t)] \quad (4)$$

Note that, a constant delay value τ which is applied to all the edges in the network. In case of heterogeneous delays, i.e. non-similar delays to the edges of the network, we replace scalar constant τ with a matrix τ which elements τ_{ij} describe the delay between i^{th} and j^{th} node.

Chimera is defined as a hybrid dynamics consisting of a coherent and an incoherent state. In the presented work, the dynamical state of a monoplex network or a particular layer of a multiplex network (represented by $z_i^t, \forall i=1,\dots,N, \forall t \geq T_0$; T_0 being the transient time) is termed as coherent state [52] if

$$\lim_{N \rightarrow \infty} \sup_{i,j \in U_\xi^N(x)} |z_i(t) - z_j(t)| \rightarrow 0 \text{ for } \xi \rightarrow 0 \quad (5)$$

where $U_\xi^N(x) = \{j : 0 \leq j \leq N, |\frac{j}{N} - x| < \xi\}$ represents the network neighborhood of any point $x \in S^1$, i.e., of the regular (S^1 ; ring) network. Geometrically, coherence means that in the continuum limit $N \rightarrow \infty$, the spatial profile at time t (i.e. the z_i^t - i curve) of the state z_i^t approach a smooth profile $z(x, t)$. A smooth spatial profile signifies very small spatial distance between the neighboring nodes. The extreme case is the completely coherent state, which can be represented as $z_i^t = z_j^t \forall t \geq T_0, \forall i, j$ (T_0 being the transient time). The completely coherent state (having a constant value for all nodes i.e. zero spatial distance with neighbors) geometrically leads to a straight line spatial profile in the $z_i^t - i$ plane. Any discontinuity appearing in the profile reflects the spatial incoherence and therefore show co-existence of coherence-incoherent, leading to a chimera state. We have used several measures throughout the thesis to detect the coexistence of coherence and incoherence, i.e., the chimera state in the parameter space of the system under investigation.

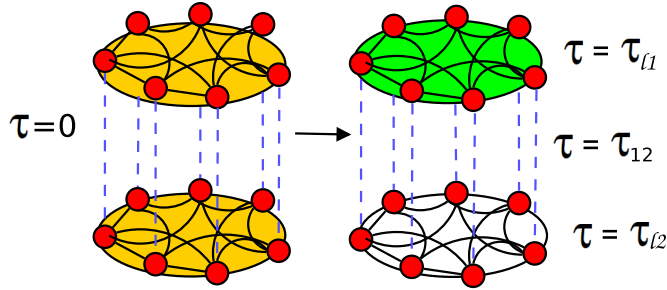


Figure 1: Schematic diagram of a multiplex network consisting of two identical regular networks with left panel (LP) and right panel (RP) describing undelayed and delayed systems, respectively.

Summary of the work done

Emergence of chimera in multiplex network.

We report an observation of the chimera state in the multiplex networks where an individual layer is represented by a regular network (S^1 ; ring) with non-local interactions (Fig. 1; LP). We show that while multiplexing retains the multi-chimera state displayed by the single-layer network in the same parameter regime, it changes the spatial location of the region of the incoherence. We demonstrate identical chimera patterns in the mirror layers of the multiplex network arising due to the underlying symmetry of the network and chosen setup of initial conditions. Moreover, the temporal behavior of the network remains periodic even after multiplexing. The chimera in the multiplex network is found to be sensitive to the changes in the initial conditions as well, which is revealed through the changes in the incoherent regions, obtained through temporal evolution from different sets of initial conditions.

We, furthermore, include system-wide delayed interaction in both inter- and intra-layer connection for a better representation of real-world dynamics on multiplex networks (Fig. 1; RP). We find that an interplay of delay and multiplexing brings about an enhanced or suppressed appearance of chimera state depending on the distribution as well as parity of delay values in the layers. Additionally, we report a *layer chimera state* with the existence of one layer displaying coherent and another layer demonstrating incoherent dynamics. This study showcases the importance of incorporating the multiple layers (representing different types of interactions) in the context of chimera state, to gain insight into the real-world networks which inherently possess such multi-layer architecture as well as delayed interactions.

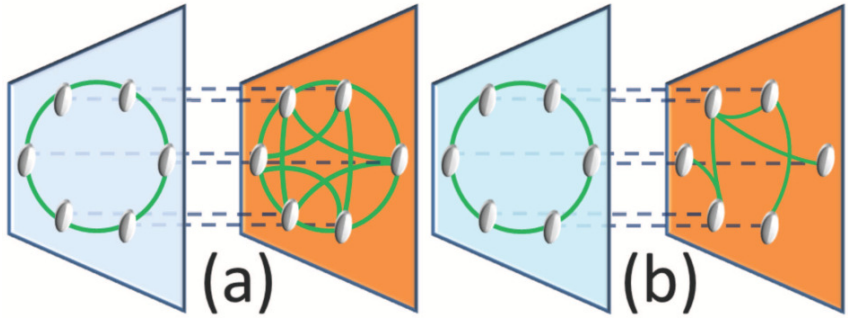


Figure 2: Schematic diagram depicting a multiplex network consisting of a regular network and (a) a regular network with different node degree (i.e., with different coupling range) and (b) a random network, respectively.

Promoting chimera through non-identical multiplexing.

We present the emergence of chimera state in a multiplex network consisting of two non-identical layers, which are interconnected. Note that, chimera state is classically defined in a network with an identical coupling environment for all nodes. Therefore, we define chimera state only in layers which are represented by regular networks (S^1 ; ring), interchangeably called homogeneous networks (due to the constant node degree). We demonstrate that the parameter range, displaying the chimera state in the homogeneous layer of the multiplex networks, can be tuned by changing the link density or connection architecture of the same nodes in the other layer. We focus on the impact of the other layer (where we are modifying the connection density or connection architecture) on the enlargement or shrinking of the coupling regime for which chimera is displayed in the homogeneous layer. We find that a denser homogeneous layer promotes chimera in a sparse homogeneous layer (Fig. 2; a), where chimeras do not occur in isolation (i.e., in a single-layer setup). Furthermore, while a high connection density is required for the second layer if it is homogeneous, this is not true if the second layer is inhomogeneous. We demonstrate that even a sparse inhomogeneous layer, can promote chimera states in a sparse homogeneous layer (Fig. 2; b). Therefore, the connectivity of the multiplexed layer plays a crucial role in the appearance of the chimera state in other layers.

Enhancing chimera through inhibition.

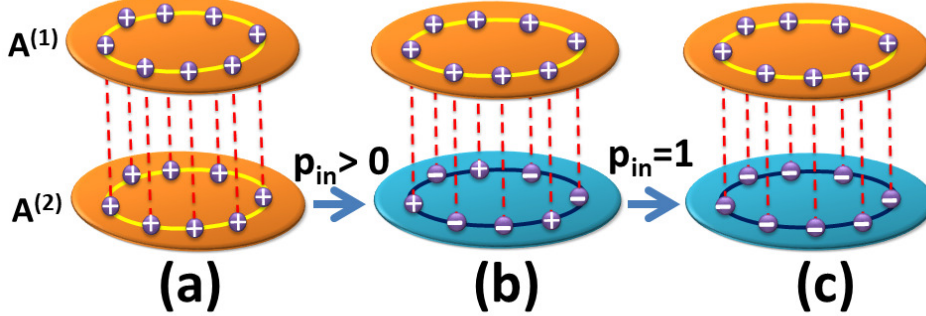


Figure 3: Schematic diagram depicting a multiplex network consisting of two regular networks where the second layer is, (a) attractively coupled, (b) repulsively coupled with some probability, (c) all repulsively coupled.

We have explored an impact of inhibitory (repulsive) coupling on the appearance of chimera state in a multiplex network. We have systematically studied the impact of multiplexing of a layer having repulsively coupled oscillators on the occurrence of chimeras in the layer having attractively coupled identical oscillators.

We report that there exists an enhancement in the appearance of chimera state in one layer of the multiplex network in the presence of all repulsive coupling in the other layer (Fig. 3; c). Due to the multiplexing with a layer having all inhibitory nodes thereby all repulsive coupling, global synchrony among oscillators with all attractive couplings is destroyed, leading to a chimera state. Furthermore, we report that the range of parameters for which chimera is demonstrated in one layer can be controlled by changing the probability of inclusion of inhibitory nodes in another layer. Importantly, we found that a minimal number of inhibitory nodes can bring an enhancement in the appearance of the chimera state destroying the synchronized state (Fig. 3; b).

Engineering Chimera states.

Chimera state consisting of coherent and incoherent regions, represents an exotic hybrid state which is very difficult to harness due to its peculiar nature and stringent conditions required for its appearance. However, due to the fundamental im-

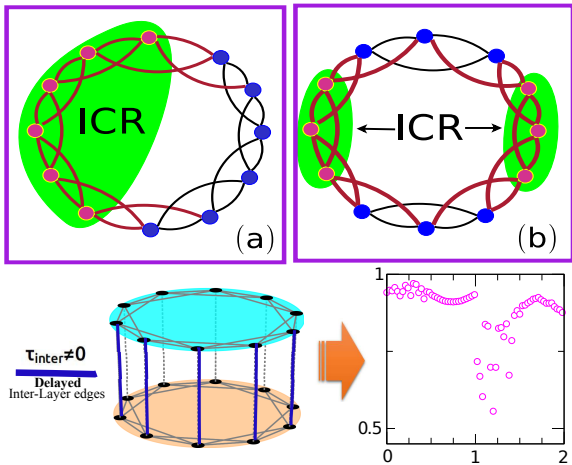


Figure 4: Schematic diagram of the proposed engineering scheme for designing the incoherent region (ICR) and, in turn, the chimera state in single layer (top panel; TP) and multiplex network (bottom panel; BP).

portance as well as potential applicabilities, there have been persistent efforts to control the appearance of the chimera state. Here, we present a novel technique to engineer a chimera state by using an appropriate distribution of heterogeneous time delays on the edges of a network. Using a coupled chaotic map with the identical coupling environment and starting from a coherent state, we demonstrate that control over the spatial location of the incoherent region of a chimera state in a network can be achieved by appropriately introducing time delays in sequence (Fig. 4). This method allows engineering one-cluster (Fig. 4; TP,(a)) or multi-cluster (Fig. 4; TP,(b)) chimera patterns.

Furthermore, we extend the proposed technique to provide a recipe to construct chimera states in the multiplex networks with the aid of multiplexing-delays. The chimera state in multiplex networks is produced by introducing heterogeneous delays in a fraction of inter-layer links, referred to as multiplexing-delay, in a sequence (Fig. 4; BP). Additionally, we demonstrate that the emergence of the incoherence in the chimera state can be regulated by making appropriate choice of both inter- and intra-layer coupling strengths, whereas the extent and the position of the incoherence regime can be regulated by appropriate placing and strength of the multiplexing delays. The proposed technique to construct such engineered chimera equips us with multiplex network's structural parameters as tools in gaining both qualitative- and quantitative-control over the incoherent section of the chimera states and, in turn, the chimera state.

Conclusion

Through a series of investigations involving the study of dynamics on multiplex networks, this thesis on one hand, demonstrates emergence of chimera state in multiplex networks and how interplay of system parameters like delay impede or expedite the appearance of chimera state, while on the other hand present a recipe to precisely control the design of the chimera state. Additionally, revealing the impact of one layer on the dynamical behavior of another layer of the multiplex network, this thesis marks the importance of incorporating multiple layers of interaction while investigating collection dynamics in real-world complex systems which inherently possess such architecture.

Keywords : Network, Multiplex Network, Chimera State, Partial synchronization

LIST OF PUBLICATIONS

Publications from thesis

1. **Saptarshi Ghosh**, Leonhard Schülen, Ajay Deep Kachhvah, Anna Zakharova and Sarika Jalan (2019) *Taming Chimeras in Networks through Multiplexing Delays*, EPL, **127**, 30002 (DOI: 10.1209/0295-5075/127/30002)
2. **Saptarshi Ghosh** and Sarika Jalan (2018) *Engineering chimera patterns in networks using heterogeneous delays*, Chaos (Fast Track) **28**, 071103 (Editors Pick Article) (DOI: 10.1063/1.5042133)
3. **Saptarshi Ghosh**, Anna Zakharova and Sarika Jalan (2018) *Non-identical multiplexing promotes chimera states*, Chaos, Solitons & Fractals **106**, 56-60 (DOI: 10.1016/j.chaos.2017.11.010)
4. Sarika Jalan, **Saptarshi Ghosh**, Bibhabasu Patra (2017) *Is repulsion good for the health of chimeras?* Chaos (Fast Track) **27(10)**, 101104 (DOI: 10.1063/1.5005576)
5. **Saptarshi Ghosh**, Anil Kumar, Anna Zakharova and Sarika Jalan (2016) *Birth and death of chimera: Interplay of delay and multiplexing*, EPL **115(6)** 60005 (DOI:10.1209/0295-5075/115/60005)
6. **Saptarshi Ghosh** and Sarika Jalan (2016) *Emergence of Chimera in Multiplex Network*, Int. Journ. of Bifurc. and Chaos **26(07)**, 1650120 (DOI: 10.1142/S0218127416501200)

Other publications

7. Aradhana Singh, **Saptarshi Ghosh**, Sarika Jalan and Jürgen Kurths (2015) *Synchronization in delayed multiplex networks*, EPL **111**, 30010 (DOI: 10.1209/0295-5075/111/30010)
8. **Saptarshi Ghosh**, Sanjiv K. Dwivedi, Mikhail V. Ivanchenko and Sarika Jalan (2016) *Interplay of inhibition and multiplexing: Largest eigenvalue statistics*, EPL **115**, 10001 (DOI: 10.1209/0295-5075/115/10001)
9. Jakub Sawicki, **Saptarshi Ghosh**, Sarika Jalan and Anna Zakharova (2019) *Chimeras in Multiplex Networks: Interplay of Inter- and Intra-Layer Delays*, Frontiers in Applied Mathematics and Statistics **5**, 19 (DOI: 10.3389/fams.2019.00019)
10. Leonhard Schülen, **Saptarshi Ghosh**, Ajay Deep Kachhvah, Anna Zakharova and Sarika Jalan (2019) *Delay engineered solitary states in complex networks*, Chaos, Solitons & Fractals, **128**, 290-296 (DOI: 10.1016/j.chaos.2019.07.046).

Table of Contents

1	Introduction	1
1.1	Dynamical systems	3
1.1.1	Logistic Map	4
1.2	Networks	5
1.2.1	Regular Network	7
1.2.2	Random and Scale-Free networks	8
1.3	Dynamics on Networks	8
1.4	Synchronization	9
1.5	Chimera State	10
1.6	Multiplex and Multilayer Networks	11
1.7	Plan for the thesis	13
2	Emergence of chimera in multiplex network	17
2.1	Overview	17
2.2	Theoretical Framework	18
2.2.1	Dynamics on Networks	18
2.2.2	Chimera State	20
2.2.3	Identification of chimera state	21
2.2.4	Initial conditions	21
2.3	Results	22
2.3.1	Chimera in undelayed multiplex networks	22
2.3.2	chimera in delayed single-layer network	25
2.3.3	chimera in the delayed multiplex network: Role of symmetric intra-layer delay	27
2.3.4	Chimera in delayed multiplex network: Role of asymmetric intra-layer delay	30
2.4	Conclusion	33

3 Promoting chimera through non-identical multiplexing	37
3.1 Overview	37
3.2 Theoretical Framework	39
3.2.1 Construction of the network	39
3.2.2 Dynamics on the network	39
3.2.3 Identification of chimera state	40
3.3 Results	40
3.3.1 Chimeras in multiplex network with connectivity mismatch	40
3.3.2 Chimeras in multiplex network with architecture mismatch .	44
3.4 Conclusion	47
4 Enhancing chimera through inhibition	49
4.1 Overview	49
4.2 Theoretical Framework	51
4.2.1 Dynamics on Network	51
4.2.2 Introduction of inhibition (repulsive coupling)	51
4.2.3 Identification of chimera	52
4.3 Results	54
4.3.1 Multiplexing with a completely inhibitory (repulsively coupled) layer	54
4.3.2 Multiplexing with a partially inhibitory (repulsively coupled) layer	56
4.4 Conclusion	58
5 Engineering Chimera states	59
5.1 Overview	59
5.2 Theoretical Framework	60
5.2.1 Chimera state	60
5.2.2 Construction of networks	61
5.2.3 Dynamical evolution on networks	62
5.2.4 Delay driven engineering scheme	62
5.2.5 Spatial Inverse participation Ratio (sIPR): A measure for identification of chimera	63
5.3 Results	65
5.3.1 Engineering chimera state with heterogeneous delay in the single-layer network	65
5.3.2 Impact of the heterogeneous delay	69

5.3.3	Engineering chimera state with multiplexing-delays in the multiplex network	72
5.3.4	Role of the D_x & E_y parameters	75
5.3.5	Investigating the temporal behavior	78
5.3.6	Designing the incoherent region by multiplexing delays . . .	80
5.3.7	Designing the Chimera by multiplexing delays in Henon Map	80
5.4	Conclusions	81
6	Discussions and Future Scope	85
6.1	Summary	86
6.2	Future direction	88
Bibliography		90

List of Figures

1	Schematic diagram of a multiplex network consisting of two identical regular networks with left panel (LP) and right panel (RP) describing undelayed and delayed systems, respectively.	x
2	Schematic diagram depicting a multiplex network consisting of a regular network and (a) a regular network with different node degree (i.e., with different coupling range) and (b) a random network, respectively.	xi
3	Schematic diagram depicting a multiplex network consisting of two regular networks where the second layer is, (a) attractively coupled, (b) repulsively coupled with some probability, (c) all repulsively coupled.	xii
4	Schematic diagram of the proposed engineering scheme for designing the incoherent region (ICR) and, in turn, the chimera state in single layer (top panel; TP) and multiplex network (bottom panel; BP).	xiii
1.1	Schematic diagram depicting different types of coupling on a network. The left panel (LP) shows a network with all to all global coupling. The mid panel (MP) demonstrates a non-local coupling and the right panel (RP) describes the local coupling architecture. . .	5
1.2	Schematic diagram depicting a Regular network in left panel (LP); a Random network in mid panel (MP); and a Scale-Free network in right panel (RP).	9

1.3 Schematic diagram of a two-layer multiplex network consisting of two random networks. The connection among the nodes in a particular layer is represented by the solid lines and referred to as intra-layer edges. The connections among the mirror nodes in different layers is depicted by dashed lines and termed as inter-layer edges. . .	12
2.1 Schematic diagram of a multiplex network consisting of two identical regular networks. The left and right panel describes undelayed and delayed systems, respectively. $\tau_{l1}(\tau_{l2})$ signifies delay in intra-layer connections (represented as solid lines) and τ_{12} depicts delay in the inter layer connections of the multiplex network (represented as dashed lines).	20
2.2 Snapshots and spatio-temporal plots for multiplex network consisting of regular (S^1 ; ring) network layers. Coupling strength(ε) for the plots are as follows, (a,f) are for $\varepsilon = 0.1$; (b,g) are for $\varepsilon = 0.28$; (c,h) are for $\varepsilon = 0.30$, (d,i) are for $\varepsilon = 0.40$, (e,j) are for $\varepsilon = 0.44$. Number of nodes in each layer is $N = 100$ and coupling radius $r = 0.32$. Initial transient is taken as 5000 time units. The spatio-temporal plots are presented for time units in range 5000 to 5015. . .	23
2.3 Snapshots for (a) Three layer and (b) Four layer multiplex network where the layers are represented by identical regular networks. Parameters are $\varepsilon = 0.28$ and $r = 0.32$. Number of nodes is $N = 100$ for each layer.	24
2.4 Spatial entropy as a function of coupling strength (ε). Other parameters are the same as Fig. 2.2.	24
2.5 Distance measure for multiplex network consisting of regular (S^1 ; ring) network layers. Coupling strength (ε) for presented states are (a,c) with $\varepsilon = 0.44$ and (b,d) with $\varepsilon = 0.4$. Other parameters are same as Fig. 2.2.	25
2.6 Phase diagram showing different dynamical regions based on number of spatial clusters (N_{clus}) in parameter space of delay (τ) and coupling strength (ε) for single layer regular network. The shades (colors) denotes different regions: IS (incoherent state $N_{clus} = 0$), CS (coherent state $N_{clus} = 1$) and chimera (chimera state $N_{clus} > 1$). Other network parameters taken are $N = 100$ and $r = 0.32$. . .	27

- 2.11 Phase diagram and scatter diagram depicting different dynamical regions of the layers of multiplex network with different intra-layer delays. The shades (colors) in phase denotes different regions: IS (incoherent state $N_{clus} = 0$), CS (coherent state $N_{clus} = 1$) and chimera (chimera state $N_{clus} > 1$). (a,b) represents N_{clus} values for different values of delay in first layer where as (c,d) represents N_{clus} as a function of coupling strength (ε) with constant delay in second layer with (c; $\tau_{l2} = 1$) and (d; $\tau_{l2} = 2$). Other network parameters are same as Fig. 2.8. 32
- 2.12 Phase diagrams depicting different dynamical regions based on number of spatial clusters (N_{clus}) in parameter space of inter-layer delay (τ_{12}) and coupling strength (ε) for multiplex network consisting of regular network layers. The shades (colors) denotes different regions: IS (incoherent state $N_{clus} = 0$), CS (coherent state $N_{clus} = 1$) and chimera (chimera state $N_{clus} > 1$). (a) represents N_{clus} values in first layer whereas (b) represents N_{clus} in second layer with different inter-layer (τ_{12}) delay values. Other network parameters taken are $\tau_{l1} = \tau_{l2} = 0$, $N = 100$ and $r = 0.32$ 33
- 3.1 Schematic diagram depicting a multiplex network consisting of a regular network and (a) a regular network with different node degree (different value of non-local coupling range) and (b) random network, respectively. We use this multiplex architecture as modeled by Eq. (3.1). 38
- 3.2 Snapshots of the (a) single layer regular network ($\langle k \rangle = 30$) and (b) first layer of the regular-regular multiplex network with node degree $\langle k^{(1)} \rangle = 30$; $\langle k^{(2)} \rangle = 64$. Other parameters: $\varepsilon = 0.33$ and $N^{(1)} = N^{(2)} = 100$ 41
- 3.3 Snapshots of the first layer for a regular-regular multiplex network for coupling strength, (a,d,g) $\varepsilon = 0.33$; (b,e,h) $\varepsilon = 0.38$ and (c,f,i) $\varepsilon = 0.44$. The node degrees of the first layer is $\langle k^{(1)} \rangle = 20$. The node degree of the second layer is, (a,b,c) $\langle k^{(2)} \rangle = 10$; (d,e,f) $\langle k^{(2)} \rangle = 40$; (g,h,i) $\langle k^{(2)} \rangle = 64$, respectively. Other parameters: $N^{(1)} = N^{(2)} = 100$ 42

3.4	The normalized correlation measure g_0 , calculated for layer 1, is plotted in the parameter plane ($\langle k^{(1)} \rangle, \varepsilon$) for (a) regular-regular multiplex network with the same node degree in both layers ($\langle k^{(1)} \rangle = \langle k^{(2)} \rangle = \langle k \rangle$), (b) nonidentical regular-regular multiplex network where the second layer has the fixed node degree $\langle k^{(2)} \rangle = 64$. Note the chimera tongue around $\langle k^{(1)} \rangle = 64$ in (b). Parameters: $N^{(1)} = N^{(2)} = 100$ and $\delta = 0.01(\max(D))$ [100]; g_0 is averaged over 1000 time steps.	43
3.5	Correlation measure g_0 vs. ε for the first layer of a non-identical regular-regular multiplex network characterizing the chimera behavior in the sparse layer as a consequence of multiplexing. Node degrees: (a) $\langle k^{(1)} \rangle = 10, \langle k^{(2)} \rangle = 10$, (b) $\langle k^{(1)} \rangle = 10, \langle k^{(2)} \rangle = 64$, (c) $\langle k^{(1)} \rangle = 64, \langle k^{(2)} \rangle = 80$. Other parameters as in Fig. 3.4. The highlighted area indicates the parameter regime for chimera states.	44
3.6	Correlation measure g_0 vs ε for the homogeneous first layer of a (a) 1D-ER (b) 1D-SF multiplex network. Node degrees $\langle k^{(1)} \rangle = \langle k^{(2)} \rangle = 10$. Other parameters as in Fig. 3.4. Highlighted area indicates parameter regime for chimera states.	45
3.7	Map of regimes for a multiplex network consisting of one 1D layer and one inhomogeneous layer, where g_0 is calculated for layer 1: (a) 1D-ER multiplex networks and (b) 1D-SF multiplex network. The first layer has the node degree $\langle k^{(1)} \rangle = 10$. Other parameters as in Fig. 3.4.	46
4.1	Schematic diagram of multiplex network consisting of two layers. Each layer is represented by identical regular network (S^1 ring), where each node (open circle) has the same coupling architecture. In the second layer of the multiplex network, nodes are (a) attractively coupled, (b) repulsively coupled with probability p_{in} , (c) all repulsively coupled corresponding to $p_{in} = 1$. Inter layer connections between two layers are represented as dashed lines.	50

- 4.2 (a) Realization of the initial condition which is taken from a uniform random distribution multiplied by a Gaussian profile. The Gaussian is of the form $\theta_i(t = 0) = \exp[-30(\frac{i}{N} - \frac{1}{2})]$. Same initial condition is considered for both the layers of regular - regular multiplex network, (b) Snapshot of spatial phase profile of kuramoto oscillators of the first layer of the multiplex network consisting of two attractively coupled layers, (c) Laplacian distance measure $|\bar{D}|$ of the spatial phase profile (d) normalized probability distribution function $g(|\bar{D}|)$ of the Laplacian distance measure $|\bar{D}|$. Parameters: Network size $N = N^1 = N^2 = 100$, node degree $\langle k^1 \rangle = \langle k^2 \rangle = 64$, coupling strength $\lambda = 1.29$, natural frequency $\omega = 0.5$ and lag parameter $\alpha = 1.45$ 53
- 4.3 Normalized probability distribution function $g(|\bar{D}|)$ for the Laplacian distance measure $|\bar{D}|$ of the first layer of the regular-regular multiplex network consisting of (a) two positive layers, and (b) positive-negative layers. Parameters: Network size $N = N^1 = N^2 = 100$, node degree $\langle k^1 \rangle = \langle k^2 \rangle = 64$, natural frequency $\omega = 0.5$ and lag parameter $\alpha = 1.45$ 55
- 4.4 Snapshots and spatio-temporal patterns depicting emergence of chimera in positive layer upon multiplexing with a negative layer. The regular-regular multiplex network consists of (a,c,e,g) two positively coupled layer, (b,d,f,h) positively and negatively couples layers. (a,b,c,d) presents a snapshot of the spatio-temporal patterns presented in (e,f,g,h) respectively. The figures represents emergence of chimera in case of multiplexing with negative layer at coupling strength $\lambda = 1.86$ (a,b) and at $\lambda = 3.7$ (c,d). Other parameters are same as Fig. 4.3 . . . 56
- 4.5 (a) Plot of the adjacency matrix of regular-regular multiplex network consisting of one positive and one inhibitory layer with inhibition probability $p_{in} = 0.1$. The black lines in the down-right block represents the rows corresponding to inhibitory nodes. (b) Normalized probability distribution function $g(|\bar{D}|)$ of the Laplacian distance measure $|\bar{D}|$ of the positive layer as a function of inhibition probability p_{in} . Inset: Snapshot and spatio-temporal profile of the first layer of a multiplex network consisting of one positive layer and one inhibitory layer. Parameters: Coupling strength $\lambda = 3.57$, Inhibition probability $p_{in} = 0.1$, Other parameters are same as Fig. 4.3. 57

- 5.1 Schematic diagram of the proposed engineering scheme for designing the incoherent region (ICR) and, in turn, the chimera state in single layer (upper panel; UP) and multiplex network (lower panel; LP). Parameters are $N = 100$, $\langle k \rangle = 64$ for both single-layer network and for individual layers of the multiplex network. 63
- 5.2 Diagrams representing (b)-(e) snapshots of the state variable (x_i) and (f)-(i) Laplacian distance variable (d_i), respectively, for different dynamical states for the regular network (S^1 ring) corresponding to various sIPR values as mentioned; [(b) and (f)] for $\varepsilon = 0.1$ and sIPR = 0.029, [(c) and (g)] for $\varepsilon = 0.34$ and sIPR = 0.048, [(d) and (h)] $\varepsilon = 0.4$ and sIPR = 0.25, [(e) and (i)] $\varepsilon = 0.76$ with sIPR = 0.015, where ε is the coupling strength as mentioned Eq.5.3 and coupling matrix as $C = \varepsilon A$. Other parameters are same as Fig.5.1. . . 64
- 5.3 Delay matrices and corresponding snapshots of chimera state engineered by heterogeneously distributed delays. The delay matrices are overlapped with the adjacency matrices to showcase both the delayed and the undelayed edges. (a) & (c) Regular network with a large and relatively smaller cluster of the delayed nodes, respectively. These delay configurations result in a large ICR denoted in (b) and a smaller ICR in (d). (e) & (f) Delay configuration and a corresponding snapshot of a chimera state, respectively, with different locations of the ICR. Note due to the S^1 symmetry of the regular ring lattice, the positions are not unique. (b), (d), & (f) correspond to schematic diagram Fig. 5.1 UP(a), and (g) and (h) represent two delayed clusters resulting in the multi-chimera state, corresponding to the schematic diagram Fig. 5.1 UP(b). The (green) boxes represent clusters of the delayed nodes introduced in the network. Other parameters are $\varepsilon = 0.77$, $\tau_{max} = 10$ and rest are same as Fig. 5.1. . . 66
- 5.4 Snapshots of the dynamical state of the regular network for different delay configurations with (a) being no delay configuration, (b) being homogeneous delay ($\tau = 1$) case, (c) being heterogeneous distributed delays case ($\tau_{max} = 10$). Note that the typical spatial profile for chimera state is visible for (c). Other Parameters are $\varepsilon = 0.61$ and rest are same as Fig. 5.1 68

5.10	A schematic phase diagram of D_x - E_y space for (a) layer 1 and (b) layer 2 with undelayed inter-layer edges and (c) layer 1 and (d) layer 2 with delayed inter-layer edges. Half of the inter-layers edges are heterogeneously delayed (in c & d), and the delay values are chosen from a uniform random distribution with $\tau_{max} = 20$. The parameters are the same as Fig. 5.7. The boundaries of various regions are drawn from visual inspection and measures (See SM [132]).	77
5.11	Time series of nodes connected with delayed and undelayed inter-layer edges along with a diagram of a multiplex network consisting of two identical regular network layers. Half of the interlayer edges are heterogeneously delayed (represented by Bold blue lines). Appropriate networking parameters ($D_x = 5$, $E_y = 0.2$) are used to induce chimera in the second layer. Region I (Shaded pink circle) consists of nodes connected with delayed edges and shown to have an incoherent time evolution in the middle panel, whereas the nodes of region II (connected to undelayed edges) are shown to have coherent evolution in the rightmost panel. Together, they display a chimera pattern, as shown in Fig. 5.7(c). Other parameters are the same as in Fig.5.7.	79
5.12	(Color online) Snapshots of both the layers of the multiplex network where (a) 20% and (b) 80% inter-layer edges are heterogeneously delayed. The network parameters are $D_x = 5$, $E_y = 0.2$. Other parameters are the same as described in Fig.5.7.	80
5.13	(Color online) Snapshot profiles of the two layers of the considered multiplex network for (a) the undelayed interlayer links, (b) the delayed interlayer links with parameters $D_x = 5$, $E_y = 0.6$. The local dynamics is described by henon map (Eq. 5.6) with parameters, $\alpha = 1.4$ and $\beta = 0.3$, $\varepsilon = 0.9$, $\tau_{max} = 20$, $r = 0.32$, $N = 100$ in each layer.	81

List of Tables

- 2.1 Critical coupling strengths for different delay values in the layers of multiplex network. upper and lower triangles represent $\varepsilon_{critical}$ for layer 1 and layer 2, respectively. Other network parameters for each layer of the multiplex network are $N = 100$ and $r = 0.32$ 34

Chapter 1

Introduction

In Greek mythology, the chimera was a fire-breathing hybrid monster from Lycia in Asia Minor, usually depicted with the body of a lion, and the head of a goat protruding from its back, and a tail with a snake's head [1]. Since then, the word “chimera” has come to refer anything comprising of disparate parts. Chimera is introduced to the study of dynamics on coupled non-linear systems through a symmetry-breaking Spatio-temporal phenomenon, comprising of different groups of constituent elements of the underlying system, exhibiting distinctly disparate dynamics [2, 3]. The mechanisms for the appearance of chimera in a multi-layered coupled systems and exploration of different system parameters controlling its emergence and design form the core of the work presented in the thesis.

The study of dynamical systems on interacting entities, represented as networks describe the foundation of the present work. The concept of the dynamical systems theory has its roots in Newtonian Mechanics where Newton and Leibniz developed the calculus to describe the motion and trajectories of celestial bodies through coupled differential equations [4]. Furthermore, the coupling architecture describing the interaction among basic entities initiated the field of Network Science. The

concept of networks describing the interaction patterns originated from the famous work on Seven Bridges of Königsberg by Leonhard Euler in 1735 [6]. His depiction of the constituent entities as vertices (nodes) and interactions as edges (links) lay the foundations of Graph Theory [7]. Owing to the nearly exponential growth of the computational power and availability of the colossal amount of information to the masses in the late twentieth century, the graph theory evolved into modern network science penetrating entire spectrum of science and technology [8]. The present-day aim of the study of dynamics on networks is in providing insight into the qualitative and quantitative behavior of a complex system ranging from as small as cells in our body to as big as celestial bodies in the galaxy, framed through a combined mathematical framework of coupled differential equations [9, 10].

Among diverse aspects of dynamics on networks, the study of synchronization narrates one of the great success stories of network science and dynamical systems theory [11]. The term “Synchronization” refers to the coordination of multiple events to operate a system in unison. In 1665, Christiaan Huygens first reported the tendency of two pendulums, mounted to a common wall, to exhibit synchronized motion [12, 13]. Later on, Famous Works by Wiener [14], Winfree [15], Kuramoto [16] and Crawford [17] laid the foundations of the Synchronization theory. In 1990s Steven Strogatz presented a general approach to understanding the coupled dynamical systems and popularized the synchronization phenomenon, attracting a tremendous amount of work done in the field in subsequent years [18]. Presently synchronization is known as one of the cornerstones of network science successfully providing insight into a diverse range of subjects ranging from Physics to Biology to Social Science and many more [19].

Furthermore, at the dawn of 21st century, a massive outburst in technological advancements in all the fields of science bough a massive influx of data pertaining to various natural and artificial complex systems, providing new insights and presenting new challenges to the existing theoretical frameworks. The emergence of partial synchronization patterns of chimera state, which is found to be more frequent in natural systems [20], is one of such directions that recently added a new dimension to

the study of coupled dynamics on the Networks. The thesis aims at providing new insights into the emergence of chimera state utilizing a new multi-layered approach to network science.

In the following, we present a brief sketch of the dynamical systems theory followed by an account of key concepts of the networks science. Next, combining both dynamical systems and networks, we show the mathematical framework for the collective dynamics on networks and synchronization. Next, we add a brief background on the research pertaining to chimera state and multiplex networks. In the final section, we discuss the motivation behind this thesis and append a reader's guide to the thesis for ease of reading.

1.1 Dynamical systems

The theory to describe dynamics of a system is at heart, a collection of differential equations that governs the temporal evolution (or dynamics) of the state of the system of interest [4, 5, 21, 22]. **State Variables** describe a set of dynamically changing quantities that are required to completely describe the system under consideration (for example, position and velocities of a particle). **System's Parameters** are the quantities that remain constant when the state variables evolve dynamically (for example, mass or charge of a particle). A set of **differential equation** presents how the state variables change in time as a function of the current state and the systems parameters (for example, Newton's second law of motion). If n state variables are required to describe a system of interest, then the state of the system can be denoted by a vector $\mathbf{Z}_{n \times 1} \in \mathbb{R}^n$. Considering time t as a continuous variable and the system's parameter as μ , a set of n first-order differential equations describing the temporal evolution of the state or more precisely, the dynamics of the system can be written symbolically as

$$\frac{d\mathbf{Z}}{dt} = \mathcal{F}(\mathbf{Z}, \mu, t) \quad (1.1)$$

Where the function \mathcal{F} depict the evolution of different variables. In some cases, time t can be treated as a discrete variable, and in such situations, the dynamics of the system can be described as difference equations or maps, expressed as

$$\mathbf{z}^{t+1} = \mathcal{F}(\mathbf{z}^t, \mu, t), \quad t \in \mathbb{Z} \quad (1.2)$$

Note that, the function $\mathcal{F} : \mathbb{R}^n \mapsto \mathbb{R}^n$ is a vector function of the state variables $\mathbf{z} = (z_1, z_2, \dots, z_n)^T$ with suitable intrinsic time dependence. Given an initial state, the differential equation (or map in time-discrete case) can calculate the state of the system at any point of time depending on the nature of the function \mathcal{F} [23]. In case of a deterministic system, the function \mathcal{F} can be written explicitly, and a fixed initial condition will always lead to the same output state at a given time point. In case of a chaotic system, the function \mathcal{F} is deterministic, but a slight perturbation in the initial state will diverge exponentially leading to random appearing output state in large time scales. A stochastic function \mathcal{F} have build-in randomness and will always produce random output states given an initial state. In this thesis, we primarily have used the time-discrete logistic map in the chaotic regime to study the dynamics of the underlying system [24].

1.1.1 Logistic Map

In 1976, Sir Robert May presented a simplistic mathematical model to describe the growth of biological population, which can be depicted as a time-discrete map written as following [25]

$$\begin{aligned} z^{t+1} &= f(z^t, \mu) \quad z^t \in \mathbb{R} \\ &= \mu z^t (1 - z^t) \end{aligned} \quad (1.3)$$

where the state variable z^t denotes a population at time t , and z^{t+1} the same one year later. μ represents the system's parameter (also known as bifurcation parameter) denoting the rate of growth. This model is known as the non-linear logistic difference equation or logistic map, which is very simple yet demonstrate very complex

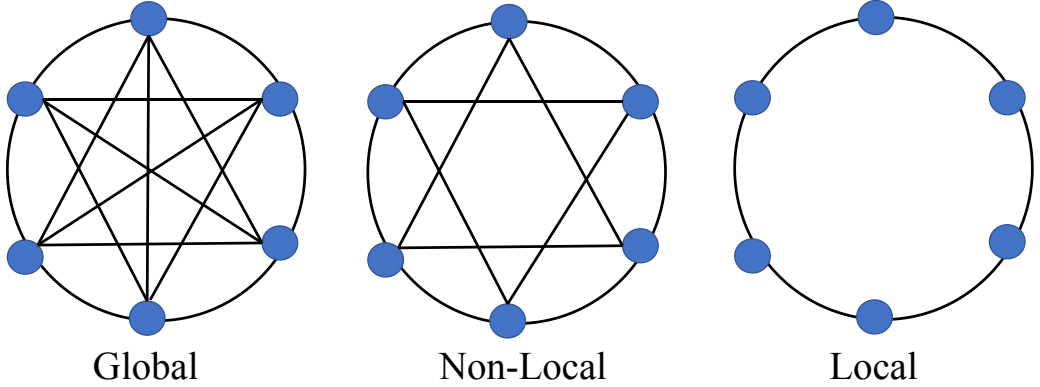


Figure 1.1: Schematic diagram depicting different types of coupling on a network. The left panel (LP) shows a network with all to all global coupling. The mid panel (MP) demonstrates a non-local coupling and the right panel (RP) describes the local coupling architecture.

dynamical phenomena. Here the state variable z or the population is treated as a fraction of maximum population between zero and one representing, extinction and the maximum population, respectively ($z \in (0, 1)$). The logistic map shows chaotic behavior for a particular range of the parameter μ [26], which is used throughout the thesis.

1.2 Networks

In the previous section, the dynamics of a system is narrated in terms of a set of uncoupled differential equations, depicting the time evolution of the state variables of the system. However, natural systems rarely evolve in an isolated fashion. The constituent entities of the system often interact with each other, demonstrating a collective output which may be quite dissimilar to the output state resulted from temporal evolution of isolated entities. Therein lays the core concept of networks which describe the constituent entities as vertices (nodes) and the interactions among them as edges (links). Thus, a network is a collection of vertices and edges, collectively showcasing the entire coupling architecture of the system. Mathematically networks are described in terms of graphs [8]. A graph (or network) is depicted by an ordered pair of sets $\mathcal{G} = (\mathcal{V}, \mathcal{E})$, where $\mathcal{V} = \{v_1, v_2, \dots, v_N\}$ and $\mathcal{E} = \{e_1, e_2, \dots, e_M\}$ repre-

sent the sets of vertices and edges, where N and M denote the size of the sets \mathcal{V} and \mathcal{E} , respectively. The graph (or network) \mathcal{G} posses N number of vertices, connected by M number of edges. The network also can be presented in terms of an adjacency matrix (A), corresponding to the graph \mathcal{G} such that the elements of the matrix are defined as $a_{ij} = 1$ if i^{th} and j^{th} nodes are connected and $a_{ij} = 0$, otherwise. Note that, We have considered simple (no self-loop and no multiple edges between the same pair of nodes), connected (no set of nodes exist which are disconnected from the rest of the network) and undirected (all the edges in the network are bi-directional) network in the thesis unless specified otherwise.

Here, we furthermore describe some key terms related to the networks that have been used throughout the thesis.

- *Node Degree.* Degree of a node is defined as the number of edges which are incident on that particular node. Mathematically, degree of a node, i , is denoted by $k_i = \sum_{j=1}^N a_{ij}$. Furthermore, the average degree of a network ($\langle k \rangle = \frac{1}{N} \sum_{i=1}^N k_i$) is defined as the average of all degrees of the nodes in the network. Additionally, a degree distribution ($P(k)$) denotes the probability distribution of all degrees of the nodes in the network. The degree distribution curve $P(k)$, in turn, describe the probability that a randomly selected node will have a degree k .
- *Global and Local Coupling.* Global coupling (Fig. 1.1 LP) refers to a case where all the nodes are connected with all other nodes of the network formulating an all to all coupling architecture. Therefore, global coupling will have a node degree of $N - 1$ (ignoring the self-connection) for a network consisting of N nodes (Degree 5 for $N = 6$ in Fig. 1.1, LP). In comparison, a purely local coupling (Fig. 1.1, RP) refers to a situation when all nodes possess connections only with their nearest neighbors.
- *Non-Local Coupling.* In general, non-local coupling (Fig. 1.1, MP) refers to an intermediate stage between global or purely local coupling architecture where the nodes are connected to some of the other nodes of the network.

Most of the natural system possess such kind of connection architecture. The chimera state had initially been demonstrated for a non-locally coupled network [2, 3].

- *Delayed coupling.* Due to the finite speed of information transmission, delay naturally arises between the transmission ends (nodes) connected through links (edges). Therefore, a delayed system possessing delayed edges portray a more realistic model of the natural systems. The time-delayed coupling (incorporating time delay τ) can be generally written as $\dot{\mathcal{Z}} = \mathcal{F}(\mathcal{Z}^t, \mathcal{Z}^{t-\tau}, \mu)$ [27] and discussed in details in the subsequent chapters of the thesis.

Now, depending on the connectivity patterns, a network can have different types of connection architectures [8–10], among which we describe two in the following, which is relevant to our work presented in the thesis.

1.2.1 Regular Network

A Regular network posses a special type of connection architecture where all the nodes have same node degree ($\langle k \rangle = k_i, \forall i = k$) (Fig. 1.2, LP). A regular network of N nodes can have a global coupling with all nodes having node degree $k = N - 1$ (without self-loop) (Fig. 1.1, LP) or a purely local coupling with all nodes having node degree $k = 2$ (Fig. 1.1, RP). A non-locally coupled regular network can have nodes with only even node degrees between $2 < k < N - 1$. Therefore, considering $k = 2P$ node degree for all the nodes in a regular network, where P denotes the number of neighbors on each direction (clockwise or anti-clockwise), P will have a range of $1 < P < (N - 1)/2$ for a non-locally coupled regular network. For ease of depiction, we further denote the node degree of a regular network by coupling radius r defined as $r = k/2N = P/N$. Due to the symmetry of the regular network, it also referred to as S^1 or ring network [2, 3] and used so, in the subsequent chapters of the thesis.

1.2.2 Random and Scale-Free networks

Unlike the regular network with same degrees for all nodes, a random network (Fig. 1.2, MP) possess a random connection architecture where all the edges are drawn with a particular probability. Starting with a set of isolated nodes, a random network is formed by adding edges between the nodes with a probability p . In the thesis, we use the famous “Erdős - Rényi” (ER) random network [28] which considers equal probability p for all introduced edges, resulting in a Poisson’s degree distribution. An ER random network is constructed by considering with isolated set of N nodes and then by connecting every pair of nodes with probability p . It creates a network with approximately $M = p\frac{N(N-1)}{2}$ edges distributed randomly among the nodes of the network. A Scale-Free network(Fig. 1.2, RP) is referred to as a network with a power-law degree distribution, characterized by a large number of low degree nodes and a small number of high degree nodes. The famous Barabási - Albert model [29] describes the characteristic power-law degree distribution as $P(k) = k^{-\lambda}$ where the exponent λ typically lies in the range $2 < \lambda < 3$. These networks are constructed by considering a small number of connected nodes and adding a new node with a constant number of edges to be connected to the existing nodes. The incoming node connects with other nodes according to the preferential attachment model, which describe that the nodes having a higher degree will have a higher probability to connect to the incoming nodes. The Scale Free nature has been found in a diverse range of real-world networks, making it one of the most successful models in network science.

1.3 Dynamics on Networks

The dynamics of a system describes the temporal evolution of the elements of a system, whereas, a network describes the interaction patterns among the elements of the system. Combining both the aspects of the network architecture and the governing equation for local temporal evolution, the collective dynamics of the whole

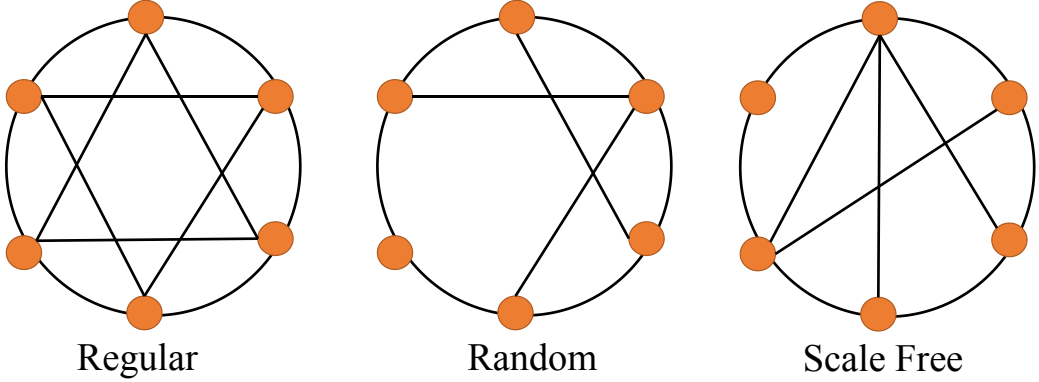


Figure 1.2: Schematic diagram depicting a Regular network in left panel (LP); a Random network in mid panel (MP); and a Scale-Free network in right panel (RP).

network can mathematically be represented as [30]

$$z_i^{t+1} = f(z_i^t, \mu) + \varepsilon \sum_j A_{ij} \mathcal{H}(z_j^t, \mu) \quad (1.4)$$

where f denotes the contribution from local temporal evolution of individual node, i and \mathcal{H} depicts the influences from its neighbors, coupled through the adjacency matrix A , representing the coupling architecture of the network. ε showcase the coupling strength of the connections among the nodes. This general framework is used throughout the thesis to present the study of the dynamics on networks.

1.4 Synchronization

Synchronization refers to an emergent phenomenon where coupled entities adjust their dynamical behavior in such a way that they collectively exhibit common dynamics [11, 19]. The generalized synchronization corresponds to a case where the state variables associated with the elements possess a functional correlation among them i.e. when a function Ψ can be defined such that $z_i^t = \Psi(z_j^t); \forall t \geq 0, \forall i, j \in N$. Depending on the system's parameters, complete synchronization can also be observed for coupled systems where all the state variables have identical values, i.e., the case where $\Psi(z_j^t) = z_j^t$. Moreover, coupled dynamical systems can also exhibit Phase synchronization, lag synchronization, cluster synchronization, and more im-

portantly, partial synchronization, which is the focus of this thesis [19, 30].

1.5 Chimera State

A dynamical system comprising of identically coupled elements is naturally expected to make the transition from an asynchronous state to a synchronous state, depending on the system's parameters. One would expect such a system to exhibit complete synchronization for a suitable choice of system's parameters as all the elements experience uniform coupling environment. In 2002, Kuramoto & Battogtokh reported a peculiar state with co-existing asynchronous and synchronous domain in a network of identical elements under some special conditions [2]. In 2004, Abrams & Strogatz christened this state as a chimera and provided a firm understanding over its emergence [3]. The discovery of this intriguing dynamical state has recently attracted considerable attention due to both its fundamental significance as well as its new-found applicabilities to the different fields [5, 31, 32] including neuroscience [20, 33].

Initially, the investigation pertaining to the chimera state is primarily restricted to the phase oscillators [2, 3] arranged on a regular network with identical coupling architecture but later they had been reported for a variety of different systems including non-identical networks [34], time-varying networks [35], 2D and 3D lattices [36–40], bi-partite networks [41], modular networks [42], inhibitory networks [43] and many others. It has been reported using various dynamical models including neural [20, 33], planar [44], Stuart-landau [48, 49], Van der Pol [50], chaotic oscillators [51], and for the time-discrete maps [52–54] as well. It has recently been extended to quantum oscillators [55, 56]. Although chimeras was initially reported for non-local, non-global coupling [2, 3], it have also been demonstrated for purely local[57] as well as globally [49, 58] coupled networks.

Various types of chimeras have been reported in the literature, including multi-cluster [59, 60], breathing chimeras [62], delayed-feedback chimeras [61] and globally clustered chimera [64]. There have been persistent efforts to gain a more in-

depth insight into analyzing and controlling [65–67] chimera states which also been realized recently through application of heterogenous delays [68, 69]. Experimentally, chimeras have been demonstrated for optical [70], chemical [45, 46], mechanical [47], electronic [71] and electro-chemical oscillators [72, 73], superconducting metamaterials [74, 75].

Furthermore, the chimera state has been closely related to various biological processes ranging from uni-hemispheric sleep in mammals [31, 76, 77] to cognitive process [20] in human brain networks. Hybrid dynamics of chimera state also has been reported to emerge in neural networks of two well-studied, Cat [79] and C Elegans [78] Brain networks. Studies on the synchronization in epileptic seizures indicated a huge collapse of synchronization just before high coherence event of the seizure [80]. Recently, observation of chimeric patterns has been reported at the onset of the transition to a seizure state in epilepsy [81, 82]. All the investigations indicate that chimera state with its co-existing synchronous and asynchronous activities play a significant role in neural dynamics [38, 40] and present a great candidate to develop understanding in neural systems [83]. Moreover, the chimera-like state has also been reported in other biological systems like neural “bump” states [84], the cardiac rhythms in ventricular fibrillation [85] as well as social systems [86].

The chimera state provides a powerful tool to study the dynamical path from asynchrony to complete synchrony and has amassed considerable works literature owing to its exotic nature and its appearance in various natural systems. We devote this thesis to the study of the chimera state and add a new dimension to the field by investigating its appearance in multi-layer complex systems.

1.6 Multiplex and Multilayer Networks

The theory of network science has been tremendously successful in describing the intricate interaction patterns among the constituent entities of a complex system. However, the interactions among the constituents are primarily considered to be of the same type until now, which is not right for most of the cases of real-world net-

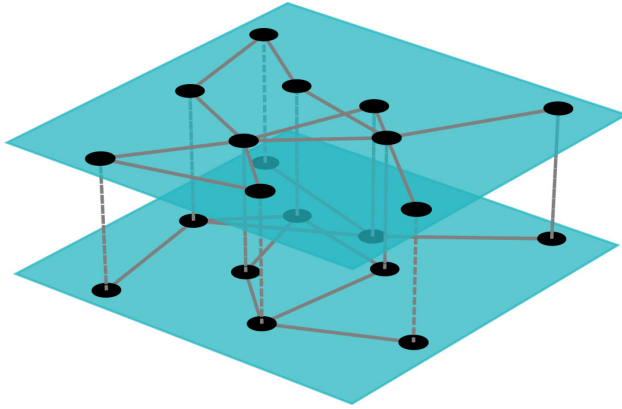


Figure 1.3: Schematic diagram of a two-layer multiplex network consisting of two random networks. The connection among the nodes in a particular layer is represented by the solid lines and referred to as intra-layer edges. The connections among the mirror nodes in different layers is depicted by dashed lines and termed as inter-layer edges.

works. For example, two geographical regions may be connected through Air or Train or Buses depending on their distance or two people may have different types of relations (academic or friendship or business-related) between them. A single layer network representation of these systems (transport and social, respectively) provide an incomplete model to understand the underlying dynamics of these systems. Recent advancements in data accusations for real-world systems, made it possible to incorporate multiple types of interactions, leading to the incorporation of the multiplex network framework [87].

The multiplex approach to network science which incorporates the existence of various types of interactions (edges) between the same pair of entities (nodes) by categorizing them in different layers with each layer reflecting a specific type of interaction, provide a more realistic portrayal of real-world complex systems [88–91]. As in the case of previous examples, the transportation network may be considered as a multiplex network where each layer depict a particular mode of transportation or the social network where each layer may represent a particular type (academic or friendship or business) of the relationship among the people [87].

Mathematically, the adjacency matrix representation of a multiplex network (\mathcal{A}) consisting of m layers can be expressed as [54, 87]

$$\mathcal{A} = \begin{pmatrix} A^1 & I & . & . & . & I \\ I & A^2 & I & . & . & I \\ . & I & A^3 & . & . & . \\ . & . & . & . & . & . \\ . & . & . & . & . & . \\ I & . & . & . & . & A^m \end{pmatrix}, \quad (1.5)$$

Where the layers are encoded by a set of adjacency matrices $\{A^1, A^2, \dots, A^m\}$. The unit matrices I denote one to one connection between the mirror nodes across layers of the multiplex network. This particular setup is termed as the multiplex network where both the layers possess same number of nodes and all the mirror nodes are connected across different layers. A general form of the multiplex networks is referred to as multi-layer network where different layers might possess different number of nodes leading to one to many connections across layers [87, 92]. However, we have considered a simple multiplex network in subsequent chapters to showcase the thesis works.

The inclusion of multiplex framework presents a wide variety of novel dynamical phenomena, which is impossible to emerge in single-layer networks [34, 53], which lead to the investigations that are presented in this thesis.

1.7 Plan for the thesis

This thesis embraces the multi-layer approach to network science and explores the coupled dynamics on multiplex networks. The main focus of the thesis is to investigate the emergence of chimera state in multiplex networks and study the enhanced or suppressed appearance of chimera state under different factors which play a crucial role in its emergence. The thesis is divided into five chapters other than the introduction.

Chapter 2 reports the emergence of the chimera state in the multiplex networks consisting of two identical regular networks and presented the required conditions

for its emergence. It furthermore provides a treatise on the behavior of chimera state in a multiplex network under homogeneous delay coupled dynamics. A constant system-wide delay is considered in intra- and inter-layer edges of the multiplex network and the enhanced or suppressed appearance chimera state is demonstrated under different values and parity of the delay values. A complete table is presented considering all combinations of inter and intra-layers delays with corresponding critical coupling strengths (coupling strength required for the transition from chimera to coherent state). Furthermore, a layer-chimera state is also showcased, which is unique to the multiplex networks.

Chapter 3 is devoted to finding the parameter regime for which chimera appears in a multiplex network where the layers of the multiplex network are not identical. Specifically, two cases are considered where (I) two-layer posses a mismatch in connection densities keeping the regular network architecture same in both the layers and (II), two layers have a connection architecture mismatch, i.e., one layer has a regular and other layer has a non-regular connection architecture. We presented a systematic study of the entire parameter space and shown and enhanced the appearance of chimera state arising due to the non-identical multiplexing.

Chapter 4 describes the appearance of chimera state a layer of the multiplex network in the presence of inhibitory or repulsive coupling in another layer. The investigation presents the destruction of synchronized regime and arises of chimera state due to the presence of inhibition, even in a small amount in the multiplexed layer.

Chapter 5 puts forward a technique to engineer chimera state in both single-layer and multiplex networks by heterogeneous delays, suitably placed in sequence in intra- and inter-layer edges, respectively. The technique is shown to exert complete control over the position and the extent of the incoherent region and thus, in turn, the chimera state. Additionally, inter- and intra-layer coupling strengths are demonstrated to have complete regulatory control over the emergence of the incoherence regions of the chimera state in the multiplex network case.

Finally, Chapter 6 summarizes of the works included in the thesis and discuss the possible scopes of future research as an extension of the studies discussed here.

So briefly, the chapters of the thesis are as follows:

- Chapter 2: Demonstration of the emergence of *chimera states in multiplex networks* and description of the *impact of delay* on chimera state in the multiplex network.
- Chapter 3: Investigation on the enhanced appearance of chimera state in *a multiplex network consisting of non-identical layers*.
- Chapter 4: Study on the *impact of inhibition* on the appearance of chimera state in multiplex networks.
- Chapter 5: Presentation of a novel recipe to *engineer chimera state* in single layer and multiplex network with the aid of *heterogeneous delays in sequential intra- and inter-layer edges*, respectively.
- Chapter 6: Summary of the thesis and discussion on the future scope of the thesis research.

Chapter 2

Emergence of chimera in multiplex network

2.1 Overview

This study demonstrates the emergence of the chimera state in a multiplex network and presents the role of inter- and intra-layer delay on the enhanced or suppressed appearance of chimera state. Complex systems, found in the world around us, often exhibit novel emergent phenomena which are impossible to decipher without a wholistic multi-layer approach [87]. In Chapter 1, we have described the importance of incorporation of multi-layer network framework while investigating coupled dynamics on networks. Adding to that, in this chapter, we explore the impact of delayed interaction among nodes of the network on the collective dynamical behavior, especially on the emergence of a chimera state. Due to the finite speed of information transmission, delay naturally arises between the transmission ends (nodes) connected through channels (edges) in complex systems. An analysis of the impact of time delay on dynamical properties of a coupled system is therefore very crucial to predict and explain the dynamic evolution of such systems [27].

Numerous dynamical phenomena, including enhancement or suppression of synchronization, have been found for time-delayed networks [93, 94]. Although it has been recently shown that chimera states exist in time-delayed networks [41, 61, 64], the occurrence of this complex spatio-temporal pattern is yet not well understood in the presence of time delay in multiplex networks.

In this chapter, we first demonstrate the emergence of the chimera state in multiplex networks. We show that while multiplexing two layers do not change the type of the chimera state and retain the multi-chimera state displayed by the single-layer networks, it changes the regions of the incoherence. Furthermore, we show the role of the interplay of the delay and the multiplexing on the occurrence of a chimera state. We find that small delays lead to enhancement or suppression in the range of parameters for which chimera state appears, depending upon the parity of the delay value, and large delays always lead to the suppression in the range of parameters for which the chimera state appears. The parity of delay value denotes the odd/even nature of the numerical value assigned as delay, which plays an important role in the enhancement and the suppression of range of the parameters, displaying chimera state. In multiplex networks, this enhancement or suppression depends upon the distribution of delay in the individual layers, which further results in a new type of chimera state, henceforth called as *layer chimera state*. The *layer chimera state* exhibit the existence of one layer showing coherent and another layer demonstrating incoherent dynamical evolution, which is unique to the delayed multiplex systems. Therefore, this chapter encompasses the emergence of the chimera state and its dependence on the delay on the multiplex network.

2.2 Theoretical Framework

2.2.1 Dynamics on Networks

We again describe the governing equations for investigating dynamics on the networks in context of multiplex networks having both delayed and undelayed edges. To showcase our findings, we consider a multiplex network (\mathcal{A}) of $2N$ nodes where each layer is represented by a regular network (S^1 ; ring) consisting of N nodes

(Fig. 4.1). The dynamical state of the nodes of the network at time t can be represented by a real variable $z_i^t \in \mathbb{R}, \forall i = 1, \dots, 2N$. The local dynamics of the nodes is realized as the famous logistic map $z_i^{t+1} = z_i^t(1 - z_i^t)$ in chaotic regime ($\mu = 4.0$) [26]. This simple model, which has the ability to display complex chaotic behavior, have been widely investigated to understand various complex phenomena manifested by a diverse range of real-world systems [19, 95]. Adding the network architecture, the dynamical evolution equation for the whole network can be written as [53, 54]

$$z_i^{t+1} = f(z_i^t) + \frac{\varepsilon}{(k_i)} \sum_{j=1}^{2N} \mathcal{A}_{ij} [f(z_j^t) - f(z_i^t)] \quad (2.1)$$

Where ε represents the overall coupling strength ($0 \leq \varepsilon \leq 1$) and $k_i = (\sum_{j=1}^{2N} \mathcal{A}_{ij})$ is the normalizing factor. The function $f(z^t)$ is the logistic map described above. The regular networks considered in the individual layers possess the coupling radius $r = 0.32$, where r represents the coupling radius defined by $r = \frac{P}{N}$, with P signifying the number of neighbors in each direction in a layer. Therefore, the node degree of the regular network considered in the individual layers is $2P = 2rN = 64$.

The adjacency matrix (\mathcal{A}) of the multiplex network with two layers (encoded by a set of adjacency matrices $\{A^1, A^2\}$) can be expressed as [54]

$$\mathcal{A} = \begin{pmatrix} A^1 & I \\ I & A^2 \end{pmatrix}, \quad (2.2)$$

The adjacency matrix of the s^{th} layer is described by $(A^s, s = 1, 2)$ where each element is defined as $A_{ij}^s = 1(0)$ depending upon whether i^{th} and j^{th} nodes are connected (or not) in the s^{th} layer. The matrix A^s is a symmetric matrix with diagonal entries $A_{ii}^s = 0$ depicting no self-connection. I is a unit $N \times N$ matrix representing one to one connection between the mirror nodes across layers of the multiplex network. We consider bi-directional inter-layer connections which maintain symmetric coupling environment required for defining a chimera state. We further describe the equation governing the temporal evolution, incorporating the time delay τ as [53]

$$z_i^{t+1} = f(z_i^t) + \frac{\varepsilon}{(k_i)} \sum_{j=1}^N \mathcal{A}_{ij} [f(z_j^{t-\tau}) - f(z_i^t)] \quad (2.3)$$

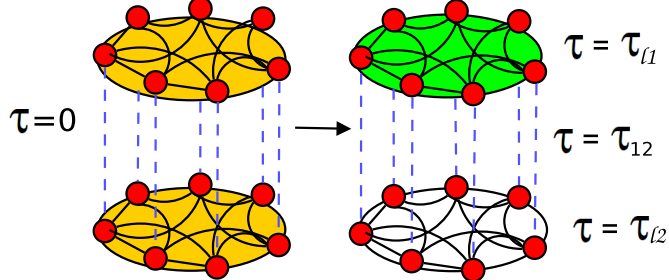


Figure 2.1: Schematic diagram of a multiplex network consisting of two identical regular networks. The left and right panel describes undelayed and delayed systems, respectively. $\tau_{l1}(\tau_{l2})$ signifies delay in intra-layer connections (represented as solid lines) and τ_{l12} depicts delay in the inter layer connections of the multiplex network (represented as dashed lines).

Note that, we have considered a constant delay value τ which is applied to all the edges in the network. Further, we have denoted τ_{l1} and τ_{l2} as the intra-layer delays for first and second layer, respectively. τ_{l12} is used for delay, applied to all inter-layer edges. Fig.2.1 present a schematic description of the arrangement for ease of reading.

2.2.2 Chimera State

Chimera is defined as a hybrid dynamics consisting of a coherent and incoherent state. The dynamical state of the network (represented by $z_i^t, \forall i=1,\dots,N, \forall t \geq T_0$; T_0 being the transient time) is defined as coherent [34, 52] if

$$\lim_{N \rightarrow \infty} \sup_{i,j \in U_\xi^N(x)} |z_i^t - z_j^t| \rightarrow 0 \text{ for } \xi \rightarrow 0 \quad (2.4)$$

where $U_\xi^N(x) = \{j : 0 \leq j \leq N, |\frac{j}{N} - x| < \xi\}$ represents the network neighborhood of any point $x \in S^1$, i.e., of the regular (S^1 ; ring) network. Now due to a near zero spatial distance between neighboring nodes, the coherent state can be geometrically represented as a smooth curve in the spatial plot where amplitudes of all the nodes are plotted as a function of node indices for a particular time value (i.e., in $z^t - i$ plane) [34, 52]. In the continuum limit $N \rightarrow \infty$, the snapshots of the state z_i^t (in $z^t - i$ plane) approach a smooth profile $z(x, t)$. Additionally, a completely synchronized state, which can be represented as $z_i^t = z_j^t \forall t \geq t_0 \forall i,j$, leads to a

straight line in the spatial profile (i.e. in the $z^t - i$ plane. This straight line represents a completely synchronized state ($z_i^t = z_j^t \forall i, j$). Any discontinuity appearing in the profile reflects the spatial incoherence and therefore show co-existence of coherence-incoherent, leading to the chimera state.

2.2.3 Identification of chimera state

We quantify this absence of smoothness (i.e. the presence of chimera state) by a spatial distance based measure which can be described as [53]

$$d_i^t = |(z_{i+1}^t - z_i^t) - (z_i^t - z_{i-1}^t)| \quad (2.5)$$

Since, the chimera state is represented by a co-existence of the coherent-incoherent dynamical evolution of the nodes, the spatial plot consisting of a smooth part (continuous curve representing coherent nodes) and gaps (discontinuities representing incoherent nodes) reflect an existence of the chimera state.

This measure capturing the difference of the spatial distance between the neighboring nodes, attains a value towards zero for a coherent profile. Any discontinuity in the spatial curve is indicated by a kink in d_i -i plane [54]. Furthermore, We use the number of spatial clusters, based on a collection of nodes with coherent evolution (recognized by low values of d_i) to identify the appearance of the chimera states. These spatial clusters are counted through the identification of spatially neighboring nodes having distance measure $d_i < \delta$, where δ is a small quantity. We choose a small positive threshold value δ ($\delta \approx 0.0384$) to clearly distinguish different dynamical states [96]. We discard clusters with the node population below a certain threshold, for instance 5, as considered in few other works [96]. The number of spatial clusters identifying different types of dynamical states can be written as follows; $N_{clus} = 0$ for the spatially incoherent state, $N_{clus} = 1$ for spatially coherent or completely synchronized state and $N_{clus} > 1$ for the chimera state.

2.2.4 Initial conditions

The chimera state has been reported to be sensitive to the choice of initial conditions. A proper choice of the initial condition is required for the emergence of the

chimera state [97]. For example, a special hump-back function is used to generate initial condition for demonstration of chimera state in identical non-locally coupled Kuramoto oscillators [2, 3]. However, few recent works have suggested that the choice of initial condition for occurrence of the chimera state may not be so significant. For instance, Ref. [48, 61] has shown the chimera-like behavior with a set of random initial conditions. Ref. [46] utilized a quasi-random initial condition for the realization of the chimera state in a coupled photosensitive chemical oscillators. Here, we consider a uniform random distribution of initial states ($z_i^{t=0}$) for the i^{th} oscillator which is bound between an interval $[0, \exp\left(-\frac{(i-\frac{N}{2})^2}{2\sigma^2}\right)]$ where the variance σ is chosen depending on the size of the network such that $z_i^{t=0} \in [0, 1]$. We use the same set of initial conditions for both the layers in a multiplex network and find that despite choosing a quasi-random initial condition, introduction of delay in a layer leads to an enhanced or a suppressed critical coupling strength for coherent evolution of dynamical variable in that layer, depending upon distribution and parity of delay values in different layers.

2.3 Results

2.3.1 Chimera in undelayed multiplex networks

We evolve Eq. 2.1 starting with a set of special initial conditions and after an initial transient, study the spatio temporal patterns of the multiplex network. In the absence of any coupling between the nodes ($\varepsilon = 0$) or for weak couplings, all the nodes evolve independently, and no spatial coherence is observed. For instance, as demonstrated in Fig. 2.2(a), for $\varepsilon = 0.1$, the evolution of the nodes in the multiplex network yields an incoherent state with no correlations in the neighboring nodes. As the coupling strength is increased, a partially coherent state emerges at $\varepsilon = 0.28$ with correlated spatial values of the neighboring nodes in the end and in the middle regions of each layer, however, the spatial range of the incoherent region is more than the coherent region (Fig. 2.2(b)). This coexistence of the coherent and incoherent dynamics corresponds to the chimera state in the multiplex network.

The dynamical behavior of two layers of a multiplex network is a replica of

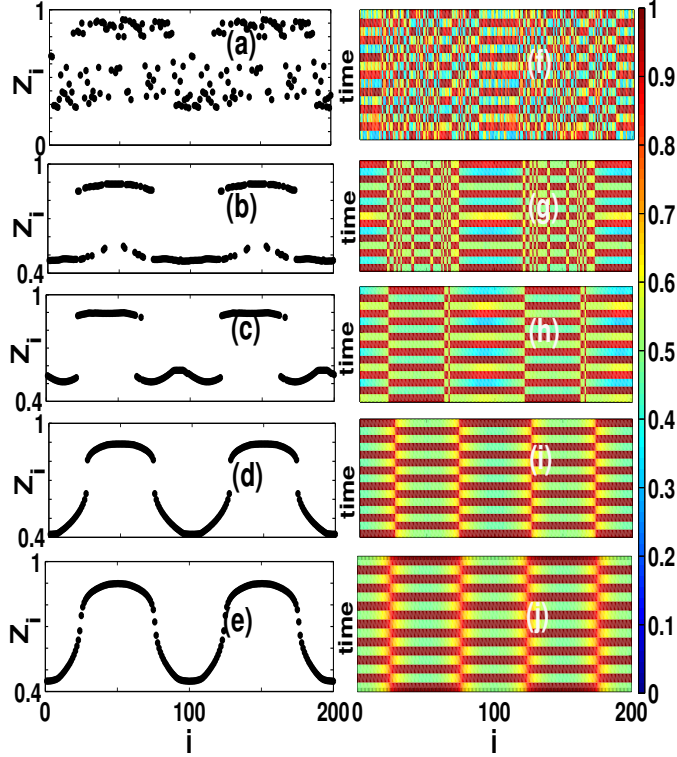


Figure 2.2: Snapshots and spatio-temporal plots for multiplex network consisting of regular (S^1 ; ring) network layers. Coupling strength(ε) for the plots are as follows, (a,f) are for $\varepsilon = 0.1$; (b,g) are for $\varepsilon = 0.28$; (c,h) are for $\varepsilon = 0.30$, (d,i) are for $\varepsilon = 0.40$, (e,j) are for $\varepsilon = 0.44$. Number of nodes in each layer is $N = 100$ and coupling radius $r = 0.32$. Initial transient is taken as 5000 time units. The spatio-temporal plots are presented for time units in range 5000 to 5015.

each other manifesting exactly the same spatio-temporal patterns (Fig. 2.2). The exact same behavior is observed for multiplex networks having more than two layers (Fig.2.3). This is, however, can be easily explained. We have considered the same realization of the quasi-random initial condition for the different layers of the multiplex network. Now, due to mirror node inter-layer coupling of the multiplex network, the inter-layer contribution of Eq. 2.1 cancels out. This reduces Eq. 2.1 to the governing equation for a single layer, consisting of the local contribution of the node dynamics and the intra-layer coupling contribution of its neighbors. Moreover, It has been shown that a different realization of the initial condition for different layers of the multiplex network leads to different chimera patterns in the multiplexed layers [54]. However, it should be noted that while different realizations in different layers induce different chimeric patterns across layers, it does not affect the overall parameter range for which chimera appears in the multiplex network. At the same coupling value, the spatio-temporal dynamics (Fig. 2.2 (g)) reflects non-regular skeletal type pattern in the incoherent regions. This irregularity of the pattern suggests that, in the multiplex network framework, a node may get

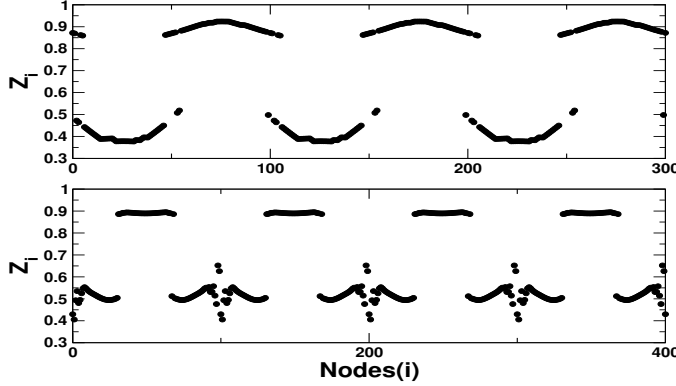


Figure 2.3: Snapshots for (a) Three layer and (b) Four layer multiplex network where the layers are represented by identical regular networks. Parameters are $\varepsilon = 0.28$ and $r = 0.32$. Number of nodes is $N = 100$ for each layer.

attracted to either of the upper or lower regions depending on its initial value as reported for the single-layer network [52].

As we increase the coupling strength further, the range of the incoherent region decreases as depicted by Fig. 2.2(c) for $\varepsilon = 0.3$. At $\varepsilon = 0.4$, we observe a sharp discontinuity in the otherwise smooth profile of $z(j)$ and the incoherency appears at two distinct points in each layer. This is a bifurcation point for the coherent-incoherent transition. Above this coupling value, all the nodes in the multiplex network acquire the complete, coherent state as indicated by the appearance of a smooth geometric profile at $\varepsilon = 0.44$ (Fig. 2.2(e)). Fig. 2.2 depicts spatial regions of incoherent nodes and thus indicates a non-zero spatial entropy with the periodic

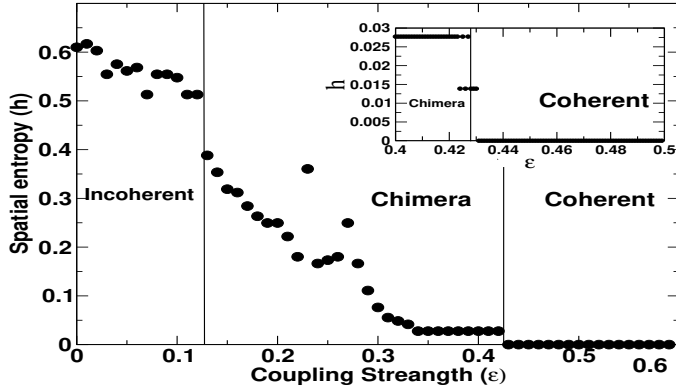


Figure 2.4: Spatial entropy as a function of coupling strength (ε). Other parameters are the same as Fig. 2.2.

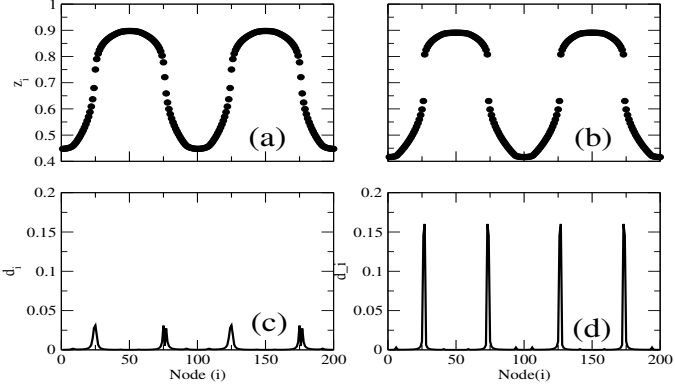


Figure 2.5: Distance measure for multiplex network consisting of regular (S^1 ; ring) network layers. Coupling strength (ε) for presented states are (a,c) with $\varepsilon = 0.44$ and (b,d) with $\varepsilon = 0.4$. Other parameters are same as Fig. 2.2.

temporal dynamics, representing a Type II chimera state [98]. Further, the regions of incoherence in the spatial profile continues to exist for narrower intervals with an increase in the coupling strength (Fig. 2.2). Furthermore, in the Chimera state, the time evolution of all the nodes in the network depicts periodic behavior with the periodicity two depicting temporal regularity. The coupled dynamics displays the spatial chaos which is defined by the non-zero spatial entropy given by $h = d \log_e(2)$, where d represents fraction of the incoherent nodes in network [52, 99]. We show that the distance measure (Eq. 2.5) is able to distinguish between coherent and chimera state easily. The discontinuous spatial profile (Fig. 2.5(b)) at $\varepsilon = 0.4$ gives rise to the kinks (Fig. 2.5(d)) in the distance measure distribution signifying transition to the chimera state. We calculate the spatial entropy as a function of the coupling strength (ε) in order to demonstrate the transition between the chimera to the coherent state. A transition from the chimera to a coherent state is indicated by the discontinuous change in spatial entropy of the network (Fig.2.4).

2.3.2 chimera in delayed single-layer network

First, we discuss the impact of delay on the dynamics of a single layer regular (S^1 ; ring) network. For the undelayed evolution, the single layer regular network exhibits a transition from the incoherent to the coherent state via chimera as coupling strength (ε) is increased. This can be clearly depicted from Fig. 2.6, where a transi-

tion from incoherence to the chimera to the coherent state at $\tau = 0$ (bottom row) can be seen, in terms of the N_{clus} employed to distinguish between different dynamical states.

However, an interesting phenomenon is discerned for the mid-range coupling values when the delay is introduced in the single-layer regular network. The overall dynamical behavior, as a function of coupling strength, remains the same as for the delayed evolution (Fig. 2.6). For the weak coupling strength, the delayed evolution also leads to the incoherent dynamics as found for the undelayed case. For mid-range coupling values, chimera dynamics is observed, but the transition from the chimera to the coherent state becomes highly dependent on the parity of the delay values (Fig. 2.6). We find that the chimera state is enhanced for the small odd delay and exists for a larger range of the coupling strength (Fig. 2.6), thus being characterized by a high critical coupling strength for the transition from the chimera state to the coherent state. Interestingly, as we increase the value of delay, we observe an immediate suppression of the chimera state for small even delay value, leading to a smaller critical coupling strength (Fig. 2.6). Therefore, the chimera state is found to be enhanced or suppressed depending upon the parity of the delay value, provided the delay value is small. For example, we observe critical coupling strength $\varepsilon_{critical} = 0.54$ and $\varepsilon_{critical} = 0.37$ for delay $\tau=1$ and $\tau=2$, respectively. However, as we increase the delay, the chimera state is found to remain suppressed as compared to the undelayed case regardless of the parity of delay (Fig. 2.6). This suppression of the chimera state becomes dominant for the large delay values.

The delayed dynamics shows a better spatial clusters formation for mid-range coupling strength as exhibited in Fig. 2.7. An introduction of the delay enhances the incoherence in the chimera state, the incoherent dynamics of the chimera state becomes larger and more pronounced. Furthermore, we find that as the time delay increases, the parameter regime for which chimera state appears, becomes suppressed leading to a completely coherent state for the mid-range coupling values (Fig. 2.6). This observation is not surprising as delays are known to enhance the synchronization [93, 94]. However, interesting enough, while high delay value enhances the

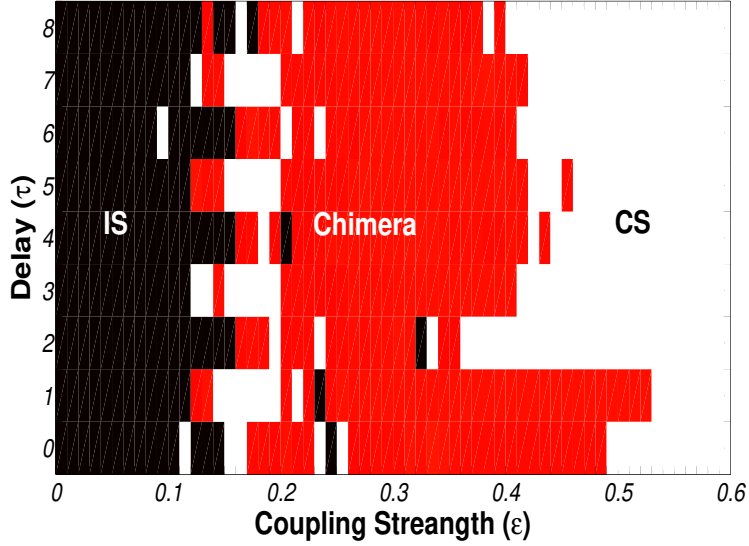


Figure 2.6: Phase diagram showing different dynamical regions based on number of spatial clusters (N_{clus}) in parameter space of delay (τ) and coupling strength (ε) for single layer regular network. The shades (colors) denotes different regions: IS (incoherent state $N_{clus} = 0$), CS (coherent state $N_{clus} = 1$) and chimera (chimera state $N_{clus} > 1$). Other network parameters taken are $N = 100$ and $r = 0.32$.

synchronization leading to suppression of chimera dynamics, the low odd delay value is shown to enhance the chimera state (Fig. 2.6).

2.3.3 chimera in the delayed multiplex network: Role of symmetric intra-layer delay

Next, we focus on the delayed temporal evolution on the multiplex network. Without any delay, the multiplex network exhibits a chimera state for the mid-range of coupling values. The dynamical behavior of the individual layer of the multiplex network is found to be exactly same to each other, leading to the identical spatio-temporal patterns. Here, we consider a multiplex network with two layers to present our findings. First, we consider a case where we introduce same delay value in the intra-layer edges on both the layers of the multiplex network with no inter-layer delay. We find that even with the introduction of delays, which is symmetric in both the layer, the multiplex chimera behavior is quite similar to the single-layer networks. Initially, for very small coupling strength value i.e., in weak coupling range ($\varepsilon \leq 2$), we find incoherent dynamics in both the layers. As the coupling strength

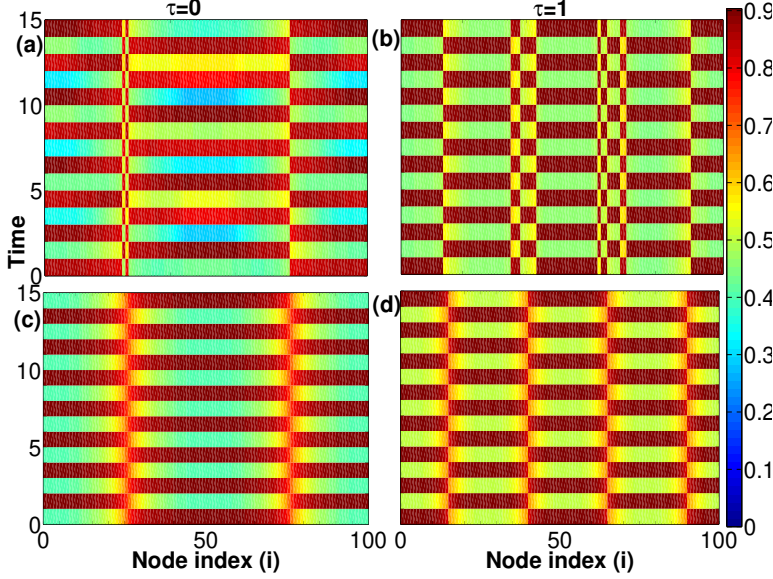


Figure 2.7: Spatio-temporal plot for the chimera state. (a,c) depict undelayed ($\tau = 0$) case whereas, (b,d) depict delayed ($\tau = 1$) case. The coupling strengths are, (a,b) with $\varepsilon=0.39$ and (c,d) with $\varepsilon=0.49$. The dynamical variable associated with the temporal evolution is color-coded in the spatio-temporal plots as a function of time. Other parameters are the same as Fig.2.6.

is increased, the chimera state emerges for mid-range coupling values followed by a coherent state in both the layers for the strong coupling. Fig. 2.8 presents the spatio-temporal patterns for different values of the delay and coupling strengths. We found that the emergent of the chimeric patterns in the layers of the multiplex network (Fig. 2.8 left column or right column), demonstrate a strong similarity with each other with no inter-layer delay. However, the nature of the delay plays a critical role in the transition from the chimera to the coherent state with the increment of the coupling strength. Analogous to the case of the single layer network, we find that small odd delay values lead to an enhancement of the chimera state with high critical coupling strength ($\varepsilon_{critical} = 0.54$ for $(\tau_{l1} = \tau_{l2} = 1)$) as presented in Fig. 2.8 (left column). An immediate suppression of the chimera state is observed for small even delay values (Fig. 2.8; right column). The critical coupling strength for intra-layer delay ($\tau_{l1} = \tau_{l2} = 2$) is found to be $\varepsilon_{critical} = 0.37$. Note that, there is no inter-layer delay present for both the cases ($\tau_{l2} = 0$). Fig. 2.9(a) (with $\tau_{l1} = \tau_{l2} = 1$) and Fig. 2.9(b) (with $\tau_{l1} = \tau_{l2} = 2$) display the enhancement

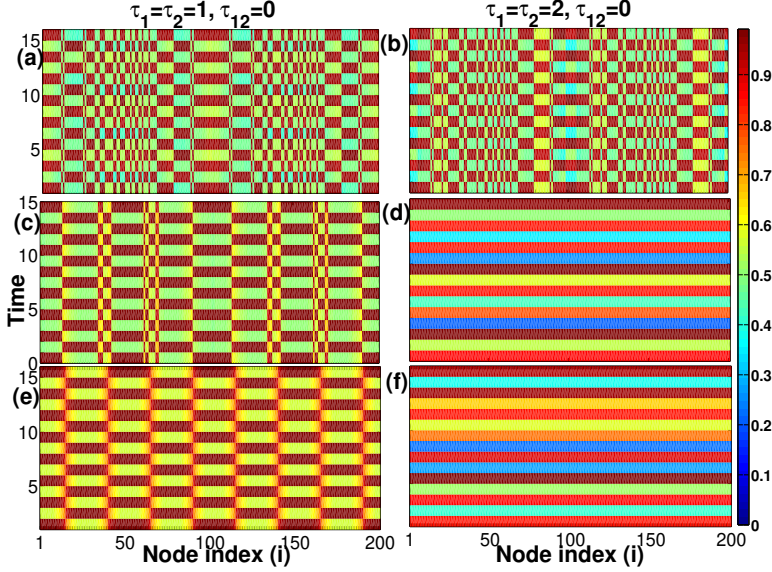


Figure 2.8: Spatio-temporal plots for the chimera state with (a,c,e) odd intra-layer delay ($\tau_{l1} = \tau_{l2} = 1$) and with (b,d,f) even intra-layer delay ($\tau_{l1} = \tau_{l2} = 2$) in the layers of the multiplex network. The coupling strengths are, (a,b) $\varepsilon = 0.31$; (c,d) $\varepsilon = 0.4$ and (e,f) $\varepsilon = 0.5$. Intra-layer delay in both the layers is the same. The space-time plots presented here are color coded for the first layer (with identical second layer) of the multiplex network. Dynamical variable associated with the temporal evolution is color-coded in the spatio-temporal plots as a function of time. Other network parameters are $N = 100$ and $r = 0.32$ for each layer of the multiplex network.

and subsequent suppression of the value of critical coupling strength ($\varepsilon_{critical}$) as compared to the undelayed case (with $\tau_{l1} = \tau_{l2} = 0$). Depending on the nature of the delay, the chimera state can be enhanced or suppressed to collapse into a coherent state. Moreover, we find that this enhancement is destroyed for high delay values. A high intra-layer delay always leads to the suppression of the chimera state as compared to the undelayed case. Fig. 2.9(c) and Fig. 2.9(d) display the range of coupling strength (ε) for which chimera state is observed for high even and odd delays. A vital point to note here is that despite having intra-layer delays, the individual layers of the multiplex network is found to behave like a single network as long as the delays in both the layers remain the same.

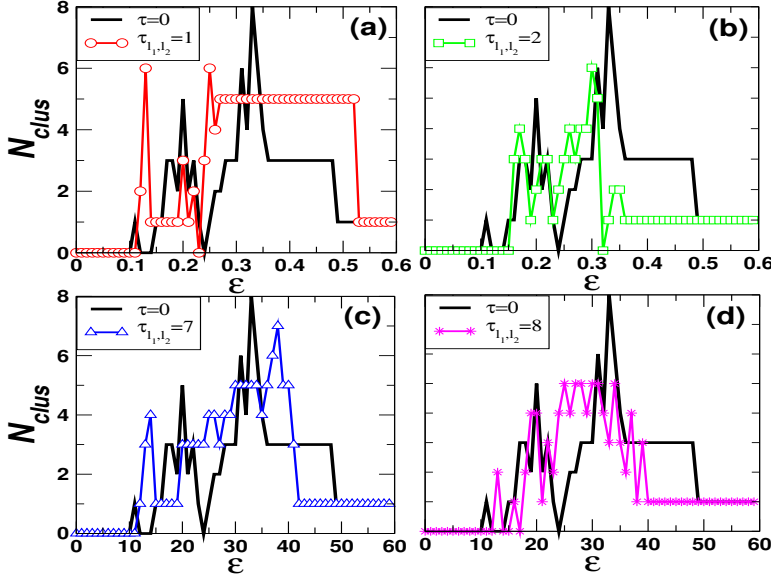


Figure 2.9: Scatter diagram depicting number of spatial clusters (N_{clus}) as a function of coupling strengths (ε) for different delay values, (a) $\tau_{l1} = \tau_{l2} = 1$, (Red circle) (b) $\tau_{l1} = \tau_{l2} = 2$ (Green square), (c) $\tau_{l1} = \tau_{l2} = 7$ (Blue triangle), (d) $\tau_{l1} = \tau_{l2} = 8$ (Magenta star). The thick black line represents N_{clus} for the undelayed case ($\tau_{l1} = \tau_{l2} = 0$). The values demonstrated here are for first layer (with identical second layer and same intra-layer delay). Other parameters are same as Fig. 2.8.

2.3.4 Chimera in delayed multiplex network: Role of asymmetric intra-layer delay

Next, we study the trade off between the delay and the multiplexing for occurrence of the chimera dynamics for delayed multiplex networks. In real-world systems, having a similar delay for all the layers of the corresponding multiplex network is very rare. Asymmetric intra-layer delay in layers of the multiplex network leads to a rich variety of emergence of the chimera state. First, we investigate the dynamical behavior of the nodes when a small value of delay is introduced into only one layer. The chimera dynamics of the delayed layer is found to be enhanced due to the introduction of small value of odd delay (Fig. 2.11). Mismatch in the delay value leads to a suppression of the identical behavior of the layers (Fig. 2.10). We find that for weak coupling strength, the delay (say in layer 2) enforces a coherent dynamics in the delayed layer while the undelayed layer (say layer 1) still keeps showing an incoherent dynamics (Fig. 2.10). Although the nodes in one layer are

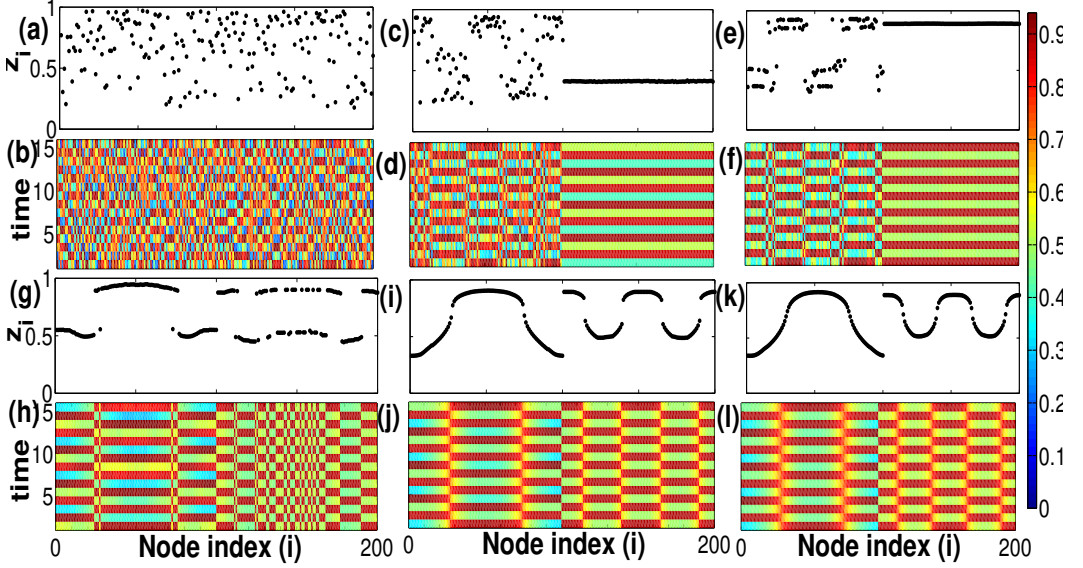


Figure 2.10: Snapshots and spatio-temporal plots for the multiplex network for various coupling strengths, (a,b) are for $\varepsilon = 0.1$; (c,d) are for $\varepsilon = 0.14$; (e,f) are for $\varepsilon = 0.17$; (g,h) are for $\varepsilon = 0.24$, (i,j) are for $\varepsilon = 0.49$, (k,l) are for $\varepsilon = 0.52$. Dynamical variable associated with the temporal evolution is color-coded in the space time plots as a function of time. Other network parameters for each layer of the multiplex network are $N = 100$, $r = 0.32$, $\tau_{l1} = \tau_{l2} = 0$ and $\tau_{l2} = 1$.

identically connected to their mirror nodes in another layer, we witness a surprising co-existence of the coherent and the incoherent dynamic evolution of nodes in the layers of the multiplex network. One population (layer) exhibits a spatial synchrony while its mirror population retains asynchronous behavior. We term this particular state as *layer chimera* state which can only emerge in a delayed multiplex network. With an increment in the coupling strength, both layers start exhibiting the chimera state. For strong coupling strength, the undelayed layer reaches to the coherent state before the delayed layer as depicted in Fig. 2.10.

Now keeping the same delay value in one layer (say in layer 2), we increase the delay in another layer (in layer 1). The same value of delay in both the layers leads to the enhancement in the chimera behavior (Fig. 2.9). However, we find that the nature of the chimera dynamics in layer 2 remains enhanced regardless of the delay in layer 1. Moreover, except for the same intra-layer delay, layer 1 always exhibits a suppressed chimera state as compared to the undelayed case with a small fluctuation in the critical coupling strength value. Next, our study denotes the impact of par-

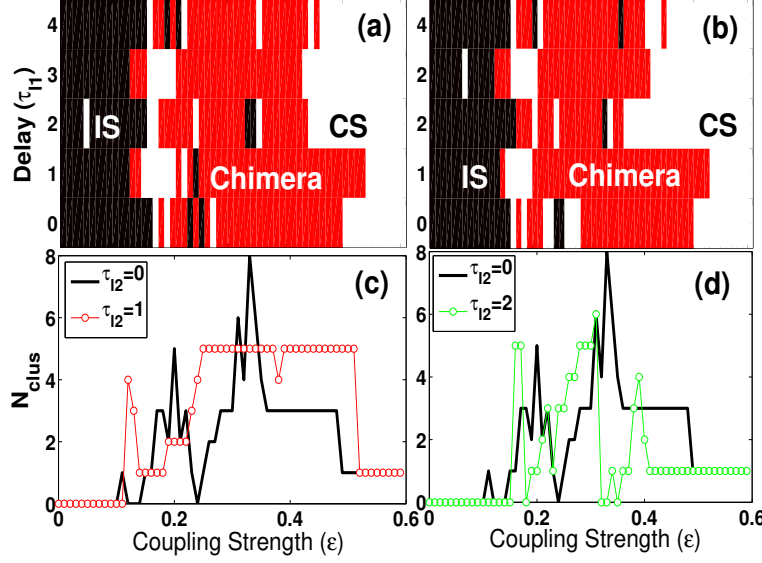


Figure 2.11: Phase diagram and scatter diagram depicting different dynamical regions of the layers of multiplex network with different intra-layer delays. The shades (colors) in phase denotes different regions: IS (incoherent state $N_{clus} = 0$), CS (coherent state $N_{clus} = 1$) and chimera (chimera state $N_{clus} > 1$). (a,b) represents N_{clus} values for different values of delay in first layer where as (c,d) represents N_{clus} as a function of coupling strength (ε) with constant delay in second layer with (c; $\tau_{l2} = 1$) and (d; $\tau_{l2} = 2$). Other network parameters are same as Fig. 2.8.

ity of delay on the layer dynamics of the multiplex network. We introduce a small value of even delay in one layer (say layer 2), keeping another layer un-delayed. We find an immediate suppression of the chimera state in the delayed layer. Moreover, the chimera dynamics in the second layer remains suppressed regardless of the delay values in the first layer except for the small value of odd delay in layer 1 where it shows an enhancement. We find that as there is an increase in the delay value in both the layers, the suppression of chimera state against the enhancement in coupling strength becomes a dominant trait of the dynamics. Table 2.1 presents the critical coupling strengths for different delay values for both the layers of a multiplex network. The higher delay values in both the layers of a multiplex network lead to a suppressed chimera state even if there is a delay mismatch between the layers (Fig. 2.11).

The chimera behavior for delayed dynamical evolution (Eq. 2.3) can have a crucial dependence on the distribution of delays in the layers of the multiplex network. For

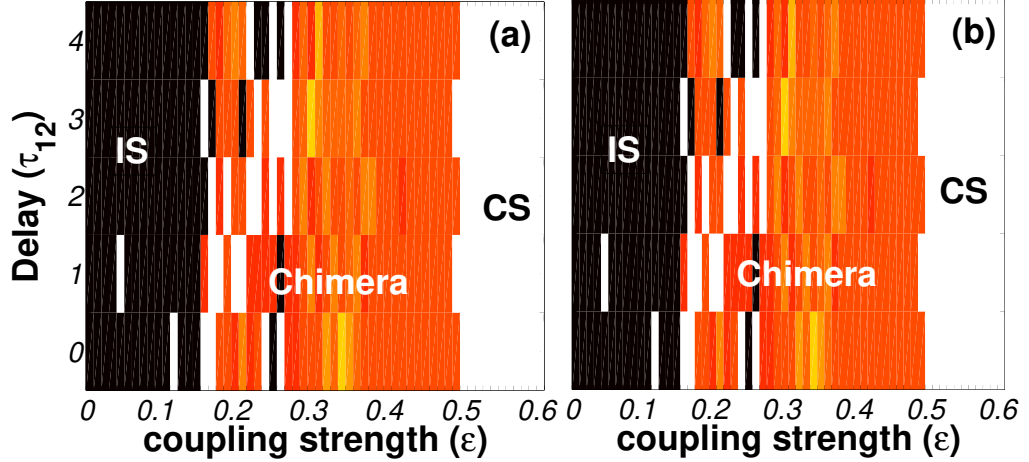


Figure 2.12: Phase diagrams depicting different dynamical regions based on number of spatial clusters (N_{clus}) in parameter space of inter-layer delay (τ_{12}) and coupling strength (ε) for multiplex network consisting of regular network layers. The shades (colors) denotes different regions: IS (incoherent state $N_{clus} = 0$), CS (coherent state $N_{clus} = 1$) and chimera (chimera state $N_{clus} > 1$). (a) represents N_{clus} values in first layer whereas (b) represents N_{clus} in second layer with different inter-layer (τ_{12}) delay values. Other network parameters taken are $\tau_{l1} = \tau_{l2} = 0$, $N = 100$ and $r = 0.32$.

a certain range of coupling strength, the appearance of a chimera state can be destroyed and then again resurrected by controlling the parity and the distribution of delay in the dynamics of the multiplexed layers. Furthermore, it is noticed that the inter-layer delay did not have any significant effect on the enhancement or suppression of the chimera state Fig. 2.12. An introduction of the homogeneous inter-layer delay ($\tau_{l1} = \tau_{l2} = 0$, $\tau_{12} \neq 0$), leads to all the nodes in both the layers experiencing the same delay in the information propagation across the layers and hence does not bring upon any significant change on the appearance of the chimera states. We find that even with high inter-layer delay and no intra-layer delay, both the layers of the multiplex network exhibit exactly the same behavior with chimera state in the mid-range coupling values.

2.4 Conclusion

In this chapter, we reported an emergence of the chimera in the multiplex networks with the layers being represented by regular network architecture having non-local

Table 2.1: Critical coupling strengths for different delay values in the layers of multiplex network. upper and lower triangles represent $\varepsilon_{critical}$ for layer 1 and layer 2, respectively. Other network parameters for each layer of the multiplex network are $N = 100$ and $r = 0.32$.

$\varepsilon_{l2}^c \backslash \varepsilon_{l1}^c$	$\tau_{(l1)} = 0$	$\tau_{(l1)} = 1$	$\tau_{(l1)} = 2$
$\tau_{(l2)} = 0$	0.49	0.52	0.41
$\tau_{(l2)} = 1$	0.49	0.53	0.43
$\tau_{(l2)} = 2$	0.41	0.43	0.36

couplings. We find that an emergence of the chimera is identical in the mirror layers arising due to the underlying symmetry of the network and the initial state. Furthermore, we have presented time-delayed dynamics for non-locally coupled chaotic maps and had observed a transition from the incoherent to the coherent dynamics via the chimera states for both single-layer and the multiplex networks. We demonstrated that the interplay of multiplexing and delay gives rise to a novel spatially clustered coherent states disconnected by incoherent regions known as chimera states. The emergence of chimera state in delayed systems shows a high dependency on the parity of the delay, which is known to influence synchronization of the coupled dynamics [93, 94]. Here, we had shown that the small odd or even value of delay leads to an enhancement or suppression, respectively, in the chimera state. Moreover, a large delay value leads to the suppression regardless of the nature of the delay. Our investigation has also uncovered the layer chimera state with one coherent and one incoherent layer directly resulting from the enhancement-suppression behavior of individual layers of the multiplex network depending on the distribution of the delays. The findings reported in this chapter can provide additional insight into the formation of spatial clusters in delayed systems. Recently, similarities between the emergence of chimera state in neural networks and Electroencephalogram (EEG) reading of a epileptic seizure state have been reported with its possible applications in early detection of seizure [81, 82]. Our result of the enhancement or the suppression of chimera state may help in the diagnosis of this kind of seizures

by introducing a delay in the neural networks. This finding may also contribute to enhancing our understanding of many biological functions known to show chimera-like states like uni-hemispheric sleep in humans and certain mammals [76, 77].

Chapter 3

Promoting chimera through non-identical multiplexing

3.1 Overview

The multiplex framework approach to network science has provided a new dimension to complex systems research [87]. We have demonstrated a rich variety of chimera states, emerging on a multiplex network consisting of two identical regular network layers, in Chapter 2. However, a multiplex network consisting of identical network architecture in both layers is not very common in real-world complex systems [92]. For example, one can consider a multi-modal transportation network, consisting of layers representing different modes of travel [87]. The air travel layer may be more sparsely connected than the rail or bus layer and vice versa, depending on the geographical area. Similarly, a communication network may have much sparser connectivity in the expensive optical fiber layer than the traditional cable network layer. Motivated by this, we investigate the behavior of chimera states for multiplex networks with non-identical layers, possessing properties which are closer to those of real-world systems in this chapter. We study the emergence of

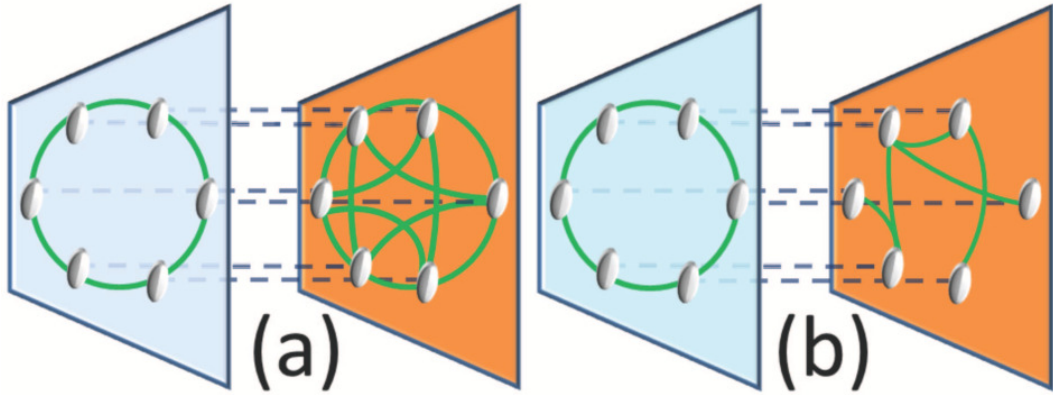


Figure 3.1: Schematic diagram depicting a multiplex network consisting of a regular network and (a) a regular network with different node degree (different value of non-local coupling range) and (b) random network, respectively. We use this multiplex architecture as modeled by Eq. (3.1).

chimera states in a homogeneous network of identical elements, which is multiplexed with networks not necessarily having an identical coupling environment. We refer to the network (layer) possessing nodes with identical coupling architecture as a homogeneous network (layer). We consider a regular network with periodic boundary conditions (S^1 ; ring) for the homogeneous network. We demonstrate that the parameter range displaying the chimera state in the homogeneous first layer of the multiplex networks can be tuned by changing the link density or connection architecture of the same nodes in the second layer. We focus on the impact of the interconnected second layer on the enlargement or shrinking of the coupling regime for which chimeras are displayed in the homogeneous first layer. We particularly consider two cases, (i) a multiplex network having two homogeneous layers with different connectivities, (ii) a multiplex network consisting of one homogeneous and one inhomogeneous layer. We find that a denser homogeneous second layer promotes chimera in a sparse first layer, where chimeras do not occur in isolation (i.e., in a single layer). Furthermore, while a dense connection density is required for the second layer if it is homogeneous, this is not true if the second layer is inhomogeneous. We demonstrate that a sparse inhomogeneous second layer, which is common in real-world complex systems, can promote chimera states in a sparse homogeneous first layer.

3.2 Theoretical Framework

3.2.1 Construction of the network

Repeating the representation technique of the network, shown in the previous chapter, We construct an undirected multiplex network (with $2N$ nodes) where the two layers of the multiplex network are encoded by a set of adjacency matrices $\{A_1, A_2\}$.

Hence, the multiplex network \mathcal{A} can be expressed as

$$\mathcal{A} = \begin{pmatrix} A^{(1)} & I \\ I & A^{(2)} \end{pmatrix}, \quad (3.1)$$

where $A^{(1)}$ and $A^{(2)}$ represent the adjacency matrix of the first and second layer, respectively. I is an identity matrix representing links between one-to-one mirror nodes in two layers.

At first, we have considered regular connection architecture (also represented by 1D or 1D lattice) in the layers of the multiplex network. We described the non-local coupling range in the layers as $P^{(1)}$ and $P^{(2)}$ neighbors to each side in the two layers, respectively. This assignment corresponds to a constant node degree of $\langle k^{(1)} \rangle = 2P^{(1)}$ and $\langle k^{(2)} \rangle = 2P^{(2)}$, in layer 1 and layer 2, respectively. Later on, We have used a multiplex network where one layer is represented by regular (or 1D) network and another layer by an Erdős-Rényi (ER) random network [28] or scale-free (SF) network [29]. Note that, we have considered the regular network as a homogeneous network, referring to the network (layer) possessing nodes with identical coupling architecture. All other networks (ER and SF) are considered as an inhomogeneous network (layer).

3.2.2 Dynamics on the network

Here again, we consider a discrete-time logistic map $z_i^{t+1} = \mu z_i^t (1 - z_i^t)$; $z_i^t \in \mathbb{R}; \forall_{i=1,\dots,2N}$ (with $\mu = 4.0$; chaotic regime) as local dynamics to describe state of the i^{th} node at time t [25, 26]. We further integrate the underlying network topology as [54]

$$z_i^{t+1} = f(z_i^t) + \frac{\varepsilon}{(k_i)} \sum_{j=1}^{2N} \mathcal{A}_{ij} [f(z_j^t) - f(z_i^t)] \quad (3.2)$$

where $k_i = \sum_{j=1}^{2N} \mathcal{A}_{ij}$ is the normalizing factor and ε is the overall coupling constant, assuming $0 \leq \varepsilon \leq 1$. Furthermore the average degree (node degree) of the layers of the multiplex network is defined as $\langle k \rangle = \frac{1}{N} \sum_{i=1}^N \left(\sum_{j=1}^N A_{ij}^{(1,2)} \right)$, where N represents number of nodes in each layer the multiplex network.

3.2.3 Identification of chimera state

The mathematical definition of chimera state referring to the coexisting coherent-incoherent dynamics has been described in the previous chapter. However, improving on the measure employed in the previous chapter, we consider a correlation measure in this chapter to identify chimera state. We define a normalized probability distribution function $g(|\bar{D}|)$ of the Laplacian distance measure $|\bar{D}(t)|$ and a correlation measure [100] as

$$g_0(t) = \int_0^\delta g(|\bar{D}(t)|) d(|\bar{D}(t)|) \quad (3.3)$$

where $|\bar{D}(t)|$ is a vector with components $d_i(t)$ defined as $d_i(t) = |(z_{i+1}(t) - z_i(t)) - (z_i(t) - z_{i-1}(t))|$ identifies the presence of strong local curvature in an otherwise smooth spatial profile [101]. The upper limit δ (Eq. 3.3) denotes a small positive threshold value. The $g_0(t)$ essentially measures the relative size of spatially coherent regions, and ideally an intermediate value between 0 and 1 indicates a chimera state [102]. However, even an incoherent state may have a small portion of nodes which can cluster together spatially, leading to a non-zero value of g_0 . We numerically find that $0.4 \lesssim g_0 \lesssim 0.8$ provides a best estimation of the parameter regime displaying Chimera states. We highlight the region in the included figures (in $g_0 - \varepsilon$ plane) for an easy comprehension.

3.3 Results

3.3.1 Chimeras in multiplex network with connectivity mismatch

First, we consider the case of both layers being represented by a homogeneous non-local coupling architecture but with a connectivity mismatch between the layers (Fig. 3.1(a)). Specifically, we choose a non-local coupling range with $P^{(1)}$ and $P^{(2)}$ neighbors to each side in the two layers, respectively. This assignment corresponds

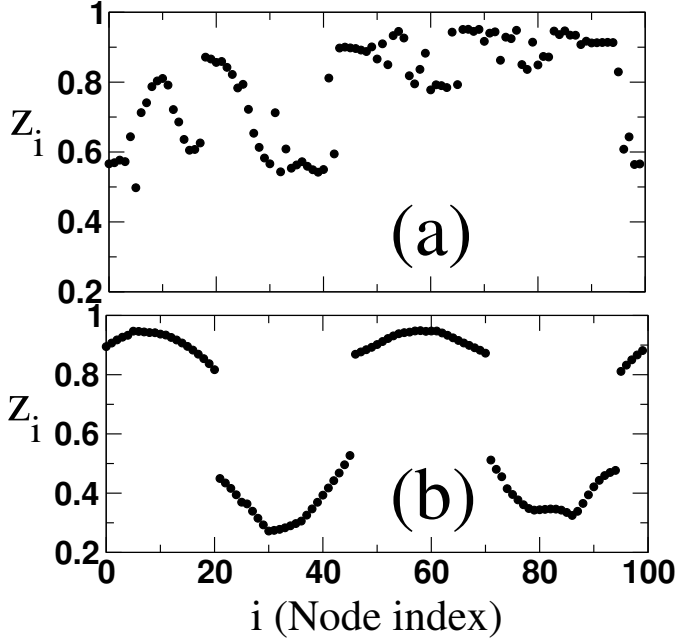


Figure 3.2: Snapshots of the (a) single layer regular network ($\langle k \rangle = 30$) and (b) first layer of the regular-regular multiplex network with node degree $\langle k^{(1)} \rangle = 30$; $\langle k^{(2)} \rangle = 64$. Other parameters: $\varepsilon = 0.33$ and $N^{(1)} = N^{(2)} = 100$.

to a constant node degree of $\langle k^{(1)} \rangle = 2P^{(1)}$ and $\langle k^{(2)} \rangle = 2P^{(2)}$, respectively. We find that chimera states emerge in the sparse first layer, in contrast to the single layer case, when it is multiplexed with a dense second layer. Fig. 3.2(a) shows that no chimera exists for the single layer network (incoherent state), and Fig. 3.2(b) depicts a chimera in the same sparse layer upon multiplexing with a dense layer. Furthermore, Fig. 3.3 display that the range of the ε for which the chimera state exists in the first layer is enlarged as the second layer becomes denser. In Fig. 3.3 (left column), when the second layer has the node degree $\langle k^{(2)} \rangle = 10$, a clear chimera state is only found for a very large value of ε (Fig. 3.3 (c)), whereas for $\langle k^{(2)} \rangle = 40$ (Fig. 3.3 (middle column)) the chimera state exists for a larger range (Fig. 3.3 (e)-(f)). With further increasing node degree of the second layer, say for $\langle k^{(2)} \rangle = 64$ (Fig. 3.3 (right column)), the chimera state in the sparser first layer exists for almost all ε values as depicted in Fig. 3.3 (g)-(i).

So far we have kept the degree of the sparse first layer fixed and have varied the node degree of the second layer, demonstrating that with increasing node degree of the second layer chimeras occur for a larger range of ε . The same is true if we fix the node degree of the dense second layer and change the degree of the sparse first layer. Again, a stronger connectivity mismatch leads to a larger range of ε for

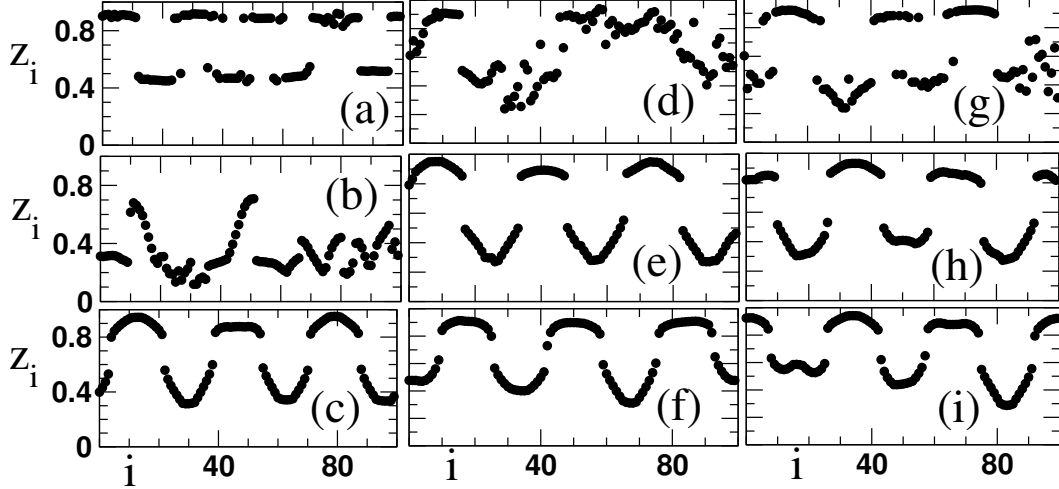


Figure 3.3: Snapshots of the first layer for a regular-regular multiplex network for coupling strength, (a,d,g) $\varepsilon = 0.33$; (b,e,h) $\varepsilon = 0.38$ and (c,f,i) $\varepsilon = 0.44$. The node degrees of the first layer is $\langle k^{(1)} \rangle = 20$. The node degree of the second layer is, (a,b,c) $\langle k^{(2)} \rangle = 10$; (d,e,f) $\langle k^{(2)} \rangle = 40$; (g,h,i) $\langle k^{(2)} \rangle = 64$, respectively. Other parameters: $N^{(1)} = N^{(2)} = 100$

which chimeras are observed in the sparser first layer. Note that the dense second layer still exhibits chimeras in an intermediate ε range (similar to the case where both layers of the multiplex network consist of dense regular coupling topology) regardless of the connection density of the sparse first layer [101]. To present a comprehensive picture of multiplexing with a denser layer that promotes chimeras in a sparse network, we plot a diagram of the parameter regimes in the plane of the node degree $\langle k^{(1)} \rangle$ and ε . The density plot shows the correlation measure g_0 of the sparse first layer (Fig. 3.4). Fig. 3.4 (a) depicts a network with the same node degree $\langle k \rangle$ in both layers. Now we keep the node degree of the dense second layer fixed and vary the node degree of the first layer from very sparse to very dense. Fig. 3.4 (b) shows that there exists a regime of chimera states in the first layer ($0 < g_0 < 1$) in the $(\langle k^{(1)} \rangle, \varepsilon)$ parameter plane at intermediate values of ε and $\langle k^{(1)} \rangle = 64$, which corresponds to two identical layers. The light-colored region to the very left of Fig. 3.4 (b), corresponding to a sparse layer (low $\langle k^{(1)} \rangle$) multiplexed with a dense layer, also indicates chimera states in a parameter regime of large ε where they are not found in a single layer (cf. $\langle k^{(1)} \rangle = \langle k^{(2)} \rangle$ in Fig. 3.4 (a)). On the other hand, for large $\langle k^{(1)} \rangle$, where both layers are dense, chimeras are only found in a small range

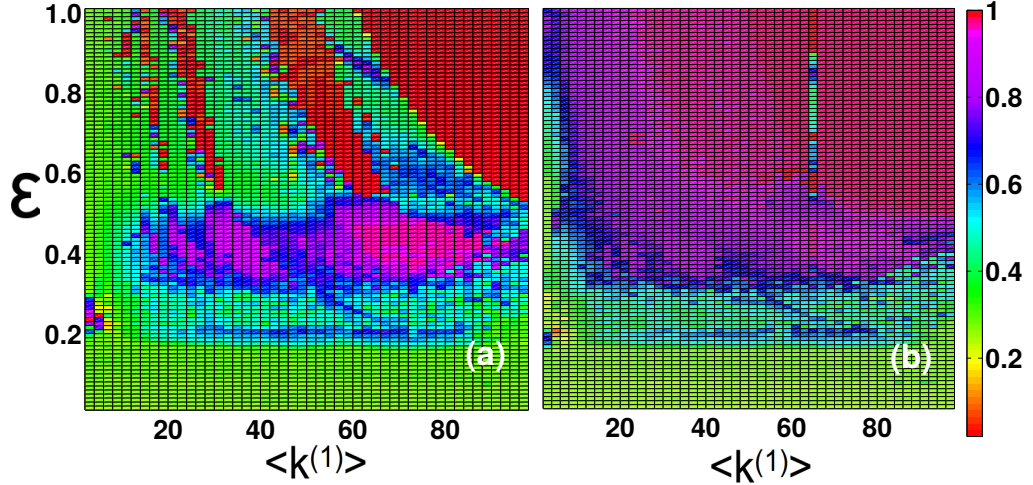


Figure 3.4: The normalized correlation measure g_0 , calculated for layer 1, is plotted in the parameter plane ($\langle k^{(1)} \rangle, \varepsilon$) for (a) regular-regular multiplex network with the same node degree in both layers ($\langle k^{(1)} \rangle = \langle k^{(2)} \rangle = \langle k \rangle$), (b) nonidentical regular-regular multiplex network where the second layer has the fixed node degree $\langle k^{(2)} \rangle = 64$. Note the chimera tongue around $\langle k^{(1)} \rangle = 64$ in (b). Parameters: $N^{(1)} = N^{(2)} = 100$ and $\delta = 0.01(\max(|D|))$ [100]; g_0 is averaged over 1000 time steps.

at intermediate values of ε (light color in Fig. 3.4 (b)).

To further illustrate this issue in Fig. 3.5, we plot the correlation measure g_0 as a function of ε for a multiplex network with mismatched node degree of the two layers. In panel (a) layers, 1 and 2 are sparse, in (b) layer 2 is more densely connected than layer 1, and in panel (c) both layers are dense. A multiplex network consisting of two sparse layers has a low value of the correlation measure g_0 indicating incoherent dynamics in layer 1 (Fig. 3.5(a)). However, with increasing connectivity of layer 2, the critical coupling strength (i.e., ε value for which the network dynamics exhibits a transition from the chimera to the completely coherent state) increases in layer 1, indicating an extended regime of chimeras. In fact, the sparse layer (layer 1) demonstrates absence of the completely coherent regime ($g_0 \approx 1$) when multiplexed with a dense layer (Fig. 3.5(b)). Furthermore, for a multiplex network consisting of two dense layers, both layers show a typical chimera regime in an intermediate range of ε as exhibited by identical dense layers (Fig. 3.5(c)). Thus, for multiplex networks with dense layers, the individual layers do not exhibit any change in the

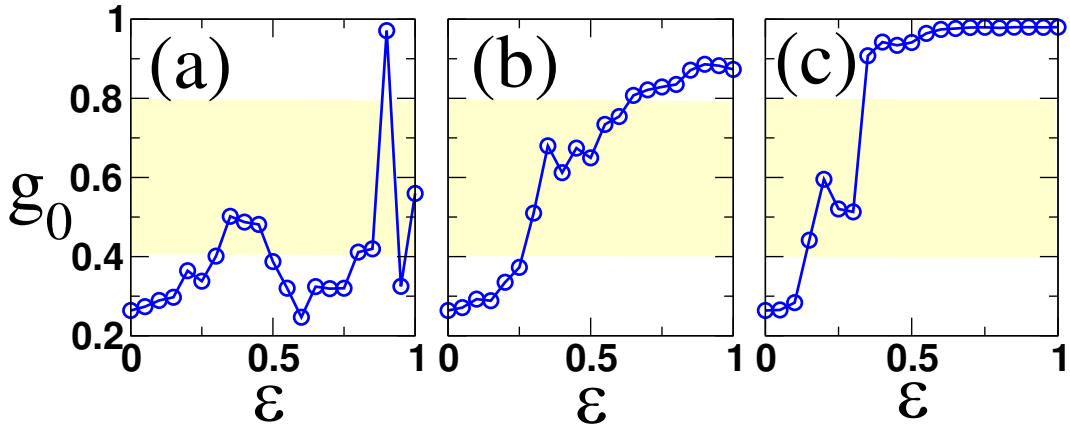


Figure 3.5: Correlation measure g_0 vs. ε for the first layer of a non-identical regular-regular multiplex network characterizing the chimera behavior in the sparse layer as a consequence of multiplexing. Node degrees: (a) $\langle k^{(1)} \rangle = 10$, $\langle k^{(2)} \rangle = 10$, (b) $\langle k^{(1)} \rangle = 10$, $\langle k^{(2)} \rangle = 64$, (c) $\langle k^{(1)} \rangle = 64$, $\langle k^{(2)} \rangle = 80$. Other parameters as in Fig. 3.4. The highlighted area indicates the parameter regime for chimera states.

critical ε value for the occurrence of chimera states.

3.3.2 Chimeras in multiplex network with architecture mismatch

Here, we discuss the impact of inhomogeneous network architecture in the second layer of a multiplex network on the emergence of chimera patterns in the homogeneous first layer. We consider a multiplex network where a regular network with homogeneous nonlocal coupling (layer 1) is multiplexed with an inhomogeneous network having a random architecture (layer 2), see Fig. 3.1 (b). Since the network architecture represented by the second layer does not consist of nodes which are ordered by nearest-neighbor coupling configurations, it is not straightforward to define chimera states in the classical sense for the second layer. All the figures and discussions in the following correspond to the dynamics of the regular network in the first layer. To construct the inhomogeneous layer, first we use an Erdős-Rényi (ER) network [28]. We consider a multiplex network consisting of a dense regular network (layer 1) and an ER random network (layer 2). The dense regular network layer exhibits chimera states at intermediate coupling values without any enhancement (as compared to the single-layer case) regardless of the connection density of the inhomogeneous ER layer [101]. An interesting phenomenon, however, oc-

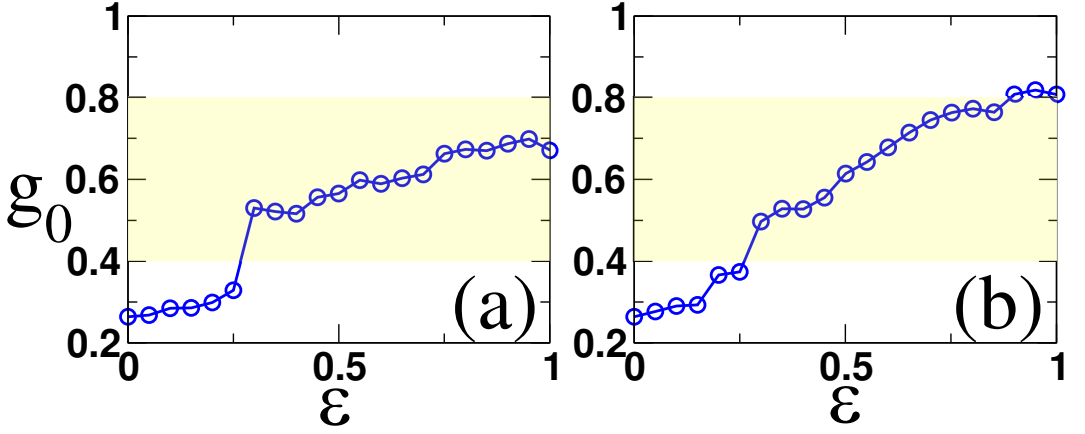


Figure 3.6: Correlation measure g_0 vs ε for the homogeneous first layer of a (a) 1D-ER (b) 1D-SF multiplex network. Node degrees $\langle k^{(1)} \rangle = \langle k^{(2)} \rangle = 10$. Other parameters as in Fig. 3.4. Highlighted area indicates parameter regime for chimera states.

curs when a sparse regular network layer is multiplexed with a random network. Unlike the case of multiplex networks consisting of two sparse homogeneous layers, if one layer is represented by a random connection architecture, for the same connection density, the homogeneous layer exhibits chimeras. The sparse regular network layer which does not exhibit chimeras upon multiplexing with a sparse homogeneous layer (Fig. 3.5 (a)), starts displaying chimeras when multiplexed with a sparse inhomogeneous layer (Fig. 3.6 (a)-(b)). Moreover, multiplexing with a sparse ER network is more favorable for the emergence of chimeras in the homogeneous layer than multiplexing with a dense layer. The critical ε value in the sparse regular network increases with decreasing average connection density $\langle k_{ER}^{(2)} \rangle$ of the ER layer (Fig. 3.7). The chimera regime expands as the ER layer becomes sparser. Fig. 3.7(a) depicts a larger range of ε for which chimeras are observed in the regular network layer due to its multiplexing with a sparser random layer. One further point to be noted is that for multiplex networks consisting of two homogeneous layers, larger average connectivity is more favorable for synchronization in one layer, however, for multiplex networks consisting of one homogeneous and one inhomogeneous (say ER) layer, enhancement in average connectivity of inhomogeneous layer leads to a shrinking coupling range for which chimeras are observed. Nevertheless, for all combinations of average degree, multiplexing with inhomogeneous

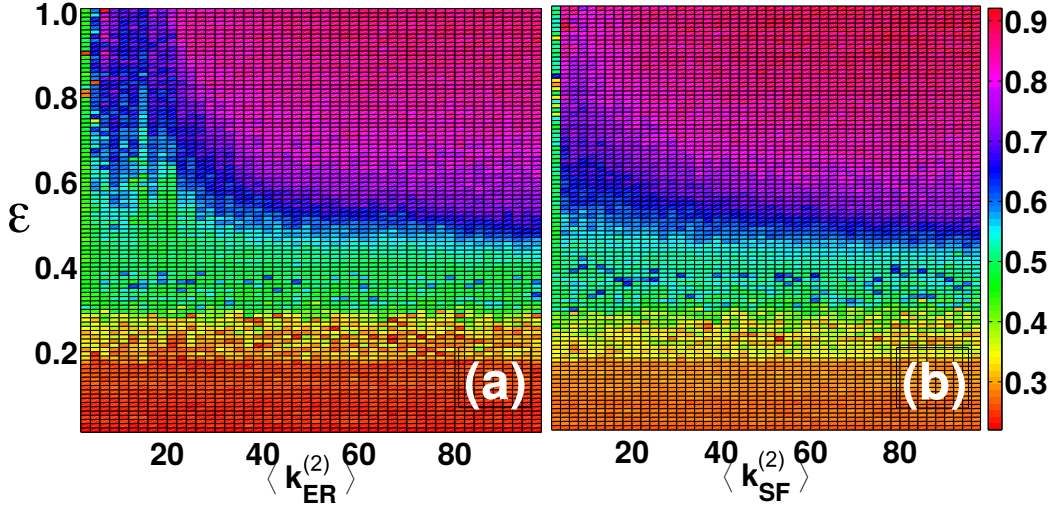


Figure 3.7: Map of regimes for a multiplex network consisting of one 1D layer and one inhomogeneous layer, where g_0 is calculated for layer 1: (a) 1D-ER multiplex networks and (b) 1D-SF multiplex network. The first layer has the node degree $\langle k^{(1)} \rangle = 10$. Other parameters as in Fig. 3.4.

layers yields a larger coupling range for chimeras than multiplexing with a homogeneous layer. Furthermore, to demonstrate the robustness of (i) the emergence of chimera states in a sparse regular network layer upon multiplexing with an inhomogeneous layer, and (ii) shrinking of the range of ε for which chimeras are observed in a sparse regular network layer with increasing connection density of the inhomogeneous region, we consider a multiplex network consisting of a regular and a scale-free (SF) layer. The SF network is generated using the preferential attachment model [29]. For this arrangement as well, chimera states emerge in the sparse homogeneous layer upon multiplexing with another sparse SF network. Additionally, an increase in the average connectivity of the SF network $\langle k_{SF}^{(2)} \rangle$ yields a similar shrinking of the chimera regime in the sparse regular network layer (Fig. 3.7(b)). Furthermore, similar to the dense 1D-ER multiplex network, a 1D-SF multiplex network consisting of a dense regular network layer does not show any enhancement or suppression of the chimera state occurring in the regular network layer as compared to the corresponding single layer regular network regardless of the connection density of the layer that it is multiplexed with [101]. The reason behind the emergence of chimera states upon multiplexing with an inhomogeneous layer

in those sparse networks which do not exhibit chimeras upon multiplexing with a homogeneous a layer of the same average connectivity seems to lie in the existence of high degree nodes in the inhomogeneous layer. To obtain high degree nodes in a layer of a regular-regular multiplex network, one needs to enhance the average connectivity of the layer. Hence, we find chimeras for the sparse regular - dense regular multiplex network and do not observe chimeras when both homogeneous layers are sparse. Whereas for a 1D-ER multiplex network, even if both layers are sparse, there may be a large mismatch in the degrees of a few pairs of mirror nodes. For 1D-SF multiplex networks, multiplexing has a more pronounced effect which may arise from a higher degree mismatch for a few pairs of mirror nodes due to the existence of hub nodes in the SF layers (Fig. 3.6).

3.4 Conclusion

To summarize, we have shown that the occurrence of chimera state in a layer of a multiplex network depends not only on the coupling strength or the initial condition but also on the network architecture of the layers that it is multiplexed with. Multiplex networks with non-identical layers promote the appearance of chimeras in a sparse homogeneous layer. Furthermore, our investigations reveal that by controlling the node degree of one layer in the multiplex network, one can tune the coupling strength for which chimeras are observed in the other layer. Moreover, the behavior of chimeras in the layer with homogeneous coupling depends on the architecture of the other layers in multiplex networks. If both layers are homogeneous, multiplexing with a denser second layer promotes the occurrence of chimeras in the sparse first layer, whereas, if multiplexing is done with an inhomogeneous layer, it enhances the parameter range for the appearance of chimera states in the homogeneous layer even if both layers are sparse. The emergence of chimeras in networks upon multiplexing with an inhomogeneous layer as well as enhancement of the coupling range for which chimeras appear in the sparse layer is more prominent if multiplexing is done with a ScaleFree network. The results presented in this chapter may help us to gain deeper insight into the emergence and impact of chimera states

in real-world networks which inherently possess a multi-layer architecture.

Chapter 4

Enhancing chimera through inhibition

4.1 Overview

Chimera, referring to a hybrid state displaying coexistence of a coherent-incoherent dynamics, provide a powerful tool to understand the transition from incoherence to complete coherence [31, 32]. Recent literature has indicated a strong connection between the emergence of chimera state and neural activities of the brain networks [20]. For example, chimera state has been related to uni-hemispheric sleep in mammals where half of the brain remains asleep while other half remains active [76, 77] which is akin to the coexisting coherent and incoherent spatio-temporal patterns of chimera state. Moreover, various brain diseases have been linked to chimera states [104]. Recent literature has shown that spatio-temporal correlation profiles, obtained from EEG readings of ecliptic seizures, bore striking similarities with hybrid patterns of chimera state [81, 82].

In this chapter, we investigate another aspect of neuronal dynamics, which is inhibition. Inhibition means to restrain or to reduce some phenomena or actions. Inhibition plays a crucial role in various cognitive functions of brain [105, 106] as well

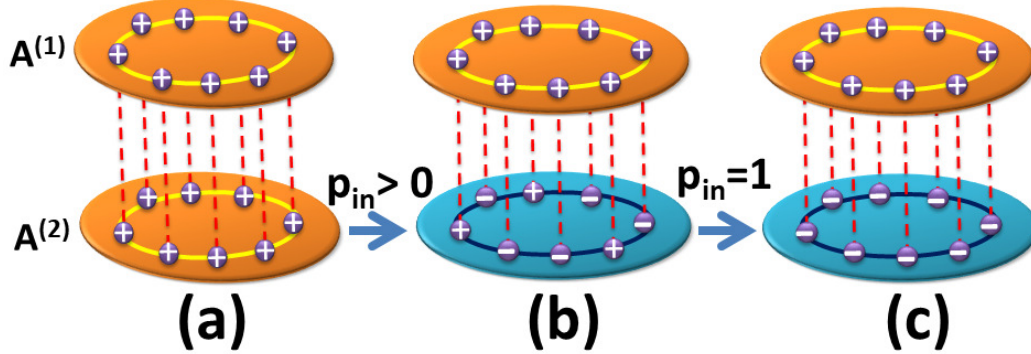


Figure 4.1: Schematic diagram of multiplex network consisting of two layers. Each layer is represented by identical regular network (S^1 ring), where each node (open circle) has the same coupling architecture. In the second layer of the multiplex network, nodes are (a) attractively coupled, (b) repulsively coupled with probability p_{in} , (c) all repulsively coupled corresponding to $p_{in} = 1$. Inter layer connections between two layers are represented as dashed lines.

as several biochemical functions in living bodies [107]. Furthermore, inhibition has also been considered in ecological networks to interpret complex predator-prey interactions among various species [108]. In the network literature, the inhibitory coupling is depicted by a repulsive coupling between the nodes of a network. A node is termed as an inhibitory node if all the edges connected to that node are inhibitory. Therefore, an inhibitory node inhibits or restrain the coupling influence from its neighbors. The repulsive couplings may either destroy a synchronized state leading to the incoherent evolution [110] or lead to an emergence of new synchronization regimes in addition to the multi-stability phenomenon [111]. The emergence of the chimera state under attractive and repulsive couplings in a globally coupled single-layer (monoplex) network has already been reported [43].

Here, we furthermore bring a different approach considering the more realistic multiplex framework. Specifically, we demonstrate the emergence of chimera state in one layer which can be controlled by changing the probability of repulsive couplings in another layer of a multiplex network. We present the impact of multiplexing of a layer having *inhibitory (repulsively coupled)* oscillators on the occurrence of chimeras in the layer having excitatory (attractively coupled) identical oscillators. We report that there exists an enhancement in the appearance of chimera

state in one layer of the multiplex network in the presence of repulsive coupling in the other layer. Additionally, we show that a small amount of inhibition or repulsive coupling in one layer is sufficient to yield chimera state in another layer by destroying its synchronized behavior.

4.2 Theoretical Framework

4.2.1 Dynamics on Network

Following the network architecture, considered in chapters 3 & 4, we consider a multiplex network where the architecture of individual layer is represented by a regular network (S^1 ; ring) network with periodic boundary conditions (Fig. 4.1). However, in this chapter, we use the famous Kuramoto oscillators [112] with diffusive coupling to showcase our findings. We express the temporal evolution of the underlying system by a state vector θ consisting of components θ_i , $i = 1, \dots, 2N$ representing phase of the i^{th} oscillator. Dynamical equation of the network state integrating the network topology can be written as follows [113]

$$\dot{\theta}_i = \omega_i + \lambda \sum_{j=1}^N \mathcal{A}_{ij} (\sin(\theta_j - \theta_i + \alpha)) \quad (4.1)$$

where ω_i depicts natural frequency of the i^{th} oscillator and λ represents the strength of the diffusive coupling. α is a constant phase lag parameter required for emergence of chimera state in a regular network of identical phase oscillators [2, 3]. We have considered a constant natural frequency $\omega = \omega_i \forall i$ for all oscillators to maintain identicity of the coupled units, a pre-requisite of definition of chimera states [2, 3].

4.2.2 Introduction of inhibition (repulsive coupling)

We again describe the architecture of the multiplex network \mathcal{A}) as,

$$\mathcal{A} = \begin{pmatrix} A^{(1)} & I \\ I & A^{(2)} \end{pmatrix}, \quad (4.2)$$

for a bi-layer multiplex network where $A^{(1)}(A^{(2)})$ represents adjacency matrix of the first (second) layer consisting of 1 or 0 entries depicting connected or disconnected pairs of nodes respectively.

We study the behavior of chimera state in the first layer ($A^{(1)}$) in the presence of repulsive couplings among the same pair of nodes in the second layer ($A^{(2)}$). In our multiplex framework, the first layer is attractively coupled (i.e., with all positive entries in the corresponding adjacency matrix $A^{(1)}$) and the second layer is repulsively coupled (i.e., with all negative entries in the adjacency matrix $A^{(2)}$). Henceforth, to avoid confusion, we will refer the first layer $A^{(1)}$ as a positive layer and the second layer $A^{(2)}$ as a negative layer. As per with the definition of the multiplex network (Eq. 4.2), we consider simple positive one to one coupling (identity matrix) for inter-layer interactions throughout the paper. Furthermore, we introduce inhibitory nodes in the second layer ($A^{(2)}$) by selecting a node (a row in $A^{(2)}$) with an probability (p_{in}). We name the probability as inhibition probability (p_{in}). Inhibition probability approximately decides the fraction of nodes in the second layer that will become inhibitory. For inhibition probability, $p_{in} = 1$, the second layer of the multiplex network becomes completely inhibitory or negative. Choosing a node to be inhibitory, leads to change in all the coupling associated to that node to inhibitory coupling (changing the signs of each 1 entry to -1 in the corresponding row of $A^{(2)}$). For an arbitrary chosen inhibitory node i ,

$$a_{i,j}^{(2)} = \begin{cases} -1 & \text{if } i \sim j \\ 0 & \text{otherwise} \end{cases}$$

We study occurrence of the chimera state in the first layer ($A^{(1)}$). The introduction of inhibition destroys the identical coupling environment of the second layer ($A^{(2)}$) except for $p_{in} = 1$ case where all couplings are negative. Due to this non-identical coupling in the negative layer, chimera state cannot be defined in the classical sense in that layer.

4.2.3 Identification of chimera

In chapter 3, we have provided a detailed discussion of the mathematical definition of the chimera and the correlation measure to identify the chimera state. However, we again provide a description for the correlation measure [34, 100] for identifying chimera in phase oscillators along with a figure describing the considered initial

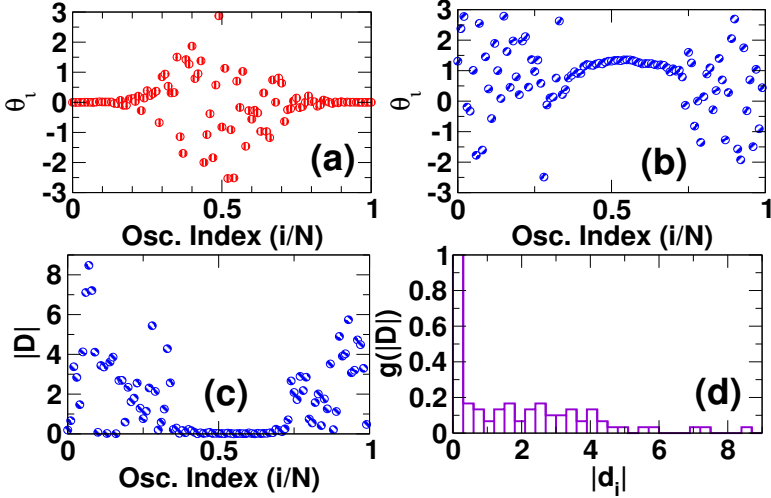


Figure 4.2: (a) Realization of the initial condition which is taken from a uniform random distribution multiplied by a Gaussian profile. The Gaussian is of the form $\theta_i(t=0) = \exp[-30(\frac{i}{N} - \frac{1}{2})]$. Same initial condition is considered for both the layers of regular - regular multiplex network, (b) Snapshot of spatial phase profile of kuramoto oscillators of the first layer of the multiplex network consisting of two attractively coupled layers, (c) Laplacian distance measure $|\bar{D}|$ of the spatial phase profile (d) normalized probability distribution function $g(|\bar{D}|)$ of the Laplacian distance measure $|\bar{D}|$. Parameters: Network size $N = N^1 = N^2 = 100$, node degree $\langle k^1 \rangle = \langle k^2 \rangle = 64$, coupling strength $\lambda = 1.29$, natural frequency $\omega = 0.5$ and lag parameter $\alpha = 1.45$.

condition, chimera state and the origin of the correlation measure, to enhance the comprehension in this chapter further. We have characterized the chimera state by studying the coexistence of spatial coherence and incoherence. The dynamical state of the network of phase oscillators can be mapped using the global order parameter [19]. However, to capture varying local dynamics for chimeras, we again adopt a correlation measure apt of identifying chimera states. We use a normalized probability distribution function $g(|D|)$ of the Laplacian distance measure $|D|$ and the correlation measure [100]

$$g_0 = \int_0^\delta g(|D|)d(|D|) \quad (4.3)$$

where $|D| = \nabla_i^2 \theta = \{d_i(t) : d_i(t) = |(\theta_{i+1}(t) - \theta_i(t)) - (\theta_i(t) - \theta_{i-1}(t))|\}$ depicts presence of a local curvature (signifying incoherence) in an otherwise smooth spatial profile (signifying spatial coherence (Fig. 4.2). Here, δ is a small threshold

value that sets a clear boundary between the coherent and incoherent states. Effectively, g_0 represents effective size of the coherent region in the spatial profile of θ at a particular time. The value of g_0 takes 0 for a complete incoherent state and 1 for the complete coherent state. A value between $0 < g_0 < 1$ theoretically signifies existence of coherence-incoherence i.e. the chimera state [34]. Though, the correlation measure g_0 identifies the chimera state, certain chimera states, for instance, breathing [62] or traveling [63] chimera, are known to depict regular repetitive patterns in the course of time evolution. A snapshot illustrates the chimera profile for only a fixed time point. To overcome this constraint, we have considered the average of the correlation measure g_0 over 1000 consecutive time steps after an initial transient. Further, we have used a uniformly distributed random number with a Gaussian envelop to satisfy special initial condition requirement of the chimera state for Kuramoto Oscillators as depicted in Fig. 4.2(a).

4.3 Results

We present results for dynamical evolution of coupled Kuramoto oscillators on multiplex networks with both layers represented by regular networks. In the first layer, all the nodes are attractively coupled, whereas in the second layer the nodes are connected via either attractive or repulsive coupling with the probability p_{in} deciding the population of inhibitory nodes.

4.3.1 Multiplexing with a completely inhibitory (repulsively coupled) layer

First, we consider a multiplex network where in one layer all nodes are positively (attractively) coupled and in another layer all nodes are negatively (repulsively) coupled. We particularly compare dynamical state of the positive layer for the following two cases; (I) a multiplex network consisting of two layers with attractive couplings in both the layers, and (II) a multiplex network with one attractive and one repulsive layer. For the case (II), all the entries in $A^{(2)}$ are negative corresponding to $p_{in} = 1$. We study changes in the oscillator dynamics in the positive layer when it is multiplexed with another positive layer (case (I)), with that of negative

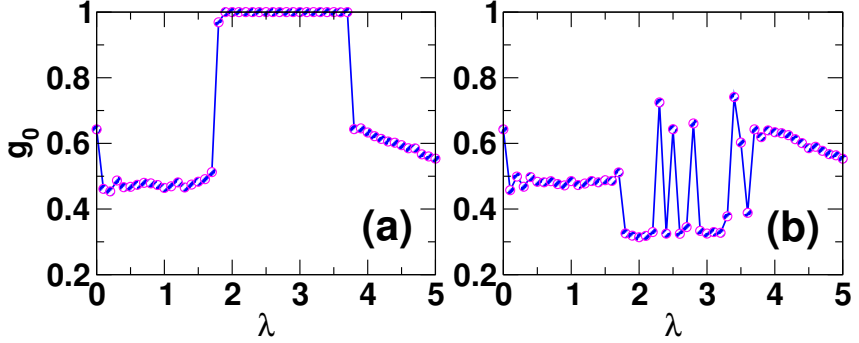


Figure 4.3: Normalized probability distribution function $g(|\bar{D}|)$ for the Laplacian distance measure $|\bar{D}|$ of the first layer of the regular-regular multiplex network consisting of (a) two positive layers, and (b) positive-negative layers. Parameters: Network size $N = N^1 = N^2 = 100$, node degree $\langle k^1 \rangle = \langle k^2 \rangle = 64$, natural frequency $\omega = 0.5$ and lag parameter $\alpha = 1.45$.

layer (case (II)). Note that, due to the symmetric coupling environment for both the layers in the multiplex network, we can define chimera state for both the layers separately in this particular combination (i.e. for $p_{in} = 1$). Fig. 4.3 plots the correlation measure indicating the range for appearance of chimera state as a function of coupling strength. We find that for lower coupling values, for both the cases, positive layer shows chimera state as depicted by $0 < g_0 < 1$ values of the correlation measure ($g_0 \approx 0.64$) at coupling strength $\lambda = 0$ arises from the fact that without the coupling, the oscillators evolve with their constant natural frequency resulting in the same spatial profile considered for the special initial condition.

Interestingly, we observe a contrasting behavior in the middle coupling range ($2 \lesssim \lambda \lesssim 4$). For the case (I), the oscillators demonstrate a transition to the synchronized state represented by $g_0 = 1$ whereas the case (II) demonstrates an intermediate correlation value ($0.3 \lesssim g_0 \lesssim 0.7$) representing the chimera state. Fig. 4.4 (a) & (e) exhibit a completely synchronized state in the positive layer when multiplexed with another positive layer (case (I)). Fig. 4.4(b) & (f) show a chimera state in the positive layer upon its multiplexing with a negative layer (case (II)). Furthermore, Fig. 4.4(c)& (d) provide another illustration of this destruction of synchrony and an enhancement in the chimera state for different coupling strength. Fig. 4.4(e)-(h)

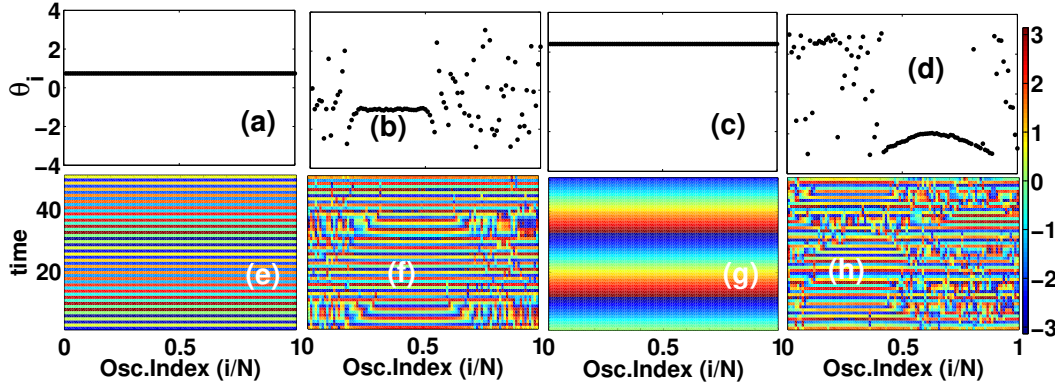


Figure 4.4: Snapshots and spatio-temporal patterns depicting emergence of chimera in positive layer upon multiplexing with a negative layer. The regular-regular multiplex network consists of (a,c,e,g) two positively coupled layer, (b,d,f,h) positively and negatively couples layers. (a,b,c,d) presents a snapshot of the spatio-temporal patterns presented in (e,f,g,h) respectively. The figures represents emergence of chimera in case of multiplexing with negative layer at coupling strength $\lambda = 1.86$ (a,b) and at $\lambda = 3.7$ (c,d). Other parameters are same as Fig. 4.3

represent the spatio-temporal patterns corresponding to Fig. 4.4(a)-(d), respectively, indicating that the emerged chimera state is stable with time. Moreover, the completely synchronized state for the case I demonstrate a periodic temporal evolution [114]. Replacing one positively coupled layer with a negatively coupled layer makes the stable periodic evolution unstable leading to a hybrid spatial chimera pattern [114]. This observation highlights the importance of repulsively coupled layer which causes an occurrence of chimera state in a attractive coupled layer due to the multiplexing.

4.3.2 Multiplexing with a partially inhibitory (repulsively coupled) layer

Next, we investigate the impact of inhibitory nodes in one layer on the emergence of chimera state in another layer. Again, we consider a multiplex network consisting of two layers where first layer ($A^{(1)}$) has all positive couplings (thus termed as positive layer). The inhibitory nodes are introduced in the second layer ($A^{(2)}$) with inhibition probability p_{in} . Fig 4.1 (c) depicts a schematic diagram of such arrangement in multiplex network and Fig. 4.5 (a) shows plot of a multiplex adjacency matrix where inhibitory nodes (represented by black lines in right-down block) are introduced

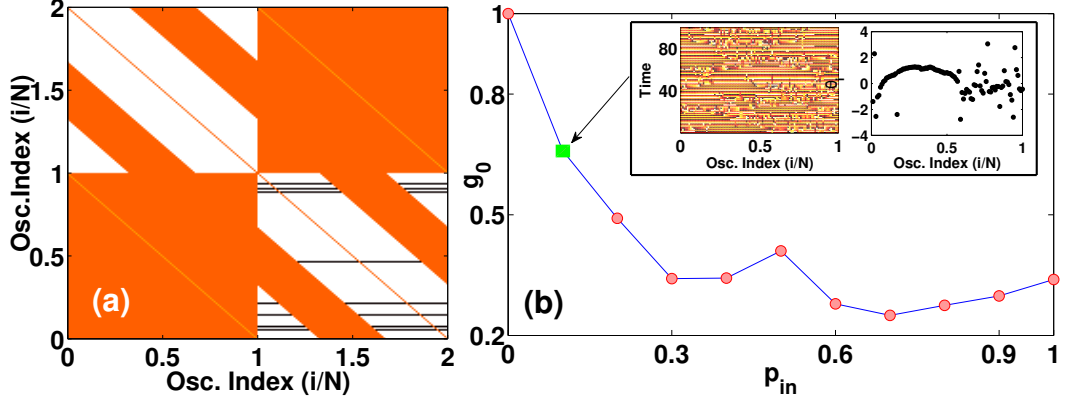


Figure 4.5: (a) Plot of the adjacency matrix of regular-regular multiplex network consisting of one positive and one inhibitory layer with inhibition probability $p_{in} = 0.1$. The black lines in the down-right block represents the rows corresponding to inhibitory nodes. (b) Normalized probability distribution function $g(|\bar{D}|)$ of the Laplacian distance measure $|\bar{D}|$ of the positive layer as a function of inhibition probability p_{in} . Inset: Snapshot and spatio-temporal profile of the first layer of a multiplex network consisting of one positive layer and one inhibitory layer. Parameters: Coupling strength $\lambda = 3.57$, Inhibition probability $p_{in} = 0.1$, Other parameters are same as Fig. 4.3.

with an inhibition probability $p_{in} = 0.1$. In this setup, a particular pair of nodes in $A^{(2)}$ may interact via either positive or negative couplings decided by p_{in} . We find that an introduction of even a small number of the inhibitory nodes is sufficient to destroy synchronized regime in $A^{(1)}$ and causes an enhancement in the range of couplings strength for which chimera is appeared in the positive layer. Fig. 4.5 depicts variation of the correlation measure with respect to the inhibition probability p_{in} for a sufficient large coupling strength ($\lambda = 3.57$). Two extreme situations, i.e. $p_{in} = 0$ and $p_{in} = 1$ correspond to a completely synchronized state ($g_0 = 1$) and a chimera state ($g_0 \approx 0.34$) respectively, which is not surprising as discussed in the previous section. However, the interesting fact is that even a small amount of inhibition in the repulsive layer (say $p_{in} = 0.1$) is sufficient to yield a non-zero correlation value ($g_0 \approx 0.65$) for the attractive layer depicting chimera state. Inset figures of Fig. 4.5 manifest this phenomena of appearance of the chimera state at low inhibition probability.

4.4 Conclusion

To summarize, we have explored an impact of inhibitory (repulsive) coupling in one layer layer on dynamical behavior of another layer in a multiplex network. We have systematically studied impact of inhibition by inserting inhibitory nodes with a probability p_{in} which is varied from zero to one. The case p_{in} being zero corresponds to a multiplex network consisting two identical layers with each layer having attractively coupled nodes. The another extreme case p_{in} being one corresponds to a multiplex network consisting of two layers which are structurally identical but vary in the nature of coupling, i.e., one layer has all attractively coupled nodes whereas another layer has all repulsively coupled nodes. We report that the range of parameters for which chimera is demonstrated in one layer can be controlled by changing probability of inclusion of inhibitory coupling in another layer. Importantly, we found that a very small number of inhibitory nodes can bring an enhancement in the appearance of chimera state destroying the synchronized state. These results promote importance of the multiplex framework to model those real-world complex systems which posses more than one type of interactions among their constituents.

Chapter 5

Engineering Chimera states

5.1 Overview

The emergence of the chimera state provides a powerful tool to study the dynamical path from asynchrony to complete synchrony and help to probe deeper into the mechanism of partial synchronization [31, 32]. Further, due to its new-found importance, special attention has been paid [116–122] to the emergent partial synchronous patterns of chimera states. There have been persistent efforts to control the chimera states [65–67]. In preceding chapters, several approaches are presented on controlling the parameter regime for which, the chimera state appear employing using several factors such as system-wide delay, and others [34, 53].

In this chapter, we approach the problem of managing the chimera states by introducing heterogeneous delay on the edges of both monoplex (single layer) and multiplex (multi-layer) network. The presence of heterogeneous delays in a network represents a more realistic scenario in the context of real-world complex systems. Due to the finite speed of information transmission, delay naturally arises between the nodes interacting through edges. Moreover, since the connection channels are

subjected to non-identical perturbations from its surroundings, the heterogeneously delayed interactions between nodes are a naturally occurring phenomenon.

Here, we demonstrate that the chimera state can be engineered in initially completely coherent dynamical state, by installing heterogeneous delays in a fraction of intra- and inter- layer links in sequence for monoplex and multiplex networks, respectively. We first demonstrate that the position and the extent of the region(s) of incoherence, thus, in turn, the chimera state can be controlled by suitably introducing the heterogeneous delays in sequence in intra-layer connections in a particular portion of the monoplex network.

Furthermore, We extend the recipe to engineer the chimera state in multiplex networks by introducing heterogeneous delays in a fraction of inter-layer links, referred to as multiplexing-delay, in a sequence. Additionally, we show the emergence of the incoherence in the chimera state can be regulated by making an appropriate choice of both inter- and intra-layer coupling strengths, whereas the extent and the position of the incoherence regime can be regulated by appropriate placing and strength of the multiplexing delays.

We also show that such manufactured chimera is independent of initial conditions, which is otherwise conventionally mandatory for the existence of chimera in coupled maps. Additionally, we introduce an entirely new way to detect the chimera by borrowing an eigenvector localization measure from spectral graph theory.

5.2 Theoretical Framework

Here, we again provide a brief description of the chimera and the networks for ease of reading the results presented in this chapter.

5.2.1 Chimera state

A chimera state is defined as a hybrid dynamical state consisting of coexisting coherent and incoherent domains that appear in structurally symmetric networks. As mentioned, we consider a regular network architecture with the periodic boundary condition (S^1 ; ring) to showcase the occurrences of the chimera state. The coherent

dynamical state on the network can be expressed as [52]

$$\lim_{N \rightarrow \infty} \sup_{i,j \in U_\xi^N(l)} |x_i(t) - x_j(t)| \rightarrow 0 \text{ for } \xi \rightarrow 0 \quad (5.1)$$

where $U_\xi^N(l) = \{j : 0 \leq j \leq N, |\frac{j}{N} - l| < \xi\}$ represents the neighborhood of a node in regular(ring) network ($l \in S^1$). Thus, the dynamical state assumes a profile such that all the nodes possess low spatial distance with their neighbors, approaching a smooth spatial curve of a coherent state in the asymptotic limit of $N \rightarrow \infty$. Any break in the profile,i.e., high spatial distance in neighboring nodes, is denoted as the incoherence [34]. Therefore, the snapshots or the spatial curves refer to a chimera state if a smooth region (the coherent part with closely placed neighboring nodes) coexist with a region characterized by scattered points (the incoherent part with distantly placed neighbors). Furthermore, a complete coherence can be attributed to the state when all nodes assume the same constant value with zero spatial distance in neighbors, thus producing a straight spatial curve [34, 113].

5.2.2 Construction of networks

In the current chapter, we focus on demonstrating chimera in both monoplex and multiplex networks, arising due to distinct time-delays present in a fraction of the intra- and inter-layer links, respectively. To achieve this, we consider first consider a monoplex network with regular connection architecture (S^1 : ring) consisting of N nodes. The monplex network is represented by adjacency matrix A such that [34]

$$A_{i,j} = \begin{cases} 1 & \text{if } i \sim j \\ 0 & \text{otherwise} \end{cases} \quad (5.2)$$

Furthermore, we construct an undirected multiplex network from two identical regular networks, each having N nodes. Two layers of the multiplex network are encoded by a set of adjacency matrices $\{A_1, A_2\}$, hence multiplex network \mathcal{A} can be expressed as [54]

$$\mathcal{A} = \begin{pmatrix} A_1 & D_x I \\ D_x I & E_y A_2 \end{pmatrix}, \quad (5.3)$$

where I is an identity matrix representing links between one-to-one mirror nodes in two layers. The parameter D_x represents multiplexing strength by which a node

and its counterpart in another layer impact each other's dynamics. The parameter E_y denote a scaling parameter for intra-layer coupling strength of a layer [115]. We define coupling matrix as $C = \varepsilon A$, for monoplex networks and $C = \varepsilon \mathcal{A}$, for multiplex networks. The element C_{ij} denotes the effective coupling strength between i^{th} and j^{th} nodes with $\varepsilon \in [0, 1]$ representing the overall coupling strength. sm

5.2.3 Dynamical evolution on networks

The dynamical state of the nodes at time t can be represented by a real variable $x_i(t) \in \mathbb{R}, \forall i = 1, \dots, N$. The time evolution of the dynamical state of nodes can be written in terms of a time discrete map $x_i(t+1) = f(x_i(t))$ where we consider famous logistic map $f(x) = \mu x(1-x)$ in chaotic regime ($\mu = 4.0$) [26] as local dynamics. The simplistic framework of logistic map [25] have been used to understand diverse spatio-temporal phenomena in a wide range of real world networks among which chimera has also been shown in both single [52] and multiplex [53, 54] networks. Adding the network architecture, the dynamical evolution equation for the whole network can be written as [54]

$$x_i(t+1) = f(x_i(t)) + \frac{1}{(k_i)} \sum_j C_{ij} [f(x_j(t - \tau_{ij})) - f(x_i(t))] \quad (5.4)$$

where $i = 1, \dots, N$, for monoplex networks and $i = 1, \dots, 2N$ for multiplex networks, respectively. $k_i = \sum_j C_{ij}$ describe the normalizing factor. We furthermore introduce delay in the dynamics by delay matrix τ whose symmetric element $\tau_{ij} = \tau_{ji}$ represents delay between i^{th} and j^{th} node. The entries of the delay matrix τ depends on the intended investigation.

5.2.4 Delay driven engineering scheme

A chimera state refer to a hybrid state consisting of a coherent region (CR) and an incoherent region (ICR) which coexist simultaneously. Here, initially we engineer chimera state in monoplex networks by introducing delays in sequential intra-layer links (Fig. 5.1 UP). Therefore, the delay matrix τ is represented by a $N \times N$ matrix whose elements describe the delays between the nodes of the network. In the case

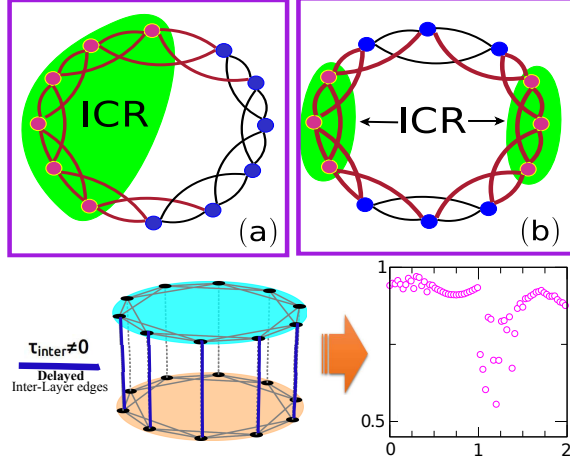


Figure 5.1: Schematic diagram of the proposed engineering scheme for designing the incoherent region (ICR) and, in turn, the chimera state in single layer (upper panel; UP) and multiplex network (lower panel; LP). Parameters are $N = 100$, $\langle k \rangle = 64$ for both single-layer network and for individual layers of the multiplex network.

of homogeneous delay, τ_{ij} takes the same value for all the edges of the network, Whereas τ_{ij} is a random variable taken from a uniform distribution bounded by $0 \leq \tau \leq \tau_{max}$ for heterogeneous delay case where delayed nodes are placed in particular spatial positions of the network. Thus, τ_{max} represents the upper limit of the random entries of the delay matrix. Note that a delayed node means the node with all the edges originating from it is delayed (Fig. 5.1 UP).

Furthermore, we design a chimera state in a multiplex network by choosing a fraction N_τ of the inter-layer links in a sequence (Fig. 5.1 LP). Each chosen link is then assigned a delay value selected uniformly randomly in the range $0 \leq \tau_{ij} \leq \tau_{max}$. Note that, for the present case, the symmetric upper right and lower left blocks I of the adjacency matrix \mathcal{A} possess the inter-layer delayed links.

5.2.5 Spatial Inverse participation Ratio (sIPR): A measure for identification of chimera

Due to the peculiarity of the spatial profiles of chimera state, a plethora of measures had been put forward in literature [53, 96, 100, 123]. In this chapter, we propose a new measure borrowed from the eigenvector localization concepts [124, 125] of the spectral graph theory. The inverse participation ratio (IPR), in the classical sense, refers the contribution of elements in a eigenvector(state) [126–128]. Following the trend, we define the spatial inverse participation ratio (sIPR) as

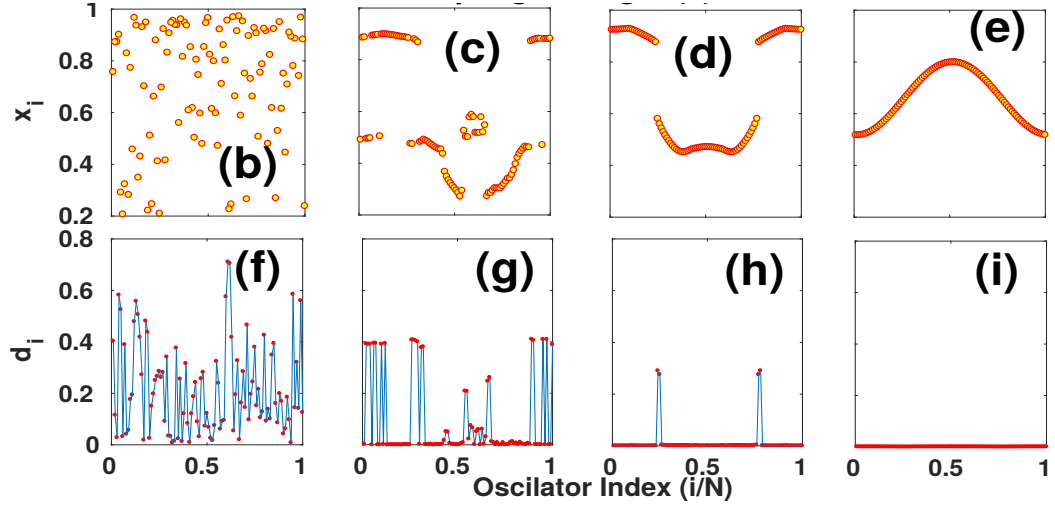


Figure 5.2: Diagrams representing (b)-(e) snapshots of the state variable (x_i) and (f)-(i) Laplacian distance variable (d_i), respectively, for different dynamical states for the regular network (S^1 ring) corresponding to various sIPR values as mentioned; [(b) and (f)] for $\varepsilon = 0.1$ and sIPR = 0.029, [(c) and (g)] for $\varepsilon = 0.34$ and sIPR = 0.048, [(d) and (h)] $\varepsilon = 0.4$ and sIPR = 0.25, [(e) and (i)] $\varepsilon = 0.76$ with sIPR = 0.015, where ε is the coupling strength as mentioned Eq.5.3 and coupling matrix as $C = \varepsilon A$. Other parameters are same as Fig.5.1.

$$sIPR = \frac{\sum_i (\langle d_i \rangle_t)^4}{\{\sum_i (\langle d_i \rangle_t)^2\}^2} \quad (5.5)$$

where $d_i = |(x_{i+1}(t) - x_i(t)) - (x_i(t) - x_{i-1}(t))|$. $\langle d_i \rangle_t$ depicts an average value of d_i over time. Overall d_i present a discrete second-order differentiation (Laplacian in general) representing the relative spatial distances between neighboring nodes. A high value of d_i corresponds to a large spatial gap between the neighbors of the i^{th} node, appearing as a discontinuity in the spatial profile (in $x_i - i$ plane), whereas a low value of d_i indicates that the i^{th} node is spatially close to its neighboring nodes. If all the d_i take high values, It represents the incoherent state where all neighboring nodes have large spatial distance between them. If all the d_i take low value, it corresponds to the coherent state where all the neighboring nodes are close by and form a smooth spatial profile (Fig. 5.2) [34, 113]. However, for both the cases, the participation of the elements are similar, i.e., all of the entries of d_i for different nodes are either high valued or low valued. This data trend of similar entries results in a low value of sIPR as dictated by the definition of the traditional IPR ((Fig. 5.2))

[124, 125].

Now, if for a particular system's parameter, d_i is high for few nodes and low for few other nodes, it indicate a chimera state where few nodes are spatially close forming CR (with low d_i values) and few others are spatially scattered forming the ICR (with high d_i values). Therefore, for hybrid patterns of chimera state, nodes forming the CR takes low d_i values, whereas the nodes in ICR produce high d_i values (Fig. 5.2) [53, 54]. This breaks the data trend of similar values in d_i , and we demonstrate that this break in the trend can be picked up by the sIPR value and can be used to identify the chimera states. Therefore, a high value of sIPR shows the presence of both high and low d_i entries denoting the coexistence of CR and ICR, forming a chimera state. On the other hand, a low value of sIPR denotes all entries of d_i are either high or low, representing an incoherent and a coherent state, respectively (Fig. 5.2).

Traditionally, the IPR value of a eigenvector for a network of dimension N is bound by $\frac{1}{N} \leq IPR \leq 1$ [124, 125]. We demonstrate that the incoherent or coherent states produce sIPR values close to $\frac{1}{N}$, Whereas the chimera state produces a significantly higher value of sIPR. Due to the lower bound of the IPR, the sIPR automatically assumes the value $\frac{1}{N}$ (with N being network size) for a non-chimera state without needing any threshold value unlike other measures of chimera state [96]. A point to note here that, due to the low values of d_i for the coherent states, sIPR value may become undefined. In that case, we manually set the IPR value as $\frac{1}{N}$ to maintain the similarity. To summarize, sIPR captures the similarity or dissimilarity in the values of d_i to identify chimera state such that it yields values closer to $\frac{1}{N}$ for the coherent or incoherent case. In contrast, it produces a high value for the chimera state.

5.3 Results

5.3.1 Engineering chimera state with heterogeneous delay in the single-layer network

Information transfer between a pair of interacting nodes takes a finite propagation time to reach from one node to another node. Therefore, a delayed interaction, particularly heterogeneous delay, is an intrinsic property of several natural and artificial

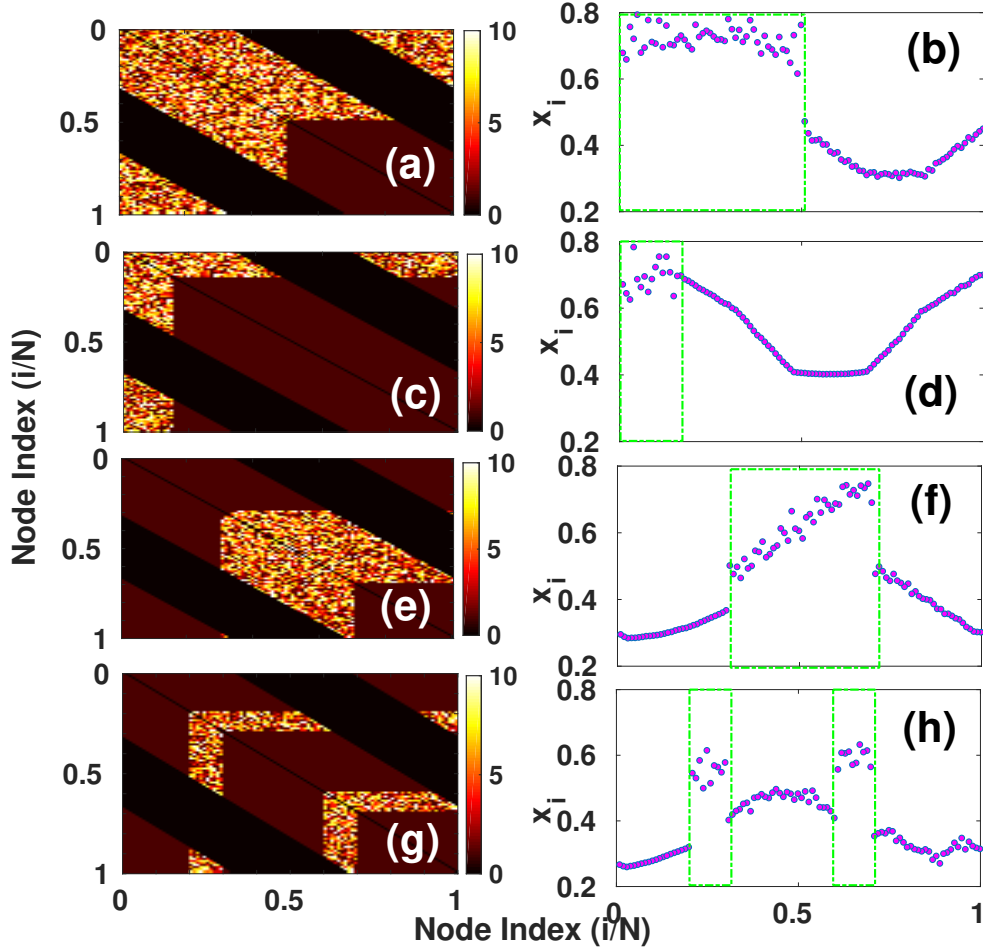


Figure 5.3: Delay matrices and corresponding snapshots of chimera state engineered by heterogeneously distributed delays. The delay matrices are overlaid with the adjacency matrices to showcase both the delayed and the undelayed edges. (a) & (c) Regular network with a large and relatively smaller cluster of the delayed nodes, respectively. These delay configurations result in a large ICR denoted in (b) and a smaller ICR in (d). (e) & (f) Delay configuration and a corresponding snapshot of a chimera state, respectively, with different locations of the ICR. Note due to the S^1 symmetry of the regular ring lattice, the positions are not unique. (b), (d), & (f) correspond to schematic diagram Fig. 5.1 UP(a), and (g) and (h) represent two delayed clusters resulting in the multi-chimera state, corresponding to the schematic diagram Fig. 5.1 UP(b). The (green) boxes represent clusters of the delayed nodes introduced in the network. Other parameters are $\varepsilon = 0.77$, $\tau_{max} = 10$ and rest are same as Fig. 5.1.

networks [27]. For example, in an aircraft network, travel time between two airports is subjected to weather conditions leading to heterogeneous delays in the system. Similarly, in a bio-chemical PPI network, the interaction time between two proteins is subjected to its chemical environment. Here, we investigate the impact of heterogeneously distributed delay in a network on the occurrence of chimera states. There are several investigations on controlling the positions of the CR/ICR, to produce custom-made chimera patterns [65–67]. We approach this problem of controlling chimera by introducing delayed nodes in the network. The delayed node means all the edges originating from that node has a delay selected randomly between 0 to τ_{max} . We choose a value τ_{max} such that it is larger than the intrinsic time scale of the underlying dynamical system, which is unity in the case of time -discrete logistic map considered here [130]. Here we show that the position of the ICR can be controlled by suitably placing the delayed nodes in a preferred spatial location. Furthermore, this scheme does not depend on the choice of the τ_{max} (See [129]). A schematic diagram depicting the protocol for delay distribution on the nodes of a regular ring network is presented in Fig. 5.1 UP. Fig. 5.1 show the clusters containing the delayed nodes (denoted by red circles in the shaded region) contributing to the ICR (corresponding to the spatial profiles depicted in Fig. 5.3 (b) & (h)). Fig. 5.1 UP(a) presents the case where a cluster consisting of neighboring nodes are heterogeneously delayed. This design produces a chimera state with one ICR and one CR (Fig. 5.3 (b)). Whereas, Fig. 5.1 UP(b) presents the case of two clusters of delayed nodes producing multiple ICRs separated by a CR (Fig. 5.3(h)).

Fig 5.3 presents different types of chimera states with a corresponding delay matrix profile, which is engineered based on our desired output. Fig 5.3(a) presents a color profile of the delay matrix. The heterogeneous delays are introduced in half of the nodes, which are clustered together in the terminal position. This protocol results in a chimera state with one CR and ICR, as depicted in Fig 5.3(b). Note that the exact position of the ICR coincides with that of the delayed nodes (green boxes in Fig. 5.3). To highlight the effect, we consider a similar delay matrix as for the previous example, however, with less number of the delayed nodes (Fig 5.3(c)).

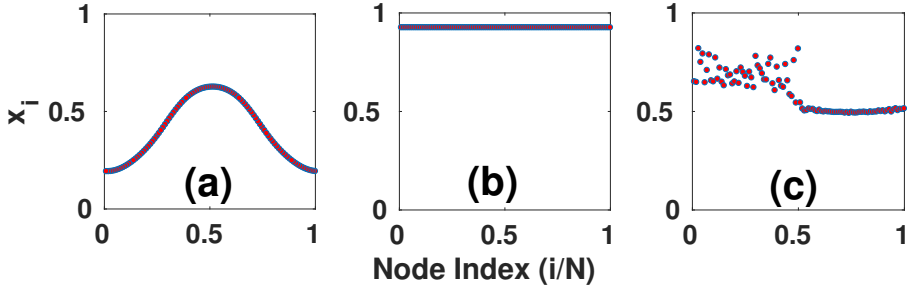


Figure 5.4: Snapshots of the dynamical state of the regular network for different delay configurations with (a) being no delay configuration, (b) being homogeneous delay ($\tau = 1$) case, (c) being heterogeneous distributed delays case ($\tau_{max} = 10$). Note that the typical spatial profile for chimera state is visible for (c). Other Parameters are $\varepsilon = 0.61$ and rest are same as Fig. 5.1

As expected, the spatial profile of the chimera state contains a reduced ICR at the position coinciding with the position of the delayed nodes. This dependence of the ICR on the position of delayed nodes holds good even if we introduce a delay in the central part of the spatial profile, as depicted in Fig 5.3(e) and (f), which results in one ICR bounded by two CRs. We further demonstrate that by appropriate engineering of the delay matrix, we can produce multi-chimera states with multiple ICRs. Fig 5.3(g) shows that the delays are introduced in the terminal positions separated by a region of undelayed nodes. This brings forward a multi-chimera state with two ICRs separated by a CR (Fig 5.3(h)).

Therefore, the location of the ICR(s) can be controlled by adopting the appropriate protocol of distribution of delays on the edges of the network. Note that due to S^1 symmetry of the regular ring network considered in this paper, there is no unique position of the nodes. However, we have referred to the unique numerical naming of the nodes (node number 1 to node number N) to refer their positions for an easy depiction of our results. The relative positions of the single-cluster or multi-cluster chimera state reflect that an appropriate distribution of heterogeneous delay can accurately engineer the spatial profile of the chimera states regardless of the nomenclature of the nodes.

5.3.2 Impact of the heterogeneous delay

The previous section demonstrates that the chimera patterns can be engineered by suitable placement of the heterogeneous delays. However, this fine control is possible only in the high coupling regions. In these regions, the chimera state does not appear for the undelayed or homogeneously delayed case. Furthermore, a protocol of distribution of heterogeneous delays on all the nodes of a network, i.e., all the nodes in the network are delayed, also does not produce the chimera states. For this protocol, a direct transition from the incoherent to the coherent states takes place. In the following, we present an elaborate discussion of this point.

For the partial heterogeneous delay case (i.e., only a few nodes are delayed), an incoherent evolution is observed in the weak coupling region, followed by a chimera state in the mid coupling range. This chimera state appearing in the mid-coupling region is completely random and cannot be controlled using the appropriate placement of the delays. However, the high coupling range yield a drastic change in the dynamical evolution and we achieve a direct relationship between the position of delayed nodes and ICRs. Note that, for both the protocols of the undelayed and homogeneously delayed networks, the high coupling regions yield a coherent dynamics [53] as depicted in Fig 5.4(a) and (b). Fig 5.4(c) demonstrates a chimera state in the same region engineered by suitably placed heterogeneous delays. Therefore, we can conclude that the heterogeneous delays not only can lead to an enhancement in the parameter region for which chimera states appear but also offer control in a limited parameter regime where we can produce tailor-made chimera patterns.

Furthermore, we find that a complete envelopment of edges by heterogeneous delays can be harmful to the chimera states. In the previous section, we demonstrated that the ICR coincides with the heterogeneous delayed nodes. Using this approach, we had shown that the production of both single and multi-cluster chimera states could be achieved. However, we had found that if heterogeneously distributed delays span over all the edges in the network, the chimera state is ceased to exist. Fig 5.5(a) presents a typical sIPR profile for a homogeneous delay case. We observe a transition from the incoherent to the coherent state via a chimera state. The mea-

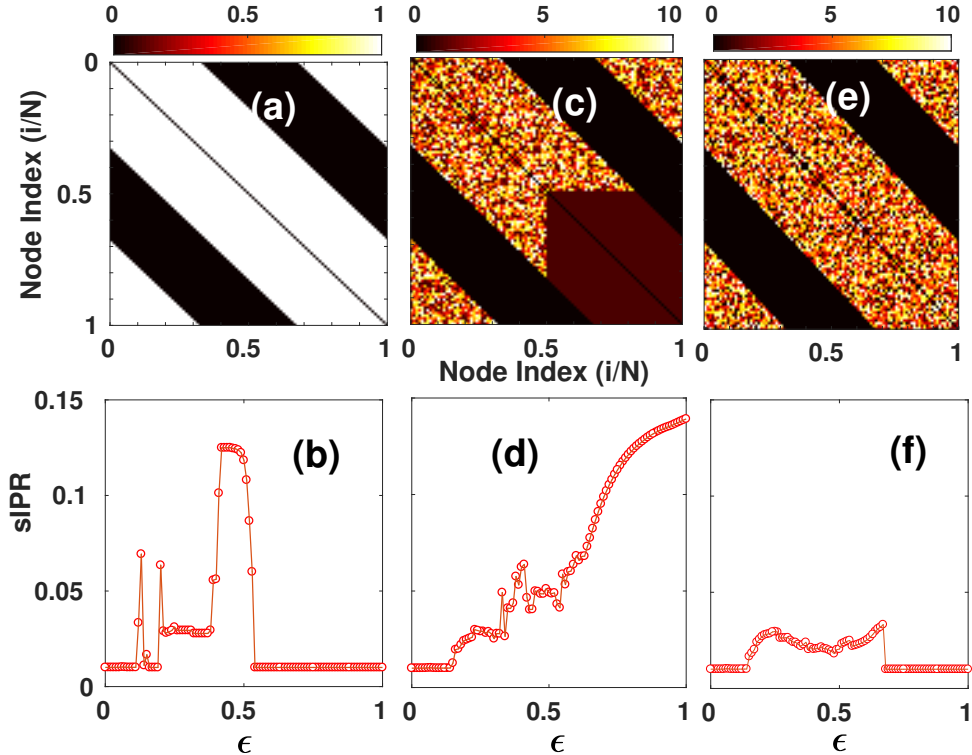


Figure 5.5: Delay matrices, representing the heterogeneous delay induced in the network and corresponding sIPR profile for the delay configuration. the delay matrices are overlapped with the adjacency matrices to show both the delayed and the undelayed edges. (a) A network with homogeneous delay ($\tau = 1$) with a typical color profile for regular network adjacency matrix, (b) sIPR profile indicating incoherent, chimera, and coherent states, respectively. (c) Delay matrix with partial heterogeneous delay represented by the mosaic pattern extended by shaded region representing edges with no delay. (d) sIPR profile indicating incoherent and subsequent chimera state (e) Delay matrix with full heterogeneous delay represented by mosaic pattern inhibiting whole adjacency matrix (f) sIPR profile with direct incoherent to coherent transition. Other parameters are $\tau_{max} = 10$ (for c & e), and rest are same as Fig. 5.1.

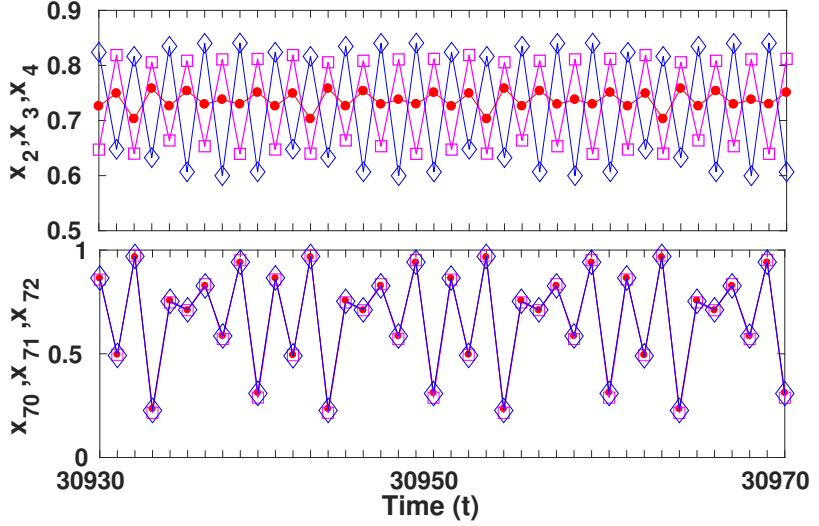


Figure 5.6: Time series of delayed and undelayed nodes of a regular ring network. A snapshot of the nodes (2,3,4,70,71,72) at a particular time can be found in Fig. 5.10(c) presenting an engineered chimera state. Time series of the node number 2,3,4 with heterogeneous delays demonstrate a non-synchronized evolution whereas bottom figure plots time series of undelayed nodes 70,71,72 showing a synchronized evolution. Other parameters are the same as in Fig. 5.4.

sure sIPR cannot clearly distinguish between the completely incoherent and a completely coherent state. For example, Fig. 5.4(b) presents that homogeneous delays (corresponding delay matrix is depicted in Fig. 5.5(a)) renders the coherent state for the high coupling region. Fig. 5.5(b) presents the enhanced parameter regime for the appearance of chimera states in the partial heterogeneous delay case where we can also observe chimera state in the high coupling regimes, as demonstrated in Fig. 5.3 & Fig. 5.4. However, Fig. 5.5(c) shows that sIPR profile maintains a low value regardless of the coupling strength, reflecting a direct transition from the incoherent to the coherent dynamics. This observation reflects that not only the introduction of delays but also the exact number of the delayed nodes in a network affects the CR and ICR distributions. As we increase the number of heterogeneously delayed nodes, the ICR expands shrinking the CR. However, for a large number of nodes having heterogeneous delays, the perturbation spreads in the entire network destroying the cohesion of the CR. This can be easily understood from Fig. 5.1 (UP), where the neighboring nodes of the delayed cluster (green shaded region) posses

some undelayed and some delayed edges. This imposes a dynamical “tug-of-war” onto the neighboring nodes. For a sufficiently large delayed node cluster, the relatively small undelayed nodes loose coherence and converts the small CR into ICR and hence chimera state lost.

This investigation indicates that partial heterogeneous delays play a crucial role in the emergence of the chimera states. The influence of delayed nodes in the engineering of the chimera state can be explained by comparing the time evolution of the delayed with those of the undelayed nodes. At high coupling values, the undelayed nodes reach a coherent state, and the delayed nodes lag due to the existence of the heterogeneous delays. Fig. 5.6 demonstrates a typical time series of the six nodes belonging to ICR (Node 2,3, & 4) and CR (Node 70,71,72), respectively, as depicted in Fig. 5.10(c). The time series of undelayed nodes (node number 70,71,72) reflect a coherent synchronous evolution (bottom subfigure of Fig. 5.6) whereas heterogeneously delayed nodes (node number 2,3,4) evolve in an incoherent fashion producing a coherent-incoherent hybrid dynamical state referred to as chimera. The disorderly “phase lags” introduced by the heterogeneous delays result in the ICR. Note that an arrangement of partial homogeneous delays will produce two clusters of nodes having a fixed lag between them. This, in turn, manifests in two CRs separated by a point discontinuity. To avoid such spatial states, we have considered a heterogeneous delay in our demonstration.

5.3.3 Engineering chimera state with multiplexing-delays in the multiplex network

In this section, we explore the emergence of chimera state in the multiplex network due to the presence of multiplexing-delays, i.e., delays in sequential inter-layer links in multiplex networks. Furthermore, we demonstrate how the emergent chimera can be regulated by means of structural parameters of the multiplex network. For all the simulations, we introduce heterogeneous delays $\tau \in (0, \tau_{max} = 20]$ drawn from a uniform random distribution, at half of the inter-layer links $N_\tau = N/2$ chosen sequentially, unless otherwise mentioned elsewhere. An identical set of initial states for the two layers give rise to identical states for both the layers [54]. Hence

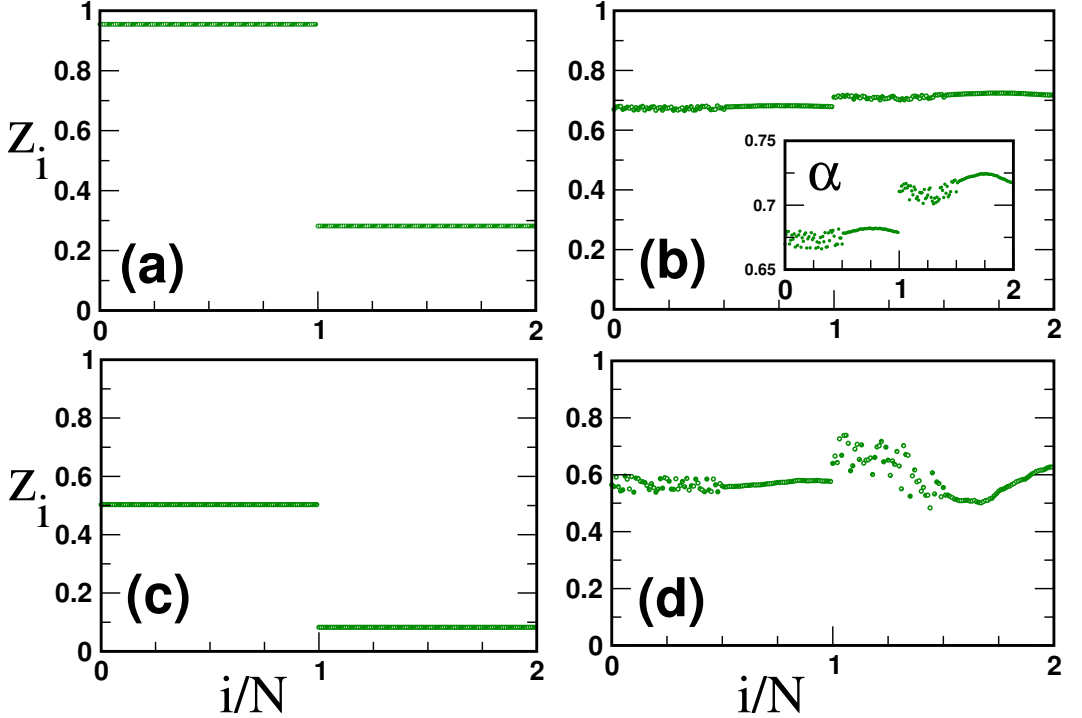


Figure 5.7: Snapshot profiles of the two layers of the multiplex network for (a) the undelayed interlayer links, (b) the delayed interlayer links with parameters $D_x = 1, E_y = 1$ and similarly, (c) the undelayed interlayer links, and (d) the delayed interlayer links with parameters $D_x = 1, E_y = 0.6$. The inset curve ($b(\alpha)$) displays the slight disturbance in (b) in the magnified Y-axis. The parameters are $\varepsilon = 0.9, \tau_{max} = 20, r = 0.32, N = 100$ in each layer.

to demonstrate the robustness of our technique we have opted two distinct sets of initial states for the maps, which are selected randomly $z \in [0, 1]$ for the two multiplexed layers. The system of networked maps is updated for a sufficiently large time 5×10^4 , and the snapshot of final states of all the nodes for both the layers is recorded. The coupling parameter is kept fixed at $\varepsilon = 0.9$, so that the system of networked maps initially remains in the coherent state as shown in the Fig.5.7(a) when there is no delay present in the system ($\tau_{i,j} = 0; \forall i, \forall j$). Fig. 5.7(b) presents the dynamical profile of the multiplex network in which the induction of delays leads to a slight disturbance (Fig. 5.7(b); inset α) in the pattern of coherent state of the nodes. However, no chimera pattern is observed in this case. The reason is that both the multiplexed layers are dense networks, and the mirror nodes which are connected by delayed interlayer links are also connected to a large number of neighbors by un-

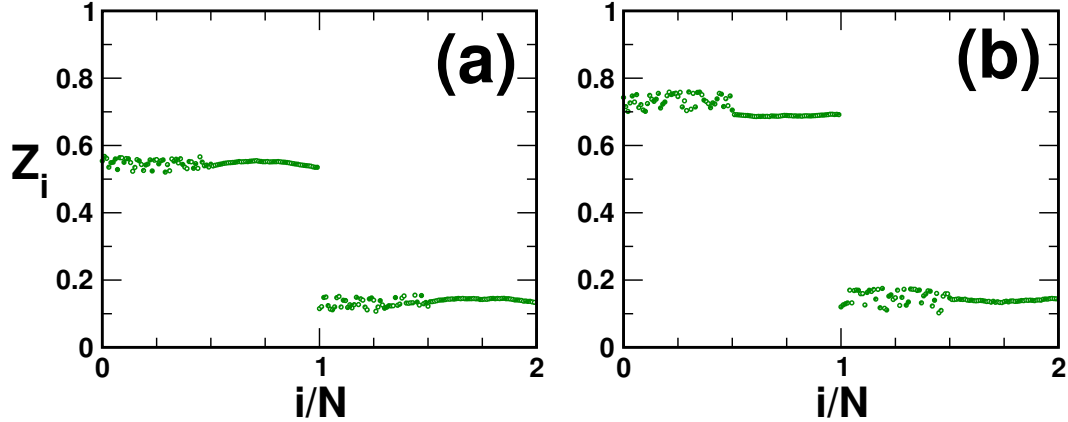


Figure 5.8: Snapshots of both the layers of the multiplex network where half of the inter-layers edges are heterogeneously delayed for the multiplexing parameters (a) $D_x = 3, E_y = 1$, (b) $D_x = 5, E_y = 1$. Others are the same as described in Fig.5.1 LP.

delayed intra-layer links. Therefore, the delayed mirror nodes fail to get completely separated from the rest of the coherent nodes in both the layers. This situation can be made to favor the emergence of chimera by varying structural parameters in such a way that the perturbative (incoherent) effects arising from delayed inter-layer links become more dominant. Fig. 5.7(d) shows that the contribution of the delayed interlayer links can be enhanced by setting D_x and E_y appropriately. However, Fig. 5.7(c) displays a coherent dynamical profile with the same of D_x and E_y values (as Fig.5.7(c)), but without the multiplexing delays. Thus, a combination of a high value of D_x and a very low value of E_y is perfect, along with the multiplexing delays, to obtain chimera state. In Fig. 5.7(d), chimera state emerges in the second layer, while the nodes in the first layer experience only faint disturbance. Thereby, this recipe helps us to attain complete regulatory control over the emergence of chimeric patterns in both the layers by suitably choosing D_x & E_y values. Additionally, we can entirely suppress the chimera induced by appropriate placement of the multiplexing delays, in one layer while having the desired chimera pattern in another layer by tuning the D_x and E_y values.

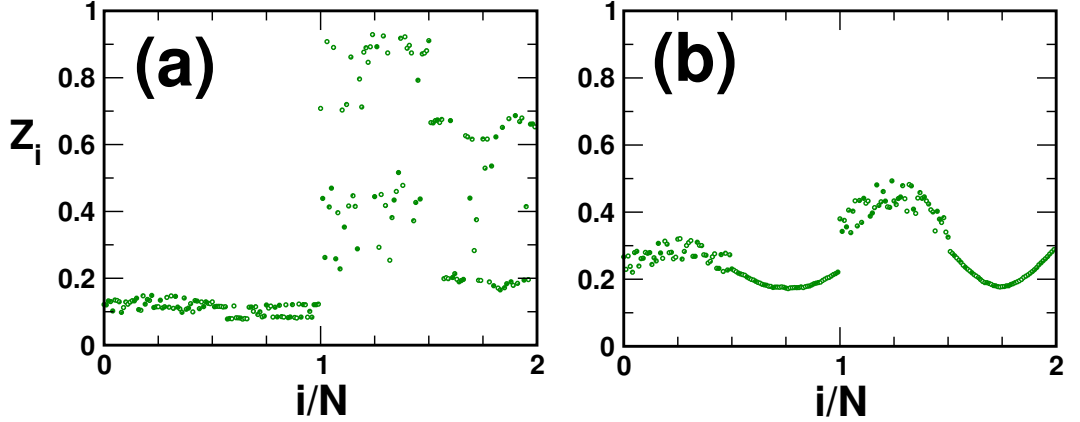


Figure 5.9: Snapshots of both the layers of the multiplex network where half of the inter-layers edges are heterogeneously delayed for the multiplexing parameters (a) $D_x = 5, E_y = 0.2$, (b) $D_x = 5, E_y = 0.8$. Others are the same as described in Fig.5.1 LP.

5.3.4 Role of the D_x & E_y parameters

Next, we take a closer look at the role of multiplex network's structural parameters, namely E_y and D_x to understand the collective dynamical behavior of the layers. Fig. 5.8, represents chimera states for different choices of D_x with usual scaling value of intralayer coupling strength $E_y = 1$. Fig 5.7(b) shows that the usual choice of $D_x = 1, E_y = 1$ yields a slight wobbling in the nodes connected with the delayed inter-layer links. A high value of D_x changes the situation drastically as can be seen in Fig. 5.8. A high value of D_x causes an enhancement in the connection strength between each pair of the mirror nodes permitting the interlayer links dominating over the intralayer links in influence. Thus, the mirror nodes disperse more freely in both the layers because of the multiplexing delays. Fig. 5.8(a) shows an increment in the dispersal of nodes connected to delayed inter-layer links (thus, producing engineered chimera states) in both the layers due to higher values of $D_x (= 3)$. Increased D_x induce even larger spatial separation for the mirror nodes in both the layers even with high value of $E_y (= 1)$. An even more noticeable chimera is observed in Fig. 5.8(b) as the value of $D_x (= 5)$ is higher in this case. Next, we present the impact of E_y along with a fixed high value of $D_x (= 5)$ in Fig. 5.9. A small value of E_y dilutes the intralayer contributions among neighboring nodes in the corre-

sponding layer allowing the nodes to strew more freely under the influence of the multiplexing delays. In Fig. 5.9(a), the mirror nodes experiencing the multiplexing delays, show low spatial separation in neighboring nodes in the first layer, whereas their counterparts in the second layer experience a complete incoherent state due to very weak E_y . The dispersal of the nodes in the second layer can be tamed by increasing E_y (see Fig. 5.7(d) and Fig. 5.9(b)). Increment in E_y diminishes the relative difference between the intralayer coupling strengths of both the layers. Note that Fig. 5.8 (b) presents a well pronounced chimeric spatial profile, whereas Fig. 5.7 (b) shows a slight wobble in the mirror nodes experiencing multiplexing delays, although values of E_y are same in both cases. Thus observed chimera in the second layer can be made even more pronounced by fine-tuning E_y while keeping D_x high (see Fig. 5.9 (b)). From these observations, it is apparent that D_x helps in introducing incoherence in the mirror nodes in both the layers by means of multiplexing heterogeneous delays, whereas E_y essentially brings in incoherence in a layer by diminishing coupling intensity of intralayer links. The interplay between these two parameters can give rise to the emergence of pronounced chimera in only one layer, while the mirror nodes in another layer can cause only mild disturbance. Hence, the intensity of chimera states in a multiplex network can be regulated by inducting heterogeneous multiplexing delays with appropriate choices of the network's structural attributes. So far, we have demonstrated the existence of chimera for a few combinations of the parameters D_X and E_y , though the control scheme is applicable for a wide range of values of the parameters. Fig. 5.10 presents phase diagrams in $D_x - E_y$ space exploring different emerging states, including chimera in the multiplex network both in the absence and the presence of the inter-layer delays. Here the phase $D_x - E_y$ diagrams correspond to a high coupling strength ($\varepsilon = 0.9$) so as to have the synchronous clusters in the multiplexed layers, which could be perturbed to explore the existence of chimera by incorporating multiplexing delays. Note that the schematics and boundaries of phase diagrams in Fig. 5.10 are based on the variance [131] (upper panels; Fig. 5.10(a,b)) and correlation measure [100]. ($g_0(t)$; lower panels; Fig. 5.10(c,d)) defined and discussed in the supporting ma-

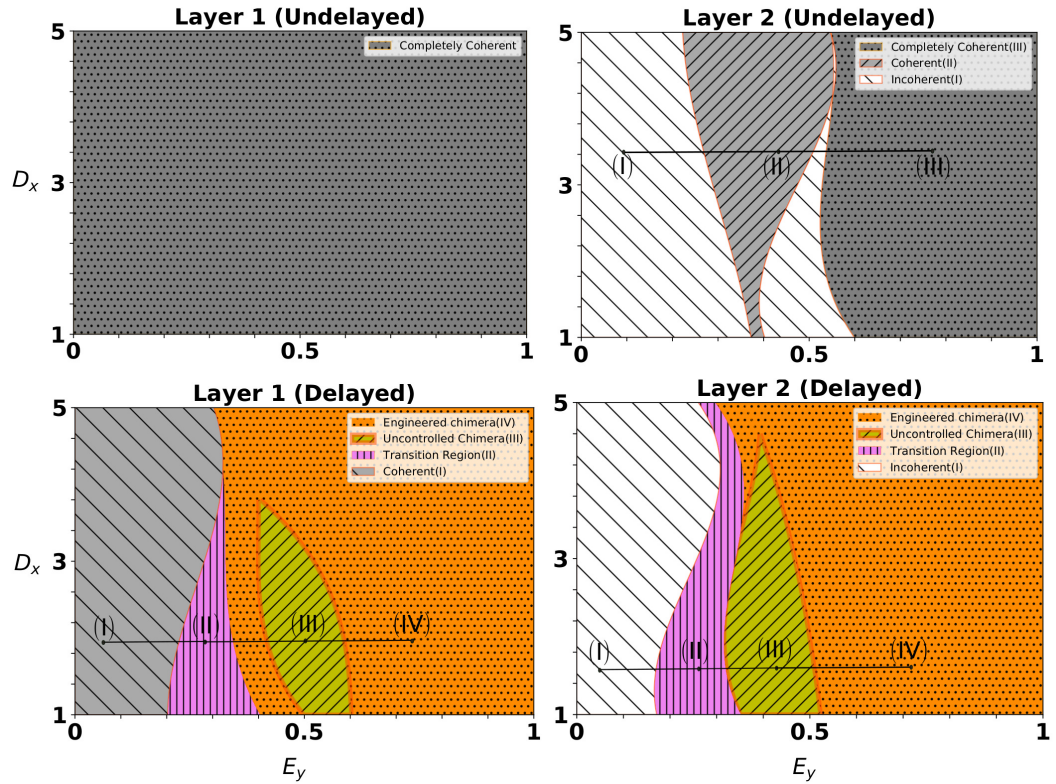


Figure 5.10: A schematic phase diagram of D_x - E_y space for (a) layer 1 and (b) layer 2 with undelayed inter-layer edges and (c) layer 1 and (d) layer 2 with delayed inter-layer edges. Half of the inter-layers edges are heterogeneously delayed (in c & d), and the delay values are chosen from a uniform random distribution with $\tau_{max} = 20$. The parameters are the same as Fig. 5.7. The boundaries of various regions are drawn from visual inspection and measures (See SM [132]).

terial [132]. Panels 5.10 (a) and 5.10 (b) show the coherence profile for Layer 1 and Layer 2, respectively, in the absence of multiplexing delays. Layer 1 displays completely coherent states spanning the entire $D_x - E_y$ space due to high coupling strength whereas Layer 2, due to the effective coupling strength $E_y * \varepsilon$, shows coherent states (regime II) in the mid-range of $D_x - E_y$ space and completely coherent states (regime III) for $E_y > 0.5$. Panels 5.10 (c) and 5.10 (d) exhibit chimera profiles for Layer 1 and Layer 2, respectively when the inter-layer delays are present. Layer 1 shows coherent region (regime I) while Layer 2 shows incoherent region (regime I) for low values of E_y and engineered chimera states (regime IV) for mid- and high-range values of E_y . Regime III for both the layers presents un-controllable chimera in the sense that the shape or area of the incoherence can not be tailored to ones preference under this parameter regime. Transition region (regime II) in both the layers yields unidentified states qualified to be neither chimera nor incoherent states. The difference in the effective coupling strength for Layer 1 (ε) and Layer 2 ($E_y * \varepsilon$) accounts for the different $D_x - E_y$ ranges of regime II and regime III for the two layers. Note that a distinct uniformly colored pattern is used to represent each region in $D_x - E_y$ diagrams; hence the dotted pattern does not show the qualitative or quantitative variation in the engineered chimera profiles (IV) with change in the value of D_x or E_y (as illustrated in Fig. 5.8 and Fig. 5.9). Hence, the phase diagrams in $D_x - E_y$ space highlight the importance of the network's structural parameters in guiding or regulating the emergent chimera in both the layers of the multiplex network.

5.3.5 Investigating the temporal behavior

A chimera state typically requires a special initial condition for its existence and generally arises in the mid-coupling range. In our work, the perturbation induced in the form of heterogeneous delays at coveted position and length of the sequence of inter-layer links gives rise to the chimera state in the coherent regime. The occurrence of such engineered chimera in individual layers of the multiplex network is not surprising. The inducted multiplexing delays disturb the respective nodes, in turn,

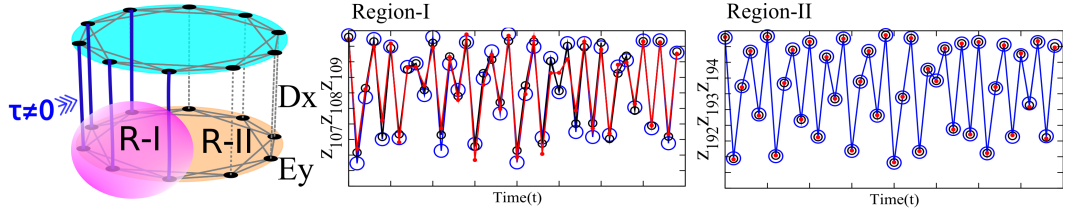


Figure 5.11: Time series of nodes connected with delayed and undelayed interlayer edges along with a diagram of a multiplex network consisting of two identical regular network layers. Half of the interlayer edges are heterogeneously delayed (represented by Bold blue lines). Appropriate networking parameters ($D_x = 5$, $E_y = 0.2$) are used to induce chimera in the second layer. Region I (Shaded pink circle) consists of nodes connected with delayed edges and shown to have an incoherent time evolution in the middle panel, whereas the nodes of region II (connected to undelayed edges) are shown to have coherent evolution in the rightmost panel. Together, they display a chimera pattern, as shown in Fig. 5.7(c). Other parameters are the same as in Fig.5.7.

causing dynamical symmetry breaking of the perturbed nodes from the rest of the nodes in the coherent bulk. We also look at the time-evolution of the perturbed (incoherent) and unperturbed (coherent) nodes to get a deeper insight into the chimera state. Fig. 5.11 shows the time series of six nodes selected from a chimera state, half of the nodes possessing delayed inter-layer links (node index $z_{107}, z_{108}, z_{109}$), while the rest half is possessing undelayed interlayer links (node index $z_{192}, z_{193}, z_{194}$). The time series of the delayed nodes ($z_{107}, z_{108}, z_{109}$) shows a desynchronized time evolution as the nodes evolve experiencing different delay values. Nevertheless, the undelayed nodes ($z_{192}, z_{193}, z_{194}$) maintain their synchronized temporal evolution as they experience no perturbation. It is important to note that if the interpolated multiplexing delays are homogeneous or identical, the impact of the perturbation will be similar to all disturbed nodes. This will produce synchronous cluster(s), possessing the same displacement from the main synchronous cluster, whose displacement in the spatial profile would depend upon the strength of homogeneous delays. However, this kind of spatial profile with detached synchronous clusters can arguably be treated either as a cluster synchronized state or as a point-wise chimera state. Therefore, heterogeneous multiplexing delays are better suited for the demonstration of engineered chimera, presented in this study.

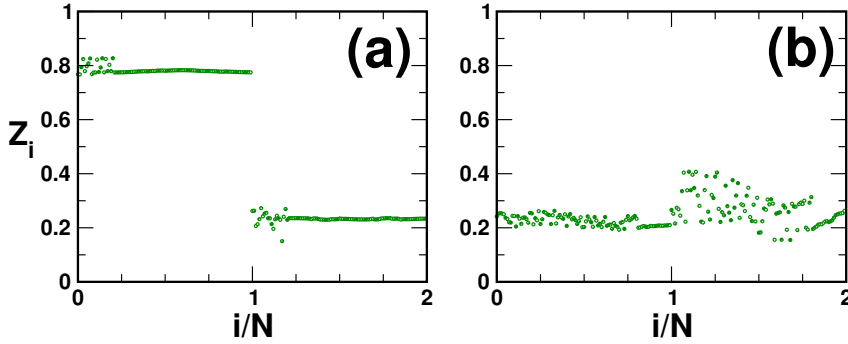


Figure 5.12: (Color online) Snapshots of both the layers of the multiplex network where (a) 20% and (b) 80% inter-layer edges are heterogeneously delayed. The network parameters are $D_x = 5$, $E_y = 0.2$. Other parameters are the same as described in Fig.5.7.

5.3.6 Designing the incoherent region by multiplexing delays

In addition, the extent of the incoherent region of the chimera state depends upon the fraction of delayed inter-layer links N_τ . The number of introduced heterogeneous delays perturbs the same number of the mirror nodes in both the layers to produce the incoherent region. Fig. 5.12 (a) exhibits a chimera state with a very small incoherent region arising due to small N_τ , whereas Fig. 5.12 (b) exhibits a chimera state having a large incoherent region because of large N_τ . This study demonstrates that besides regulating chimera state by varying network's structural parameters, the extent of the incoherent region of the chimera state can also be regulated quantitatively by varying fraction of the multiplexing delays.

5.3.7 Designing the Chimera by multiplexing delays in Henon Map

To verify if the regulating scheme is universally applicable, we also have investigated a multiplex network of non-locally coupled two-dimensional map, described as [133, 134]

$$x_i^{t+1} = f(x_i^t, y_i^t) + \frac{1}{(k_i)} \sum_{j=1}^{2N} C_{ij} [f(x_j^{t-\tau_{ij}}) - f(x_i^t, y_i^t)] \quad (5.6)$$

$$y_i^{t+1} = \beta x_i^t$$

where the local dynamics is governed by the Henon map $f(x_i^t, y_i^t) = 1 - \alpha(x_i^t)^2 + y_i^t$. As displayed in Fig.5.13, a two-dimensional Henon map also shows

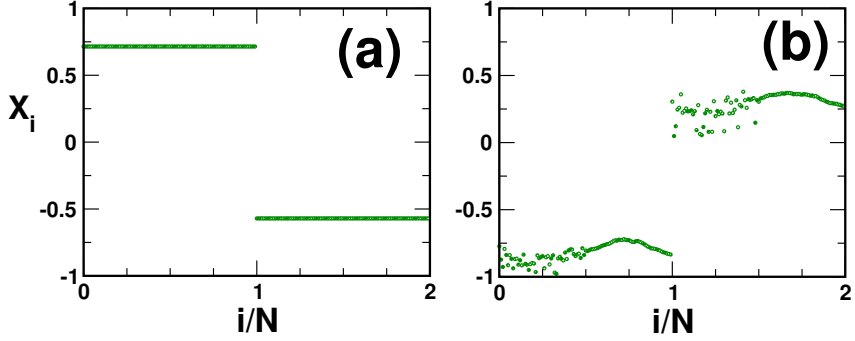


Figure 5.13: (Color online) Snapshot profiles of the two layers of the considered multiplex network for (a) the undelayed interlayer links, (b) the delayed interlayer links with parameters $D_x = 5$, $E_y = 0.6$. The local dynamics is described by henon map (Eq. 5.6) with parameters, $\alpha = 1.4$ and $\beta = 0.3$, $\varepsilon = 0.9$, $\tau_{max} = 20$, $r = 0.32$, $N = 100$ in each layer.

an engineered chimera state with delayed inter-layer links with a proper choice of D_x and E_y parameter in the high coupling regime. Therefore, we deduce that the regulatory scheme of engineering chimeric pattern(s) can be applied in a variety of systems with different underlying dynamics provided the system lies in the coherent regime.

5.4 Conclusions

In this chapter, We have presented a new approach towards control of the emergent chimera patterns in regular networks. To summarize, we have shown that in a regular network, the chimera regime can be enhanced with an introduction of the heterogeneous delays in the edges. Importantly, the chimera patterns can be designed by placing the delayed nodes in suitable spatial positions. We have demonstrated that the location of the incoherent region coincides with the edges having the heterogeneous delays. Further, by appropriate distribution of the heterogeneous delays, it is possible to engineer both the single-cluster and the multi-cluster chimera state. However, the proposed scheme works only in the high coupling region. Moreover, for both the undelayed and the homogeneous delayed cases, the high coupling region manifests an occurrence of the coherent dynamics.

Furthermore, we extend the technique to produce engineered chimera states in

the multiplex network by using any random initial condition in the presence of heterogeneous multiplexing (inter-layer) delays. We induce chimera states in the initially coherent multiplexed layers by introducing incoherence with the aid of multiplexing delays. It is also displayed that the emergent chimera can be regulated to one's choice both (a) qualitatively by tweaking the degree (level) of induced incoherence by making proper choices for multiplex network's structural parameters such as interlayer and intralayer coupling strengths, and (b) quantitatively by tweaking the amount of induced incoherence by varying fraction of the delayed interlayer links. The above-described control over the behavior of the emergent chimera can be understood in detail by the phase diagram in the interlayer and intralayer coupling parameters' space. The proposed scheme is robust against underlying time-discrete local dynamics and might be applicable as well to continuous time dynamical systems in producing engineered chimera states originating from regular initial conditions. Also there may be cases when delays in the systems are inevitable, and chimeras may not always be desirable. Such cases present a new challenge to how naturally existing chimera in a delayed system can be destroyed, and a modified application of the reported technique can be sought towards the cause.

Therefore, by introducing the heterogeneous delays, we can generate tailor-made chimera states in this high coupling region. The heterogeneous delays not only causes an enhancement in the parameter regime for which chimera appears but also offers control over chimera patterns in a limited parameter range. Further, we found that the heterogeneous delays spanned over the entire network destroy the emergence of chimera patterns for any coupling strength. The dynamical systems directly jump from the incoherent to the coherent state if all the edges of the network posses heterogeneous delays. This article sheds light on manufacturing engineered chimera in a monoplex and multiplex network, whose relevance can be found in the case of neural disorders [33].

The highly complex structure of synapses between neurons in the brain network is responsible for most of our brain functions [135]. Deterioration of these complex

interaction pathways may lead to the neural disorders which hinder the brain from functioning normally. The complex network approach presents a holistic way to watch all the activities at once and find the anomalies in the emergent pattern within the framework of network science [136]. Chimera is a promising candidate to detect these anomalous patterns in the brain. Our technique of producing chimera with the aid of heterogeneous delays can provide a new direction in understanding the underlying dynamics behind the emergence of neuronal disorder in the brain as the delays are inherently present in the neuronal interactions connecting different functional or structural regions of the brain.

Chapter 6

Discussions and Future Scope

The study of dynamics on networks provides a unique window to perceive the collective complex behavior of a system consisting of interacting entities. Furthermore, synchronization, a fascinating emergent dynamics arising due to the interacting nodes of a network, holds a special place due to its applicability in diverse areas of research [11, 19]. Recent literature however, indicates the partial synchronization patterns, termed as chimera state, describing a hybrid dynamics where a group of entities (nodes) exhibit synchrony while other entities (nodes) display asynchrony [2, 3], is even more common phenomenon in natural systems [20]. The new-found importance of chimera state in biological systems allured a large amount of literature on chimera state [31, 32]. However, despite the availability of a large volume of research, a systematic study of chimera patterns in a network incorporating multiplex architecture is scarce. The works presented in the thesis aims to bridge the gaps by providing an account of investigations pertaining to the emergence of chimera in multiplex networks and impact of several factors on the appearance of chimera state, which may be unique to the multiplex networks. Additionally, this thesis provides a recipe to design the chimera state, which may be very important

due to the fact that the chimera state is found to play a significant role in neural dynamics and cognitive functions.

6.1 Summary

In the thesis, we have explored the impact of multiple types of interactions on the collective dynamical behavior of the entire multiplex network in the context of partial synchronous patterns of chimera state.

First in the second chapter, we present the emergence of chimera in the multiplex network and the required conditions for the appearance of chimera state. We further show that while, the multiplex architecture, retains the type of chimera state, displayed by the monoplex (single -layer) networks, it changes the regions of the asynchrony. Additionally, depending on the choice of the initial condition, the layers of a multiplex network consisting of identical regular networks, display mirror chimera state regardless of the number layers included. Later on, we had extended the work, including delayed interactions in both inter- and intra-layer connections and put forward an extensive study of the parameter regime for which chimera appears in the multiplex network. We found that interplay of delay and multiplexing brings about an enhanced or suppressed appearance of the chimera state depending on the distribution as well as the parity of delay values in the layers. Furthermore, a large value delay always suppresses the parameter region, for which the chimera appears. Additionally, we reported a layer chimera state with the existence of one layer exhibiting synchronous and another layer, asynchronous dynamics, which is unique to the multiplex networks.

Then, in the third chapter, we showcase the emergence of chimera states in a multiplex network where the layers of the multiplex network may not be identical. We mainly consider two cases, (i) a multiplex network having two homogeneous layers with different connection densities, (ii) a multiplex network consisting of one identically coupled layer (homogeneous layer) and one non-identically coupled layer (heterogeneous layer). We demonstrate that the parameter range displaying the chimera state in the homogeneous layer could be tuned by changing the con-

nnection density or connection architecture of the same nodes in the heterogeneous layer. We found that a denser homogeneous second layer promotes chimera in a sparse homogeneous layer, where chimeras do not occur in isolation. Furthermore, we presented that a sparse heterogeneous layer could promote chimera states in a sparse homogeneous layer.

Proceeding to the fourth chapter, we show the impact of inhibitory couplings on the appearance of chimera state. Considering a multiplex network with a layer having inhibitory (repulsive) coupling and other layer having excitatory (attractive) coupling, we report an enhancement in the emergence of the chimera state in one layer, in the presence of repulsive coupling in the other layer. Furthermore, we show that a small amount of inhibition or repulsive coupling in one layer is sufficient to yield the chimera state in another layer by destroying its synchronized behavior.

Finally, in the fifth chapter, we turn our attention to the control of chimera states. We propose a technique to engineer a chimera state by using a specially chosen distribution of heterogeneous time delays on the edges of a single-layer (monoplex) network. We demonstrate that control over the spatial location and extent of the incoherent region of a chimera state in a network can be achieved by appropriate placement of heterogeneous time delays. Furthermore, we extend the technique to construct chimera states in the multiplex networks with the aid of heterogeneous delays in a fraction of inter-layer links, referred to as multiplexing-delay, in a sequence. We show that the emergence of the incoherence in the chimera state can be regulated by making a proper choice of both inter- and intra-layer coupling strengths, whereas the extent and the position of the incoherence regime can be regulated by fitting placement and strength of the multiplexing delays. The proposed technique to construct such engineered chimera equips us with both single and multiplex network's structural parameters as tools in gaining both qualitative- and quantitative-control over the incoherent region and, in turn, the chimera state.

To summarize, the thesis put forward an extensive study of the system parameter space in which chimera state emerges in multiplex networks and explains the role of several parameters including delay, inhibition, and non-identical multiplexing and

presents an engineering scheme to gain both qualitative- and quantitative-control over it.

6.2 Future direction

Of late, it has been realized that the presence of global synchrony is not very common, and instead, a partial synchronization is more widespread in real-world complex systems. Particularly, the interacting neurons in brain networks are more likely to show partial synchrony than a complete synchronization, which forms the future direction of the works presented in the thesis.

Recent advancements in neuroscience, especially in neuro-imaging techniques, brought a massive influx of data related to neural activities of a system as complex as the human brain. “Network Neuroscience” which deals with interacting communities of neurons under network science framework, providing an improved understanding of the brain, represented as network and, is addressing the challenges in detection and diagnosis of neural disorders. However, despite the availability of extensive data, a concrete understanding of the neural interactions is far from complete. The mechanism of emergent partial synchronous patterns or chimera state, which is proven to play a very important role in neural dynamics [33], and its relations to cognitive functions remains an open challenge. Furthermore, it remains to be seen, if these patterns can be used as a marker for early diagnosis of neural disorders like epilepsy. This presents a tremendous opportunity for a data-driven investigation on the role and importance of partial synchrony, shedding light into not only structural but functional nature of brain networks.

Chimera state has been closely related to various biological processes ranging from uni-hemispheric sleep in mammals [31, 76, 77] to cognitive process [20] in human brain networks. Hybrid dynamics of chimera state also has been reported to emerge in neural networks of two well-studied neural networks of, Cat [79] and C Elegans [78]. A seizure state has been reported to show a massive collapse of synchronization before high coherence event of seizure state [80]. Adding to that works by Andrzejak *et al.* [81] and Chouzouris *et al.* [82] indicated the emergence

of chimera-like patterns at the epileptic seizure onset, i.e., at the transition to a seizure state in epilepsy. All the investigations indicate that chimera state with its co-existing synchronous and asynchronous activities play a vital role in neural dynamics and present a great candidate to develop novel techniques and tools for early detection and disease diagnosis related to neural systems.

Additionally, recent literature have shown that a neural system showcases a perfect example of the multi-layer network [137] where the layers may be formed using anatomical and functional connectivity [138] or frequency-based acclivities [139]. However, a complete study on partial synchronization in the neural system, considering its multi-layer nature is yet unexplored. Combining both the multi-layer framework and the network neuroscience, a cross-disciplinary approach to study the mechanism behind the emergence of partial synchronization, exploring the interplay of structure and function in brain networks and investigation potential usage of these patterns as a marker in neural disorders, devise a very suitable future direction for the works pursued in the thesis.

Bibliography

- [1] Peck, H.T. (1898), Harpers Dictionary of Classical Antiquities, Harper and Brothers, New York.
- [2] Kuramoto Y., Battogtokh D. (2002), Coexistence of coherence and incoherence in nonlocally coupled phase oscillators, Nonlinear Phenom. Complex Syst., 5(4), 380-385 (DOI is not available)
- [3] Abrams, D. M., Strogatz, S. H. (2004), Chimera states for coupled oscillators, Phys. Rev. Lett., 93, 174102 (DOI: 10.1103/PhysRevLett.93.174102).
- [4] Goldstein, H., Poole, C., and Safko, J. (2011), Classical mechanics, 3rd Ed. Pearson Education (978-8131758915)
- [5] Ujjwal S.R. (2016) Spontaneous symmetry-breaking in oscillator networks. PhD Dissertation, Jawaharlal Nehru University
- [6] Euler, L. (1741). Solutio problematis ad geometriam situs pertinentis. Commentarii academiae scientiarum Petropolitanae, 128-140 (DOI is not available).
- [7] Biggs, N., Lloyd, E. K., and Wilson, R. J. (1999). Graph Theory 1736-1936, New Ed. Clarendon Press (978-0198539162)
- [8] Newman, M. (2018). Networks. Oxford university press (DOI: 10.1093/oso/9780198805090.001.0001)
- [9] Newman, M., Barabási, A. -L., Watts, D.J., (2006) The Structure and Dynamics of Networks: Princeton Studies in Complexity, Princeton University Press (9780691113579)

- [10] Barabási, A. L. (2016), Network science. 1st ed. Cambridge university press (978-1107076266)
- [11] Strogatz, S. (2004). Sync: The emerging science of spontaneous order, Reprint ed. Hachette Books (978-0786887217)
- [12] Birch, T. (1756). The History of the Royal Society of London, for Improving of Natural Knowledge from Its First Rise... As a Supplement to the Philosophical Transactions (Vol. 2). p.19 (DOI is not available)
- [13] Huygens, C. (1893). Oeuvres completes de Christiaan Huygens, vol. 5. The Hague: Martinus Nijhoff.(Includes works from 1665.), 246 (DOI is not available)
- [14] Wiener, N. (2013), Nonlinear problems in random theory, New Ed. Literary Licensing, LLC (978-1258629908)
- [15] Winfree, A. T. (1967). Biological rhythms and the behavior of populations of coupled oscillators. *Journal of theoretical biology*, 16(1), 15-42 (DOI: 10.1016/0022-5193(67)90051-3)
- [16] Kuramoto, Y. (1975). International symposium on mathematical problems in theoretical physics. *Lecture notes in Physics* , 30 , 420 (DOI is not available)
- [17] Crawford, J. D. (1994). Amplitude expansions for instabilities in populations of globally-coupled oscillators. *Journal of statistical physics*, 74(5-6), 1047-1084 (DOI: 10.1007/BF02188217)
- [18] Strogatz, S. H. (2000). From Kuramoto to Crawford: exploring the onset of synchronization in populations of coupled oscillators. *Physica D: Nonlinear Phenomena*, 143(1-4), 1-20 (10.1016/S0167-2789(00)00094-4)
- [19] Pikovsky, A., Rosenblum, M., Kurths, J., and Kurths, J., (2003) *Synchronization: a universal concept in nonlinear sciences*, Cambridge university press (9780521533522)
- [20] Bansal, K., Garcia, J. O., Tompson, S. H., Verstynen, T., Vettel, J. M., and Muldoon, S. F. (2019). Cognitive chimera states in human brain networks. *Science Advances*, 5(4), eaau8535 (DOI: 10.1126/sciadv.aau8535)
- [21] Eckmann, J. P., and Ruelle, D. (1985). Ergodic theory of chaos and strange attractors. In *The theory of chaotic attractors* (pp. 273-312). Springer, New York, NY (DOI: 10.1007/978-0-387-21830-4-17)

- [22] Ruelle, D. (1979). Ergodic theory of differentiable dynamical systems. Publications Mathématiques de l’Institut des Hautes tudes Scientifiques, 50(1), 27-58 (DOI: 10.1007/BF02684768)
- [23] Werndl, C. (2009). Are deterministic descriptions and indeterministic descriptions observationally equivalent?. Studies in history and philosophy of science part B: studies in history and philosophy of modern physics, 40(3), 232-242 (DOI: 10.1016/j.shpsb.2009.06.004)
- [24] Ott, E. (2002). Chaos in dynamical systems, 2nd Ed. Cambridge university press (978-0521811965)
- [25] May, R. M., (1976), Simple mathematical models with very complicated dynamics, Nature, 261, 5560, 459-467 (DOI: 10.1038/261459a0)
- [26] Ott, E., (2002) One-dimensional maps. In: Chaos in Dynamical Systems, 2nd edn. Cambridge: Cambridge University Press, pp. 24-70 (DOI: 10.1017/CBO9780511803260.004)
- [27] Lakshmanan, M., and Senthilkumar, D. V. (2011). Dynamics of nonlinear time-delay systems, Springer, Berlin, Heidelberg (DOI: 10.1007/978-3-642-14938-2).
- [28] Erdős, P., and Rényi, A. (1960). On the evolution of random graphs. Publ. Math. Inst. Hung. Acad. Sci, 5(1), 17-60 (DOI is not available)
- [29] Barabási, A. L., and Albert, R. (1999). Emergence of scaling in random networks. science, 286(5439), 509-512 (DOI: 10.1126/science.286.5439.509)
- [30] Boccaletti, S., Latora, V., Moreno, Y., Chavez, M., and Hwang, D. U. (2006). Complex networks: Structure and dynamics. Physics reports, 424(4-5), 175-308 (DOI:10.1016/j.physrep.2005.10.009)
- [31] Panaggio, M. J., and Abrams, D. M. (2015). Chimera states: coexistence of coherence and incoherence in networks of coupled oscillators, Nonlinearity, 28(3), R67 (DOI: 10.1088/0951-7715/28/3/R67).
- [32] Schöll, E. (2016). Synchronization patterns and chimera states in complex networks: interplay of topology and dynamics, The European Physical Journal Special Topics, 225(6-7), 891-919 (DOI: 10.1140/epjst/e2016-02646-3).

- [33] Majhi, S., Bera, B. K., Ghosh, D., and Perc, M. (2018). Chimera states in neuronal networks: A review. *Physics of life reviews*, 28, 100-121 (DOI: 10.1016/j.plrev.2018.09.003).
- [34] Ghosh, S., Zakharova, A., and Jalan, S. (2018). Non-identical multiplexing promotes chimera states. *Chaos, Solitons and Fractals*, 106, 56-60 (DOI: 10.1016/j.chaos.2017.11.010)
- [35] Buscarino, A., Frasca, M., Gambuzza, L. V., and Hövel, P. (2015). Chimera states in time-varying complex networks. *Physical Review E*, 91(2), 022817 (DOI: 10.1103/PhysRevE.91.022817).
- [36] Panaggio, M. J., and Abrams, D. M. (2015). Chimera states on the surface of a sphere. *Physical Review E*, 91(2), 022909. (DOI: 10.1103/PhysRevE.91.022909).
- [37] Omel'chenko, O. E., Wolfrum, M., Yanchuk, S., Maistrenko, Y. L., and Sudakov, O. (2012). Stationary patterns of coherence and incoherence in two-dimensional arrays of non-locally-coupled phase oscillators, *Physical Review E*, 85(3), 036210 (DOI: 10.1103/PhysRevE.85.036210).
- [38] Schmidt, A., Kasimatis, T., Hizanidis, J., Provata, A., and Hövel, P. (2017). Chimera patterns in two-dimensional networks of coupled neurons. *Physical Review E*, 95(3), 032224 (DOI:10.1103/PhysRevE.95.032224)
- [39] Maistrenko, Y., Sudakov, O., Osiv, O., and Maistrenko, V. (2015). Chimera states in three dimensions. *New Journal of Physics*, 17(7), 073037 (DOI: 10.1088/1367-2630/17/7/073037).
- [40] Kasimatis, T., Hizanidis, J., and Provata, A. (2018). Three-dimensional chimera patterns in networks of spiking neuron oscillators. *Physical Review E*, 97(5), 052213 (DOI: 10.1103/PhysRevE.97.052213)
- [41] Punetha, N., Ujjwal, S. R., Atay, F. M., and Ramaswamy, R. (2015). Delay-induced remote synchronization in bipartite networks of phase oscillators. *Physical Review E*, 91(2), 022922 (DOI: 10.1103/PhysRevE.91.022922).
- [42] Ujjwal, S. R., Punetha, N., and Ramaswamy, R. (2016). Phase oscillators in modular networks: The effect of nonlocal coupling. *Physical Review E*, 93(1), 012207 (DOI: 10.1103/PhysRevE.93.012207).

- [43] Mishra, A., Hens, C., Bose, M., Roy, P. K., and Dana, S. K. (2015). Chimeralike states in a network of oscillators under attractive and repulsive global coupling. *Physical Review E*, 92(6), 062920 (DOI: 10.1103/PhysRevE.92.062920).
- [44] Laing, C. R. (2010), Chimeras in networks of planar oscillators, *Phys. Rev. E.*, 81, 066221 (DOI: 10.1103/PhysRevE.81.066221)
- [45] Tinsley, M. R., Nkomo, S. and Showalter, K. (2012), Chimera and phase-cluster states in populations of coupled chemical oscillators, *Nat. Phys.*, 8, 662–665 (DOI: 10.1038/nphys2371)
- [46] Nkomo, S., Tinsley, M. R. and Showalter, K. (2013), Chimera States in Populations of Nonlocally Coupled Chemical Oscillators, *Phys. Rev. Lett.*, 110, 244102 (DOI: 10.1103/PhysRevLett.110.244102)
- [47] Martens, E. A., Thutupalli, S., Fourriére, A. and Hallatschek, O. (2013), Chimera states in mechanical oscillator networks, *Proc. Natl. Acad. Sci. U. S. A.*, 110, 10563–10567 (DOI: 10.1073/pnas.1302880110)
- [48] Zakharova, A., Kapeller, M., and Schöll, E. (2014). Chimera death: Symmetry breaking in dynamical networks. *Physical review letters*, 112(15), 154101 (DOI: 10.1103/PhysRevLett.112.154101).
- [49] Sethia, G. C., and Sen, A. (2014). Chimera states: The existence criteria revisited. *Physical review letters*, 112(14), 144101 (DOI: 10.1103/PhysRevLett.112.144101).
- [50] Ulonska, S., Omelchenko, I., Zakharova, A., and Schöll, E. (2016). Chimera states in networks of Van der Pol oscillators with hierarchical connectivities. *Chaos: An Interdisciplinary Journal of Nonlinear Science*, 26(9), 094825 (DOI: 10.1063/1.4962913).
- [51] Ujjwal, S. R., Punetha, N., Prasad, A., and Ramaswamy, R. (2017). Emergence of chimeras through induced multistability. *Physical Review E*, 95(3), 032203 (DOI: 10.1103/PhysRevE.95.032203).
- [52] Omelchenko, I. *et al* (2011), Loss of Coherence in Dynamical Networks: Spatial Chaos and Chimera States, *Phys. Rev. Lett.* 106, 234102 (DOI: 10.1103/PhysRevLett.106.234102).

- [53] Ghosh S., Kumar A., Zakharova A., Jalan S. (2016), Birth and death of chimera: Interplay of delay and multiplexing, EPL, 115, 60005 (DOI: 10.1209/0295-5075/115/60005).
- [54] Ghosh, S., and Jalan, S. (2016). Emergence of chimera in multiplex network, International Journal of Bifurcation and Chaos, 26(07), 1650120 (DOI: 10.1142/S0218127416501200).
- [55] Bastidas, V. M., Omelchenko, I., Zakharova, A., Schll, E., and Brandes, T. (2015). Quantum signatures of chimera states, Physical Review E, 92(6), 062924 (DOI: 10.1103/PhysRevE.92.062924)
- [56] Viennot, D., and Aubourg, L. (2016). Quantum chimera states, Physics Letters A, 380(5-6), 678-683 (DOI: 10.1016/j.physleta.2015.11.022)
- [57] Laing, C. R. (2015), Chimeras in networks with purely local coupling, Physical Review E, 92(5), 050904 (DOI: 10.1103/PhysRevE.92.050904)
- [58] Schmidt, L., and Krischer, K. (2015), Clustering as a prerequisite for chimera states in globally coupled systems, Physical review letters, 114(3), 034101 (DOI: 10.1103/PhysRevLett.114.034101)
- [59] Xie, J., Knobloch, E., and Kao, H. C. (2014). Multicluseter and traveling chimera states in nonlocal phase-coupled oscillators, Physical Review E, 90(2), 022919 (DOI: 10.1103/PhysRevE.90.022919).
- [60] Omelchenko, I., Omelchenko, E., Hövel, P., and Schöll, E. (2013), When nonlocal coupling between oscillators becomes stronger: patched synchrony or multichimera states, Physical review letters, 110(22), 224101 (DOI: 10.1103/PhysRevLett.110.224101)
- [61] Larger, L., Penkovsky, B., and Maistrenko, Y. (2013), Virtual chimera states for delayed-feedback systems, Physical review letters, 111(5), 054103 (DOI: 10.1103/PhysRevLett.111.054103)
- [62] Abrams, D. M., Mirollo, R., Strogatz, S. H., and Wiley, D. A. (2008), Solvable model for chimera states of coupled oscillators, Physical review letters, 101(8), 084103 (DOI: 10.1103/PhysRevLett.101.084103)
- [63] Bera, B. K., Ghosh, D., and Banerjee, T. (2016), Imperfect traveling chimera states induced by local synaptic gradient coupling, Physical Review E, 94(1), 012215 (DOI: 10.1103/PhysRevE.94.012215)

- [64] Sheeba, J. H., Chandrasekar, V. K., and Lakshmanan, M. (2010), Chimera and globally clustered chimera: Impact of time delay, *Physical Review E*, 81(4), 046203 (DOI: 10.1103/PhysRevE.81.046203).
- [65] Sieber, J., Omel'chenko, E., and Wolfrum, M. (2014), Controlling unstable chaos: stabilizing chimera states by feedback, *Physical review letters*, 112(5), 054102 (DOI: 10.1103/PhysRevLett.112.054102).
- [66] Bick, C., and Martens, E. A. (2015), Controlling chimeras, *New Journal of Physics*, 17(3), 033030 (DOI: 10.1088/1367-2630/17/3/033030).
- [67] Omelchenko, I., Omel'chenko, E., Zakharova, A., Wolfrum, M., and Schöll, E. (2016), Tweezers for chimeras in small networks, *Physical review letters*, 116(11), 114101 (DOI: 10.1103/PhysRevLett.116.114101)
- [68] Ghosh, S., and Jalan, S. (2018), Engineering chimera patterns in networks using heterogeneous delays. *Chaos: An Interdisciplinary Journal of Nonlinear Science*, 28(7), 071103 (DOI: 10.1063/1.5042133).
- [69] Ghosh, S., Schülen, L., Kachhvah, A. D., Zakharova, A., and Jalan, S. (2019), Taming Chimeras in Networks through Multiplexing Delays, *EPL (In Press)* arXiv:1907.10031.
- [70] Hagerstrom, A. M., Murphy, T. E., Roy, R., Hövel, P., Omelchenko I. and Schöll E. (2012), Experimental observation of chimeras in coupled-map lattices, *Nat. Phys.*, 8, 658–661 (DOI: 10.1038/nphys2372)
- [71] Gambuzza, L. V., Buscarino, A., Chessari, S., Fortuna, L., Meucci, R., and Frasca, M. (2014). Experimental investigation of chimera states with quiescent and synchronous domains in coupled electronic oscillators. *Physical Review E*, 90(3), 032905 (DOI: 10.1103/PhysRevE.90.032905)
- [72] Wickramasinghe, M., and Kiss, I. Z. (2014). Spatially organized partial synchronization through the chimera mechanism in a network of electrochemical reactions. *Physical Chemistry Chemical Physics*, 16(34), 18360-18369 (DOI: 10.1039/C4CP02249A)
- [73] Ocampo-Espindola, J. L., Bick, C., and Kiss, I. Z. (2019). Weak Chimeras with Modular Electrochemical Oscillator Networks. *Frontiers in Applied Mathematics and Statistics*, 5, 38 (DOI: 10.3389/fams.2019.00038)

- [74] Lazarides, N., Neofotistos, G. and Tsironis, G. P. (2015), Chimeras in SQUID metamaterials, *Phys. Rev. B.*, 91, 054303 (DOI: 10.1103/PhysRevB.91.054303)
- [75] Hizanidis, J., Lazarides, N., and Tsironis, G. P. (2016). Robust chimera states in SQUID metamaterials with local interactions. *Physical Review E*, 94(3), 032219 (DOI: 10.1103/PhysRevE.94.032219)
- [76] Tamaki, M., Bang, J. W., Watanabe, T., and Sasaki, Y. (2016). Night watch in one brain hemisphere during sleep associated with the first-night effect in humans. *Current biology*, 26(9), 1190-1194 (DOI: 10.1016/j.cub.2016.02.063).
- [77] Ramlow, L., Sawicki, J., Zakharova, A., Hlinka, J., Claussen, J. C., and Schöll, E. (2019). Partial synchronization in empirical brain networks as a model for unihemispheric sleep. arXiv preprint arXiv:1904.05949.
- [78] Hizanidis, J., Kouvaris, N. E., Zamora-López, G., Díaz-Guilera, A., and Antonopoulos, C. G. (2016). Chimera-like states in modular neural networks. *Scientific reports*, 6, 19845 (DOI: 10.1038/srep22314)
- [79] Santos, M. S. *et al.* (2017), Chimera-like states in a neuronal network model of the cat brain, *Chaos, Solitons & Fractals*, 101, 86-91 (DOI: 10.1016/j.chaos.2017.05.028)
- [80] Jiruska, P., De Curtis, M., Jefferys, J. G., Schevon, C. A., Schiff, S. J., and Schindler, K. (2013), Synchronization and desynchronization in epilepsy: controversies and hypotheses, *The Journal of physiology*, 591(4), 787-797 (DOI: 10.1113/jphysiol.2012.239590)
- [81] Andrzejak, R. G., Rummel, C., Mormann, F., and Schindler, K. (2016), All together now: Analogies between chimera state collapses and epileptic seizures, *Scientific reports*, 6, 23000 (DOI: 10.1038/srep23000)
- [82] Chouzouris, T., Omelchenko, I., Zakharova, A., Hlinka, J., Jiruska, P., and Schöll, E. (2018), Chimera states in brain networks: Empirical neural vs. modular fractal connectivity, *Chaos: An Interdisciplinary Journal of Nonlinear Science*, 28(4), 045112 (DOI: 10.1063/1.5009812)
- [83] Glaze, T. A., Lewis, S., and Bahar, S. (2016), Chimera states in a Hodgkin-Huxley model of thermally sensitive neurons, *Chaos: An Interdisciplinary Journal of Nonlinear Science*, 26(8), 083119 (DOI: 10.1063/1.4961122)

- [84] Laing, C. R., and Chow, C. C. (2001), Stationary bumps in networks of spiking neurons, *Neural computation*, 13(7), 1473-1494 (DOI: 10.1162/089976601750264974).
- [85] Davidenko, J. M., Pertsov, A. V., Salomonsz, R., Baxter, W., and Jalife, J. (1992), Stationary and drifting spiral waves of excitation in isolated cardiac muscle, *Nature*, 355(6358), 349 (DOI: 10.1038/355349a0)
- [86] González-Avella, J. C., Cosenza, M. G., and San Miguel, M. (2014), Localized coherence in two interacting populations of social agents, *Physica A: Statistical Mechanics and its Applications*, 399, 24-30 (DOI:10.1016/j.physa.2013.12.035)
- [87] Boccaletti, S., Bianconi, G., Criado, R., Del Genio, C. I., Gómez-Gardenes, J., Romance, M. and Zanin, M. (2014), The structure and dynamics of multilayer networks, *Physics Reports*, 544(1), 1-122 (DOI: 10.1016/j.physrep.2014.07.001).
- [88] Gómez-Gardenes, J., Reinares, I., Arenas, A., and Floría, L. M. (2012), Evolution of cooperation in multiplex networks, *Scientific reports*, 2, 620 (DOI: 10.1038/srep00620).
- [89] Sarkar, C., Yadav, A., and Jalan, S. (2016), Multilayer network decoding versatility and trust, *EPL (Europhysics Letters)*, 113(1), 18007 (DOI: 10.1209/0295-5075/113/18007)
- [90] Dwivedi, S. K., Sarkar, C., and Jalan, S. (2015), Optimization of synchronizability in multiplex networks, *EPL (Europhysics Letters)*, 111(1), 10005 (DOI: 10.1209/0295-5075/111/10005)
- [91] Shinde, P., and Jalan, S. (2015), A multilayer protein-protein interaction network analysis of different life stages in *Caenorhabditis elegans*, *EPL (Europhysics Letters)*, 112(5), 58001 (DOI: 10.1209/0295-5075/112/58001).
- [92] Kivelä, M., Arenas, A., Barthelemy, M., Gleeson, J. P., Moreno, Y., and Porter, M. A. (2014), Multilayer networks. *Journal of complex networks*, 2(3), 203-271 (DOI: 10.1093/comnet/cnu016)
- [93] Singh, A., Ghosh, S., Jalan, S., and Kurths, J. (2015), Synchronization in delayed multiplex networks, *EPL (Europhysics Letters)*, 111(3), 30010 (DOI: 10.1209/0295-5075/111/30010)

- [94] Jalan, S., and Singh, A. (2014), Impact of heterogeneous delays on cluster synchronization, *Physical Review E*, 90(4), 042907 (DOI: 10.1103/PhysRevE.90.042907).
- [95] Kaneko, K. (1991), *Coupled map lattice*, In *Chaos, Order, and Patterns* (pp. 237-247), Springer, Boston, MA (DOI: 10.1007/978-1-4757-0172-2_10);
- [96] Gopal, R., Chandrasekar, V. K., Venkatesan, A., and Lakshmanan, M. (2014), Observation and characterization of chimera states in coupled dynamical systems with nonlocal coupling, *Physical Review E*, 89(5), 052914 (DOI: 10.1103/PhysRevE.89.052914).
- [97] Martens, E. A., Panaggio, M. J., and Abrams, D. M. (2016), Basins of attraction for chimera states, *New Journal of Physics*, 18(2), 022002 (DOI: 10.1088/1367-2630/18/2/022002).
- [98] Dudkowski, D., Maistrenko, Y., and Kapitaniak T. (2014), Different types of chimera states: An interplay between spatial and dynamical chaos, *Phys. Rev. E*, 90, 032920 (DOI:10.1103/PhysRevE.90.032920).
- [99] Coullet, P., Elphick, C. and Repaux D. (1987), Nature of Spatial Chaos, *Phys. Rev. Lett.*, 58 431 (DOI:10.1103/PhysRevLett.58.431)
- [100] Kemeth, F. P., Haugland, S. W., Schmidt, L., Kevrekidis, I. G., and Krischer, K. (2016), A classification scheme for chimera states, *Chaos: An Interdisciplinary Journal of Nonlinear Science*, 26(9), 094815 (DOI: 10.1063/1.4959804)
- [101] See supporting Material at openly available Supplementary Data for (I) a phase diagram (Fig.1) depicting the correlation measure g_0 , calculated for layer 2 in the $(\langle k^{(1)} \rangle, \varepsilon)$ parameter plane for an mismatched 1D-1D multiplex network, (II) a snapshot (Fig.2) of (a) a chimera state and (b) the corresponding Laplacian distance measure in a 1D-1D multiplex network, (III) the initial conditions considered in this work (Fig.3), (IV) chimera states (Fig.4) for (a) 1D-Erdös-Rényi (ER) (b) 1D-scale-free (SF) multiplex networks (with dense 1D layer) as color density plots of the correlation measure
- [102] The Laplacian distance measure $|\bar{D}(t)| = \{d_i(t) : d_i(t) = |(z_{i+1}(t) - z_i(t)) - (z_i(t) - z_{i-1}(t))|\}$ (Eq. 3.3) captures the spatial distance between the neighboring nodes. The nodes belonging to the incoherent region posses high value

of the laplacian distance measure owing to the high local curvature in the spatial profile [101]. The normalized probability distribution function $g(|\bar{D}|)$ (Eq. 3.3) categories the number of nodes having particular spatial distances. The correlation measure g_0 (Eq. 3.3) calculates the relative amount of nodes having spatial distance below a certain threshold δ where δ (Eq. 3.3) sets a limit below which the spatial curve is considered smooth indicating coherent nodes. The $\delta = 0.01(\max(|D|))$ [100] is taken such that it distinguishes between different dynamical states. So, the $g_0(t)$ indicates the relative size of spatially coherent regions. The measure $g_0(t)$ taking value 1(0) indicates all (none) of the nodes have very small spatial distance with respect to its neighbors and thus form a smooth (discontinuous) spatial profile. Any intermediate value of g_0 between 0 and 1 shows presence of both coherent and incoherent regions denoting a chimera state [100].

- [103] Owing to the sensitivity of chimeras to the choice of initial conditions, a uniform random distribution, multiplied by a Gaussian spatial profile has been used to prepare the initial state ($z_i(t=0)$ for i^{th} node) of the network [2, 3]. A detailed discussion of the choice of initial conditions can be found in Ref. [2, 3] and in the supplemental information [101].
- [104] Ayala, G. F., Dichter, M., Gumnit, R. J., Matsumoto, H., and Spencer, W. A. (1973), Genesis of epileptic interictal spikes. New knowledge of cortical feedback systems suggests a neurophysiological explanation of brief paroxysms, Brain research, 52, 1-17 (DOI: 10.1016/0006-8993(73)90647-1)
- [105] Compte, A., Sanchez-Vives, M. V., McCormick, D. A., and Wang, X. J. (2003), Cellular and network mechanisms of slow oscillatory activity (< 1 Hz) and wave propagations in a cortical network model, Journal of neurophysiology, 89(5), 2707-2725 (DOI: 10.1152/jn.00845.2002).
- [106] Dwivedi, S. K., and Jalan, S. (2014), Emergence of clustering: Role of inhibition, Physical Review E, 90(3), 032803 (DOI: 10.1103/PhysRevE.90.032803)
- [107] Berg, J.M., Tymoczko, J.L., and Stryer, L. (2002) Biochemistry, 5th ed. W H Freeman, New York (978-0716746843)
- [108] Dwivedi, S. K., and Jalan, S. (2017), Evolution of correlated multiplexity through stability maximization, Physical Review E, 95(2), 022309 (DOI:10.1103/PhysRevE.95.022309)

- [109] Dwivedi, S. K., and Jalan, S. (2013), Extreme-value statistics of networks with inhibitory and excitatory couplings, *Physical Review E*, 87(4), 042714 (DOI: 10.1103/PhysRevE.95.022309)
- [110] Tsimring, L. S., Rulkov, N. F., Larsen, M. L., and Gabbay, M. (2005), Repulsive synchronization in an array of phase oscillators, *Physical review letters*, 95(1), 014101 (DOI: 10.1103/PhysRevLett.95.014101)
- [111] Astakhov, S., Fujiwara, N., Gulay, A., Tsukamoto, N., and Kurths, J. (2013), Hopf bifurcation and multistability in a system of phase oscillators, *Physical Review E*, 88(3), 032908 (DOI:10.1103/PhysRevE.88.032908)
- [112] Kuramoto Y. (1975) Self-entrainment of a population of coupled non-linear oscillators. In: Araki H. (eds) International Symposium on Mathematical Problems in Theoretical Physics. Lecture Notes in Physics, vol 39. Springer, Berlin, Heidelberg (DOI is not available)
- [113] Jalan S., Ghosh S., and Patra B. (2017), Is repulsion good for the health of chimeras?, *Chaos (Fast Track)*, 27(10), 101104 (DOI: 10.1063/1.5005576).
- [114] See Supplemental Material for time evolution of nodes for a multiplex network consisting of (I) two positively coupled layers (II) one positively coupled and negative layers.
- [115] Dwivedi, S. K., Baptista, M. S., and Jalan, S. (2017), Optimization of synchronizability in multiplex networks by rewiring one layer, *Physical Review E*, 95(4), 040301 (DOI: 10.1103/PhysRevE.95.040301).
- [116] Bera, B. K., Ghosh, D., and Lakshmanan, M. (2016). Chimera states in bursting neurons. *Physical Review E*, 93(1), 012205 (DOI: 10.1103/PhysRevE.93.012205)
- [117] Yao, N., Huang, Z. G., Ren, H. P., Grebogi, C., and Lai, Y. C. (2019). Self-adaptation of chimera states. *Physical Review E*, 99(1), 010201 (10.1103/PhysRevE.99.010201)
- [118] Sethia, G. C., Sen, A., and Atay, F. M. (2008). Clustered chimera states in delay-coupled oscillator systems. *Physical review letters*, 100(14), 144102 (DOI: 10.1103/PhysRevLett.100.144102)

- [119] Strelkova, G. I., Vadivasova, T. E., and Anishchenko, V. S. (2018). Synchronization of chimera states in a network of many unidirectionally coupled layers of discrete maps. *Regular and Chaotic Dynamics*, 23(7-8), 948-960 (DOI:10.1134/S1560354718070092)
- [120] Meena, C., Murali, K., and Sinha, S. (2016). Chimera states in star networks. *International Journal of Bifurcation and Chaos*, 26(09), 1630023 (DOI:10.1142/S0218127416300238)
- [121] Shepelev, I. A., Vadivasova, T. E., Bukh, A. V., Strelkova, G. I., and Anishchenko, V. S. (2017). New type of chimera structures in a ring of bistable FitzHughNagumo oscillators with nonlocal interaction. *Physics Letters A*, 381(16), 1398-1404 (DOI: 10.1016/j.physleta.2017.02.034)
- [122] Gupte, N., and Singha, J. (2019). Classification and Analysis of Chimera States. In *Proceedings of the 5th International Conference on Applications in Nonlinear Dynamics* (pp. 318-328). Springer, Cham (DOI: 10.1007/978-3-030-10892-2-33)
- [123] Gjurchinovski, A., Schöll, E., and Zakharova, A. (2017), Control of amplitude chimeras by time delay in oscillator networks, *Physical Review E*, 95(4), 042218 (DOI: 10.1103/PhysRevE.95.042218)
- [124] Pradhan, P., Yadav, A., Dwivedi, S. K., and Jalan, S. (2017), Optimized evolution of networks for principal eigenvector localization, *Physical Review E*, 96(2), 022312 (DOI: 10.1103/PhysRevE.96.022312)
- [125] Jalan, S., and Pradhan, P. (2018), Localization of multilayer networks by optimized single-layer rewiring, *Physical Review E*, 97(4), 042314 (DOI: 10.1103/PhysRevE.97.042314)
- [126] Murphy, N. C., Wortis, R., and Atkinson, W. A. (2011). Generalized inverse participation ratio as a possible measure of localization for interacting systems. *Physical Review B*, 83(18), 184206 (DOI: 10.1103/PhysRevB.83.184206)
- [127] Goltsev, A. V., Dorogovtsev, S. N., Oliveira, J. G., and Mendes, J. F. (2012). Localization and spreading of diseases in complex networks. *Physical review letters*, 109(12), 128702 (DOI: 10.1103/PhysRevLett.109.128702)
- [128] Cuevas, E. (2002). Critical generalized inverse participation ratio distributions. *Physical Review B*, 66(23), 233103 (DOI: 10.1103/PhysRevB.66.233103)

- [129] See supporting material for a diagram depicting tailored chimera states for different values of τ_{max} .
- [130] We have chosen τ_{max} to be larger than the intrinsic time scale to get a high variance in the entries of the delay matrices. As a result, a large spread in the delay values ensures that the selected delayed nodes lag considerably and randomly as compared to the undelayed nodes. Thus, in a snapshot, the selected nodes produce a high scattering owing to their different lags. However, the choice of τ_{max} does not considerably influence the results shown in the manuscript. A comparative diagram of the snapshots for different τ_{max} is presented in Sec. [129] which demonstrate same engineered chimera state with a little different scatter pattern in the ICR region.
- [131] Atay, F. M., Jost, J., and Wende, A. (2004), Delays, connection topology, and synchronization of coupled chaotic maps, *Physical Review Letters*, 92(14), 144101 (DOI:10.1103/PhysRevLett.92.144101)
- [132] See supporting material for the phase diagram of $D_x - E_y$ space drwan with variance [131] and correlation measures [100].
- [133] Hénon, M. (1976), A two-dimensional mapping with a strange attractor. In *The Theory of Chaotic Attractors* (pp. 94-102). Springer, New York, NY (DOI: 10.1007/978-0-387-21830-4-8)
- [134] Jalan, S., Jost, J., and Atay, F. M. (2006). Symbolic synchronization and the detection of global properties of coupled dynamics from local information. *Chaos: An Interdisciplinary Journal of Nonlinear Science*, 16(3), 033124 (DOI:10.1063/1.2336415)
- [135] Bassett, D. S., and Sporns, O. (2017). Network neuroscience. *Nature neuroscience*, 20(3), 353 (DOI: 10.1038/nn.4502)
- [136] Stam, C. J. (2014). Modern network science of neurological disorders. *Nature Reviews Neuroscience*, 15(10), 683 (DOI: 10.1038/nrn3801)
- [137] Muldoon, S. F., and Bassett, D. S. (2016), Network and multilayer network approaches to understanding human brain dynamics, *Philosophy of Science*, 83(5), 710-720 (DOI: 10.1086/687857)
- [138] De Domenico, M. (2017). Multilayer modeling and analysis of human brain networks. *Giga Science*, 6(5), gix004 (DOI: 10.1093/gigascience/gix004)

- [139] Buldú, J. M., and Porter, M. A. (2018), Frequency-based brain networks: From a multiplex framework to a full multilayer description, *Network Neuroscience*, 2(4), 418-441 (DOI: 10.1162/netn-a-00033)